FINAL REPORT

EVALUATION OF JOINT INFILTRATION AND DRAINAGE OF RIGID PAVEMENTS

WPI # 0510781 Contract # BA-524

University of Florida Project # 4504 567-12

State Project # 99700-3348-119

Submitted by:

UNIVERSITY OF FLORIDA
Dept. of Civil & Coastal Eng.

Principle Investigator - David Bloomquist, Ph.D., P.E.

Graduate Research Assistant – Boonchai Sangpetngam, MSCE

Graduate Research Assistant – Kenneth Kerr, E.I.

University of Florida
Department of Civil and Coastal Engineering
345 Weil Hall
P.O. Box 116580
Gainesville, FL 32611

Submitted to:

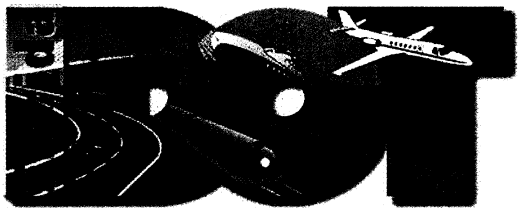

Florida Department of Transportation

Executive Summary

Rigid pavements are primarily distressed by the effects of pumping, i.e. relocation and erosion of subbase material resulting in joint faulting and transverse cracking due to loss of support. The capability of a pavement system to drain susceptible water from its subbase is a major factor governing a pavement's long-term serviceability. There are two basic methods currently in use for analyzing the drainage requirement: a steady-state flow analysis or a time-to-drain approach. This report examines the characteristics of both techniques and the factors affecting their results are discussed. Currently, the Florida Department of Transportation uses a value of 0.7 ft^3/day/ft joint infiltration rate (referenced in the FHWA design manuals) to design the subbase geometry based on the steady-state flow method. This value is derived from field tests conducted in Connecticut. Thus, applicability of this infiltration rate to Florida conditions has not been verified, since the material properties of the pavement systems tested in Connecticut are not available. Thus, a 0.7 ft^3/day/ft infiltration value may not be appropriate in providing a satisfactory cross-section design for effective rigid pavement performance.

This study examines various joint infiltration values, based on typical Florida subbase conditions and their effect on section geometry. Both steady state and time-to-drain approaches were investigated. It was found that the joint infiltration value necessary to achieve a well-drained (i.e., an effective) section deviates from the 0.7 ft^3/day/ft figure, depending on the methodology used in the steady-state-flow calculations. In addition, unlike the steady-state flow approach, which is an empirically derived method, the time-to-drain technique appears to be a more rational approach and directly connotes the drainage capability of a pavement system. Based on this procedure, it suggests that subbase materials furnish excellent drainage characteristics if they contain 5% or less fine material. However, higher percentages may also provide adequate

drainage since the standard usage of time-to-drain to 85% may not be required. Thus, both a new field infiltration test and a pore-pressure-generation lab test were developed to assess this figure. The preliminary results of both procedures are outlined in the report. Finally, design charts for both approaches are presented and reveal that soil properties and the sectional geometry have a major effect on sub-drainage quality. The information gleaned through the analysis of both design procedures led to the development of a new method for analyzing subbase drainage. The method computes the elapsed time required to achieve a particular phreatic surface level below the pavement. In fact, drainage to a finite level may provide design engineers with a useful tool in reducing subbase deterioration through pumping.

Table of Contents

Introduction

Rigid pavements traditionally have longer service lives compared to flexible pavements. However, water that is trapped in the soil beneath the pavement can lead to pavement distress. This problem, commonly referred to as pumping, can result in the erosion and ejection of soil particles, and ultimately create joint faulting and transverse slab cracking. Therefore, minimizing the amount of water retained in the underlying material should assuage the problem of deterioration. Providing an adequate sub-drainage section is considered the most effective long-term method of safeguarding pavements from pumping induced failure.

With regards to drainage, the FHWA has suggested the following two approaches for the design of a subbase layer:

1. Steady-state flow
2. Time-to-drain

The *steady-state flow* approach is based on a uniform inflow rate—the joint/crack infiltration rate—to indicate the amount of water introduced through the pavement joints. As the name implies, this method requires that the outflow rate equal the inflow rate, a condition generated by the choice of an appropriate subbase layer. Calculations for this method are developed from Darcy's steady state equation,

$$q = kiA$$

where q = flow rate (inflow/outflow)

k = coefficient of permeability

i = hydraulic gradient

A = cross-sectional area

Therefore, the inflow rate is a major contributor in layer thickness geometry.

The *time-to-drain* approach assumes water (from a rainfall event) enters the subbase until it is saturated. Then to prevent the development of excess pore pressures, the subbase must drain the water to a certain saturation level within a relatively short time. This method is more complex than the steady-state infiltration method since it uses non-steady state analysis for a given pavement section to determine a degree of saturation at a particular time. A subbase layer that provides drainage to a particular level in a recommended period of time is the section specified.

The Florida Department of Transportation (FDOT) currently utilizes a joint infiltration rate of 0.7 ft^3/day/ft to determine the subbase thickness based on typical properties of the subbase material. In this study, the two methods previously discussed will be employed to evaluate typical Florida materials. Also included is a qualified subbase section based on the FHWA and AASHTO guidelines and the factors affecting both the joint infiltration and the drainage time.

Purpose and Scope of the Study

The objectives of this research include:

1. Determine those factors affecting joint infiltration rate in the *steady-state flow* design approach, including the associated effect that permeability has on the drainage rate of typical Florida soils.
2. Verify that the 0.7 ft^3/day/ft joint infiltration rate for a subbase layer design is appropriate for Florida conditions.
3. Analyze flow patterns beneath rigid pavements as a function of geometry and boundary conditions.
4. Provide recommendations for a more rationale design standard.

Chapter 1 Literature Review

1. Pumping Distress

Deterioration of rigid pavement can be caused by many factors, the most detrimental of which is pumping. As water saturates the soil beneath a pavement structure, it reduces the strength of the soil by reducing the effective stress. In addition, heavy truck traffic can produce load cycles that create positive followed by negative water pressures at the moment the wheels pass over a transverse joint. This cyclical generation of water pressure induces flow beneath the pavement and the eventual ejection of soil particles from the subbase layer. This leads to the development of voids beneath the pavement. Ultimately, joint faulting and slab cracking result due to a lack of structural support.

Pumping generally occurs in both fine-grained materials and stabilized materials that make up an erodible subbase. Pumping is most prevalent in plastic clays and plastic silty-clayey soils and is of lesser concern in silty soils. A subbase layer material that facilitates rapid drainage will minimize pumping. Materials with a maximum amount of 7% passing the #200 sieve have been recommended. On the other hand, materials with particles 15% finer than the #200 sieve are considered virtually impermeable and are conducive to pumping [Van Wijk (1985)].

The following are the typical sources of water that is introduced into a pavement structure:

1. Surface water on the pavement flowing through longitudinal and transverse joints
2. Water from the median or shoulder ditch flowing laterally through the side edge of the pavement structure
3. A high groundwater level seeping upward
4. Capillary tension pulling water up from the water table

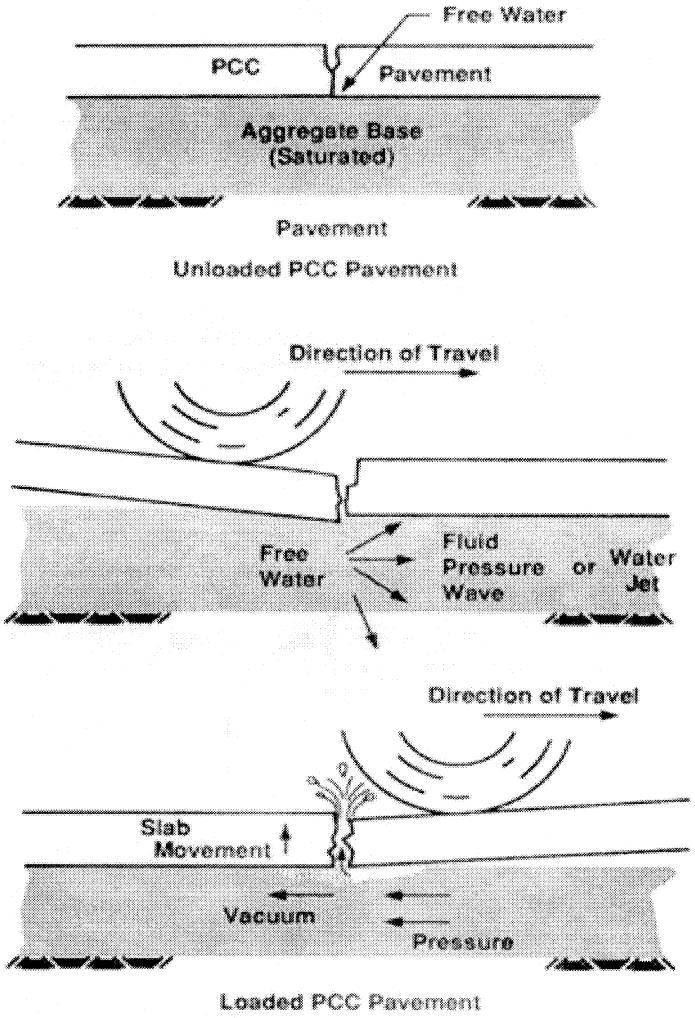

Figure 1-1. Action of free water in concrete pavements.

[From FHWA, 1992, *Drainage Pavement Systems*: Participant Notebook March 1992, Pub.No. FHWA-SA-92-008.]

Surface water is the primary source of water in a subbase [Cedergren (1987,1989)]. To reduce the water buildup in a pavement section, the following approaches are recommended [FHWA Notebook 1992]:

1. Seal all joints and cracks.
2. Provide drainable pavement systems.

A well performing sub-drainage system can be achieved by providing a well-drained subbase and edge drains. This type of system will help protect rigid pavements from deterioration by eliminating an ample amount of water from the subbase within an adequate time period in order to minimize pumping susceptibility.

2. Joint Infiltration

General Definition

The major source of subbase infiltration is surface water flowing through the joints in the pavement [Cedergren (1987,1989), FHWA Drainable Pavement Systems: notebook (1992)]. The joint infiltration rate is defined as the amount of surface water on the pavement flowing into a unit length of joint per unit time and typically has units of ft^3/day/ft or cm^3/day/cm.

Once infiltration has occurred, the water penetrates to the subbase layer and flows laterally toward the edge drain via the subbase (the subgrade soil is considered, for all practical purposes, impermeable). Given a sufficient precipitation period, a steady state condition is reached and the joint infiltration rate will be identical to the flow or seepage rate through the porous media (subbase) to the edge drains. The flow through the drains is considered the output. Therefore, the infiltration rate is mainly dependent upon the subbase properties, which is comprised of the soil permeability and subbase geometry (slope, thickness, and length of drainage path).

Quantifying the Infiltration Rate Value

A question exists as to whether a high or low rate of infiltration is preferred. Frequently it is assumed that since low rates provide minimal infiltration into the subbase pumping cannot occur. The FHWA Drainage Pavement Systems: Notebook (1992) revealed that pumping is enabled only in the presence of the following:

- truck wheel loading
- rigid pavement curling upward at the transverse joints
- subbase soil susceptible to pumping erosion
- water underneath the transverse joint

However, the fact is that only a small amount of water is necessary for pumping to occur. A low joint infiltration rate (and in turn a low outflow rate) can easily provide enough susceptible water to cause pumping. The low rate is a direct result of the low capacity of a subbase to drain infiltrated water. With poor drainage quality, water can be stored and exposed to wheel loads for days. Therefore, a high rate is favored in order to drain the entrapped water as rapidly as possible following any precipitation.

The FHWA sub-drainage design manual provides a standard joint infiltration rate for pavement sub-drainage design purposes. This joint infiltration rate represents a rate at which water enters the subbase and is removed by means of a satisfactory subbase layer and drainage system. The FHWA design procedure uses the joint infiltration rate, the pavement geometry, and the subbase material's permeability as input parameters for determining the thickness of the subbase layer based on Darcy's flow equation.

The FHWA Highway Sub-drainage Design manual [Moulton (1980)] suggests an infiltration rate of 2.4 ft^3/day/ft but noted that this value was based on minimal research. Ridgeway (1976) found that infiltration rates varied from 0 to 1.91 ft^3/day/ft and that rates up to 1.21 ft^3/day/ft were observed in sealed transverse cracks. Ridgeway's data was based on field tests of nine joints in two separate rigid pavement sections containing dense-graded subbase material in Connecticut. However, he suggested an infiltration rate of 2.4 ft^3/day/ft for design purposes. Later, Hassan-Feng-White (1997) presented results on sub-drainage analysis from an instrumented jointed concrete pavement section of Highway U.S. 36 in Indiana. Hassan-Feng-White's results from numerical modeling were in agreement with measured field results at a value of 0.61 ft^3/day/ft. The two-dimensional section was composed of a 21.6 cm thick x 3.65 m wide concrete slab with a 0.76 m wide shoulder, a 15.24 cm thick bituminous base having a 0.02 cm/s permeability, and a 30.48 cm wide x 45.72 cm deep edge drain with a permeability of 0.07 cm/s. A subgrade with a

permeability of $1.1x10^{-5}$ cm/s was imposed as an impervious boundary at the bottom of the base layer.

Chapter 3 will describe the factors that affect the infiltration rate for steady state conditions and the methods required to quantify the infiltration rate. It will then lead to back-calculation of the required subbase properties based on desired rates of infiltration. The procedures for determining a suitable infiltration rate for drainage purposes will be described in detail in Chapter 5.

To quantify the infiltration rate and identify the factors by which it is influenced, the following two methods were applied to the pavement model in this study:

1. Conventional flow equations:

   Application of Dupuit's confined & unconfined flow equations as described in "Foundation Engineering: Dewatering Chapter" [Leonards (1962)].
2. Flow simulation by computer modeling for solving seepage problems:
   - FastSEEP/SEEP2D finite element software for two-dimensional problems
   - Visual MODFLOW finite difference software for three-dimensional problems

Conventional Flow Equations

Below are the equations for unconfined, confined and combined flow developed from Dupuit's assumptions. The equations are derived in detail in the Appendix.

1. Unconfined Flow (No Pavement)

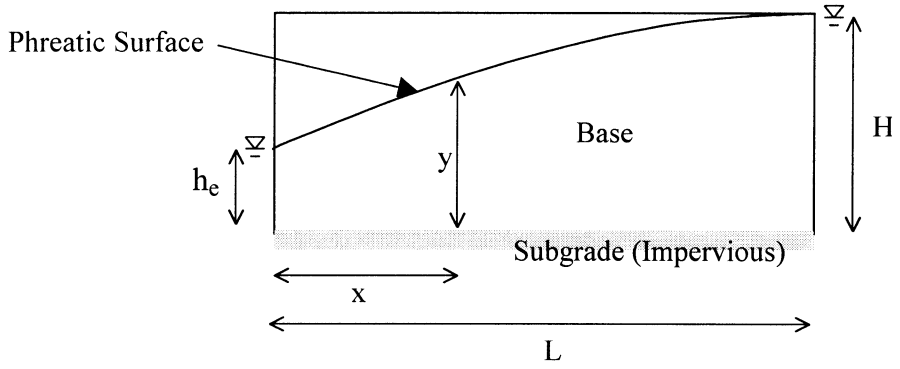

$$Q = \frac{k}{2L}(H^2 - h_e^2)$$ ← Unconfined Flow Equation

2. Confined Flow (Pavement)

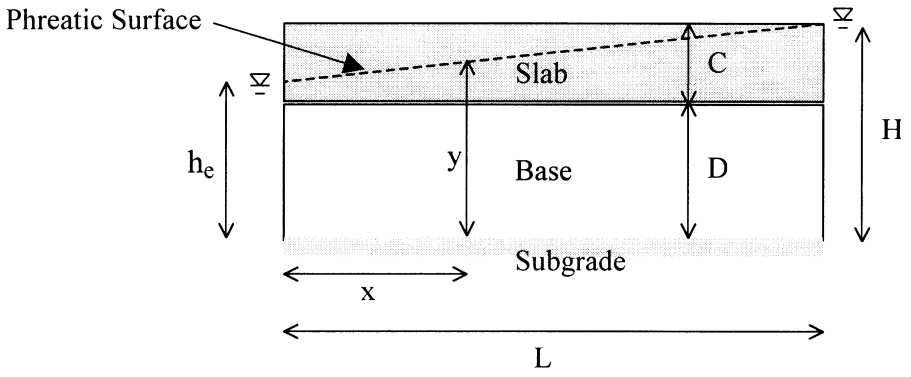

$$Q = \frac{kD}{L}(H - h_e)$$ ← Confined Flow Equation

Where Q = the flow rate (volume / time)

k = the soil's permeability

H = the total thickness

h_e = the depth of water in the edge drain

D = the base thickness

C = the slab thickness

3. Combining the Confined and Unconfined Flow Models

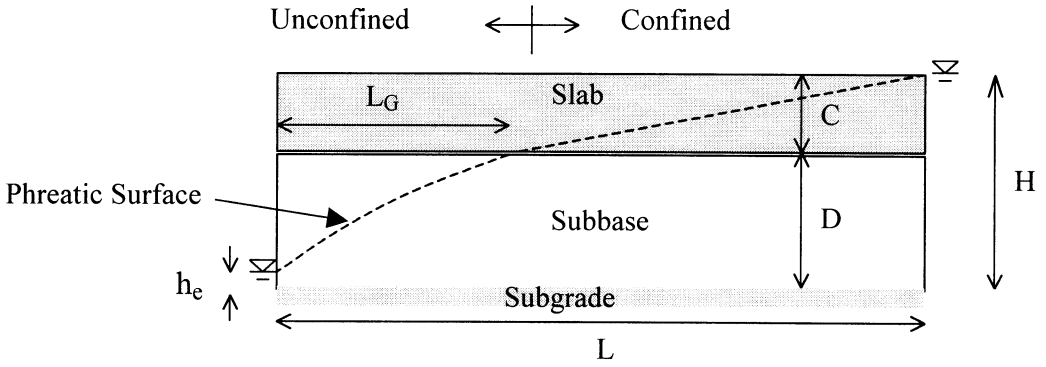

In this case, the flow under the pavement consists of both confined flow with a phreatic level in the slab (i.e. pressurized) and an unconfined flow region in the subbase as shown in the above figure. Therefore, combining the confined and unconfined flow equations will result in an equation that describes the entire flow regime beneath the pavement. The equations are combined as follows:

Unconfined flow: $$Q_1 = \frac{k}{2L_G}(D^2 - h_e^{\,2})$$

Confined flow: $$Q_2 = \frac{kD}{(L - L_G)}(H - D)$$

Where Q_1 = the flow in the subbase

Q_2 = the flow confined by the slab

L_G = the horizontal distance separating the two flow regions

But $Q_1 = Q_2$. Therefore, equating the two equations and solving for L_G gives,

$$L_G = \frac{L(D^2 - h_e^2)}{2DH - D^2 - h_e^2}$$

Consequently, $$Q = \frac{k}{2L}(2DH - D^2 - h_e^2)$$ ← Combined Flow Equation.

and $$H = C + D$$

Therefore, $$Q = \frac{k}{2L}(2CD + D^2 - h_e^2)$$

Thus, given the geometry of the section the flow rate and soil permeability are directly related to each other.

Flow Solutions using Computer Software

1. FastSEEP or SEEP/2D

As described in the user's manual reference, FastSEEP is a pre- and post-processor program designed to be used in conjunction with the SEEP2D program to solve seepage problems in two-dimensional space (*x-z* plane) for steady state conditions. In a typical application, FastSEEP is used to construct a finite element mesh of the modeled region with applicable boundary conditions. The mesh is then saved in a data file and SEEP2D is used to perform the seepage analysis. A solution file containing total head, flow potential (used in drawing flow nets), velocity at each node, etc., are used as input for FastSEEP's post-processor feature to generate flow nets and contour plots.

2. MODFLOW

VisualMODFLOW is a set of graphical pre- and post-processor programs designed to create three-dimensional groundwater flow models and observe the results from user defined simulations. Used in conjunction with MODFLOW, (a finite difference groundwater solver), enables VisualMODFLOW to estimate and present computed flow rates at designated zones, equipotential lines, velocity vectors, etc., in the form of plan and sectional views.

3. Soil Properties

Grain Size Analysis

[Davidson J.L.] The Grain Size Analysis Test (ASTM D422) provides information on the sizes of solid particles and their relative proportions within a soil. The results are used for soil classification. Two grain size analysis tests are used:

1. Mechanical (or sieve) analysis
2. Hydrometer analysis

For mechanical analysis, a representative sample of soil is shaken through a stack of wire sieves of known mesh dimensions and sorted by grain size. The fraction of the total soil retained on each sieve is determined by weighing each sieve. A plot of sieve size, or grain size, vs. the percent of the soil that passes through that sieve is generated. The percent of the soil by weight that passes each sieve is generally referred to as the *percent finer*, and is notated throughout the remainder of this report as *%fines*. The resulting plot is referred to as a grain-size distribution curve. The sieve test is suitable only for coarse-grained soils, i.e., sands and gravels. For practicality, the smallest sieve used is the #200 sieve that corresponds to a 0.075 mm square opening. According to the Unified Soil Classification System (USCS), this sieve size differentiates between sand and silt size particles, and will be referred to as *% fines*.

The hydrometer analysis test is used to obtain an approximate grain-size distribution for soils finer than the #200 sieve. For soils containing both coarse and fine fractions, the two methods can be combined to provide a single grain-size distribution curve covering the entire range of soil

particle sizes. Since the size of fine-grained soil particles is seldom of practical importance, the hydrometer test was not used in this research.

Coefficient of Permeability or Hydraulic Conductivity, *k*

Permeability, or the coefficient of permeability, of a soil is a parameter that indicates the resistance to fluid flow through a soil. The permeability is defined as the discharge velocity through a unit area under a unit hydraulic gradient. It is a constant in Darcy's law for laminar flow in porous media,

$$Q = k\, i\, A\, t$$

where k is the permeability and Q is the quantity of seepage in a cross section of area A normal to the direction of flow, under a hydraulic gradient i, during a length of time t. It has the same unit as velocity, i.e., cm/s, m/day, ft/min, ft/day, and for a granular soil is dependent on the following factors: fluid viscosity, pore-size distribution, grain-size distribution, particle arrangement, void ratio, particle roughness, and degree of saturation.

The three common methods for determining the permeability of soil are as follows:

1. Laboratory methods

The most common tests are the constant head test (ASTM D2434) and the falling head test. The more accurate test for determining permeability is the double burette test.

2. Indirect methods

The one-dimensional consolidation test provides data to compute the soil permeability by using the relationship developed by Terzaghi (1943). There have been several formulas developed to

estimate the permeability from an "effective size" value obtained from a grain size distribution curve and a soil's void ratio. A popular one developed by Hazen (1911) is:

$$k\,(\text{cm/s}) = C_1 D_{10}^2$$

where D_{10} is the effective size in cm. This represents the diameter in a distribution curve corresponding to 10% fines. The value of C_1 varies from 90 to 120, but is generally assumed to be 100. For uniform sands, indirect formulas provide reasonable approximations of a soil's permeability.

3. Field methods

Samples tested in the lab are small in size relative to the large masses in the field and may not represent the field conditions with regards to spatial variability. Also, obtaining samples from the field for laboratory testing is difficult. Thus, the *insitu* (in place) test is frequently utilized to measure the permeability of soil in the field. Various methods, such as pumped wells with observation holes, borehole tests, ring infiltrometer tests, etc., are used.

Effect of %fines on Coefficient of Permeability

Hazen's formula for estimating the permeability of sand is $k\,(\text{cm/s}) = C_1 D_{10}^2$ as previously mentioned. Several D_{10} sizes from test data are shown in Table 19.3 of *Soil Mechanics* [Lambe and Whitman (1969)] and include the following:

Soil	D_{10} (mm.)
Coarse sand	0.11
Medium sand	0.02
Fine sand	0.03
Silt	0.006

From the above data, the fine particles greatly affect the permeability of sandy material. In fact since the D term is squared based on the above table the permeability of a silt is 25 times lower

than a fine sand. Therefore, according to Hazen's formula, the amount of fine particles adversely affects the permeability of soil.

Soil-Water Drainage Properties

Any type of soil has a characteristic curve that relates the degree of saturation (or volumetric water content θ) to a corresponding applied pressure, ψ. For example, a soil subjected to atmospheric pressure will hold or retain a certain amount of water due to surface tension, but if an applied pressure is added the soil will drain additional water. The suction head or negative pressure corresponding to the break in the curve (near the saturated water content θ_s) is generally referred to as the air-entry head (ψ_a). The air-entry head is the suction head below which the soil remains fully saturated. The water content corresponding to the asymptote of the curve for a very large suction head is called the residual water content, θ_r, or residual saturation, s_r. The shape of the curve is a function of soil type. Soils with smaller pores have relatively higher values of ψ_a or they remain more saturated. Soils with a wider range of pore sizes or grain sizes have steeper slopes. The soil-water drainage curve is best determined in the laboratory from content measurements of water and applied suction head. The two common approaches to describe the data curve are the Brooks-Corey equation and the van Genuchten equation. The Brooks-Corey equation is stated as follows:

$$\frac{\theta-\theta_r}{\theta_s-\theta_r}=\frac{s-s_r}{1-s_r}=\left(\frac{\psi_a}{\psi}\right)^{\lambda} \qquad \psi > \psi_a$$

$$\theta=\theta_s,\ s=1 \qquad \psi \le \psi_a$$

Where s = degree of saturation of interest

s_r = residual degree of saturation

The constant λ is an empirical parameter called the pore-size distribution index, which is a function of the distribution of pores in the soil. The more uniform the material, the larger the value of λ. The values of λ, θ_r, ψ_a and k are all related to the grain size distribution and hence the porosity of the soil.

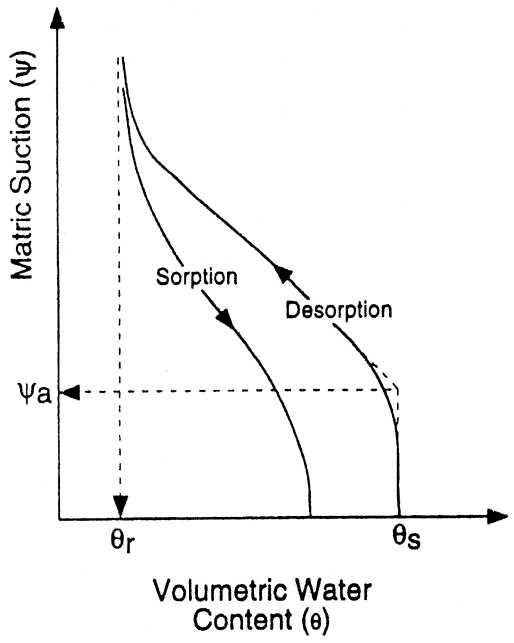

***Note:** ψ_a = air entry head, Matric Suction = applied negative pressure = suction head

Figure 1-2. Typical soil-water characteristic curves for desorption and sorption. [From *Soil-Water Characteristic Curves for Compacted Clays*, Tinjum et.al (1997), ASCE Journal of Geotech. and Geoenv. Eng.]

The SOILPROP program

Soil grain-size distribution and bulk density are more easily determined than hydraulic data from water-retention tests. SOILPROP is a program designed to estimate soil hydraulic properties from the particle-size distribution data. The results from SOILPROP include the saturated hydraulic conductivity and the parameters required in the Brooks-Corey and van Genuchten equations. Methods for estimating the saturated hydraulic conductivity are generally based on the

Kozeny-Carman equation or variations thereof, which involve a relationship between saturated conductivity, porosity and some representative particle diameter. The procedure used in SOILPROP is based on a method developed by Mishra, et al (1989).

Effective Porosity, N_e or Drainable Porosity n_d

Following the FHWA Notebook (1992), *effective porosity* is a measure of how well a soil will hold water when a saturated sample is allowed to drain under the influence of gravity. Thus, the effective porosity is the ratio of the volume of water that drains from the soil sample to the total volume of the sample.

The effective porosity is used to represent the water-retention parameters for estimating a drainage time in the FHWA design procedure. The FHWA Notebook (1992) provides a recommended table and a corresponding equation to estimate the effective porosity based on the soil type and the %fines contained in the material.

Amount of Fines	< 2.5% Fines			5% Fines			10% Fines		
Type of Fines	Filler	Sand	Clay	Filler	Sand	Clay	Filler	Sand	Clay
Gravel	70	60	40	60	40	20	40	30	10
Sand	57	50	35	50	35	15	25	18	8

Table 1-1. Water loss values as percentages of the porosity of the material.

Effective porosity, $N_e = N * W_L$,

where N = porosity of the material

W_L = water loss from Table1.1 divided by 100

A program known as DAMP used by the FHWA uses an empirical equation from Moulton (1980) related to the subbase permeability to obtain the effective porosity (or drainable porosity, n_d). This equation is given as:

$$n_d = 0.0355\, k^{0.235}$$

where k is the permeability measured in m/day. This is a lump sum equation developed for a typical range of subbase heights. Exact agreement between the FHWA N_e method and the FHWA n_d method cannot be reached because they are both empirical equations derived from different sets of field data. This is shown in Tables 1-2 and 1-3 by using typical soil property values and comparing results from each method.

Soil	Fines		Porosity,	Water Loss,	Effective Porosity,	Permeability,	Permeability,
	Type	Amount	N	W_L (%)	N_e	k (m/day)	k (cm/s)
Sand	Sand	<2.5%	0.430	50	0.215	2,130.9	2.47
Sand	Clay	10%	0.350	8	0.028	0.364	4.2×10^{-4}
Gravel	Filler	<2.5%	0.550	70	0.385	25,424	29.43

Table 1-2. FHWA N_e method for calculating effective porosity using typical porosity values (soil property averages: Lambe, 1969). The permeability shown is the corresponding back-calculated value required for equality in the FHWA n_d equation.

Soil	Fines		Permeability,	Permeability,	Effective Porosity,	Porosity,
	Type	Amount	k (cm/s)	k (m/day)	n_d	N
Sand	Sand	<2.5%	2.3×10^{-1}	200.0	0.123	0.246
Sand	Clay	10%	5.0×10^{-4}	0.432	0.029	0.363
Gravel	Filler	<2.5%	3.0	2592.0	0.225	0.321

Table 1-3 FHWA n_d method for calculating effective porosity with typical permeability values (soil property averages: Lambe, 1969). The porosity shown is the corresponding back-calculated value required for equality in the FHWA N_e equation.

4. Pavement Sub-drainage

Water Retention in Granular Subbase

After precipitation ceases, water stored in the subbase is then drained through pre-installed edge drains by gravity action. Depending on the hydraulic properties of the soil and subbase geometry, some water may remain in the subbase layer. At any vertical section from the edge drain, the degree of saturation varies from the lowest (at the uppermost level) to the highest at the bottom of the subbase, where the maximum degree of saturation is 1.0, or 100%. This drainage geometry depends on the relationship between the degree of saturation and pore-water suction head, ψ. Brooks and Corey(1964) used their equation to estimate the drainage curve in the soil and, with results from lab measurements, obtained the necessary hydraulic constants. Thus, an approximate drainage curve and its constants can be computed from grain size distribution data and the bulk density of the material using the SOILPROP program.

Definition and Importance

The minimum degree of saturation at a point in the subbase is a function of the water-retention property of the soil, head due to capillary tension and the force of gravity causing drainage. In a thick, medium-sand subbase, the minimum degree of saturation can vary from 0% at the top level to 100% approximately at the middle level of the subbase. In a thin, fine-sand subbase, the minimum degree of saturation can possibly remain 100% saturated throughout the layer. In fact, in a coarse gravel subbase, the minimum degree of saturation may equal 0% throughout the entire layer.

The *average degree of saturation* is the mean value of the degree of saturation over the entire subbase layer at any time during the drainage process. The *average minimum degree of saturation* follows the same definition, but is determined when drainage is complete. The average minimum degree of saturation indicates the amount of water that cannot be gravity drained from the subbase.

The *time-to-drain* is defined as the amount of time needed for water stored in the subbase to drain from 100% saturation to a certain average degree of saturation. As long as the pavement subbase is saturated with water, traffic will activate the pumping and erosion mechanism. Hence, it is essential to drain this water in the shortest time to keep deterioration to a minimum. The time to drain is an important indicator of the drainage quality of the subbase. Several references recommend an appropriate time to drain, however the average minimum degree of saturation still poses a challenging question of how much water must drain in order to disable the pumping process. The following two approaches consider the time to drain question:

1. Time to 50% drainage, $T_{50\%DRAIN}$

   The time to 50% drainage is the elapsed time from the start of drainage (100% saturation) until 50% of the drainable water has been removed.

2. Time to 85% saturation, $T_{85\%SAT}$

   The time to 85% saturation is the time required for a 100% saturated subbase to drain to the average degree of saturation (for the entire subbase) equal to 85%. (Note that the average minimum degree of saturation is less than 85% in this case.)

In addition to the time to drain criteria cited above, the actual level of the phreatic surface beneath the pavement may be a major determining factor in pumping causation. This hypothesis will be analyzed in order to gain information on water level in the subbase versus pore pressure generation.

Recommended Values of Time to Drain

The FHWA Design Manual (1992) includes criteria from the AASHTO Guide for Design of Pavement Structures (1986) that provides the following recommendations based on draining 50 percent of the drainable water from the subbase.

AASHTO Drainage Recommendations for Time to Drain

Quality of Drainage	Time to Drain (50% of completion)
Excellent	2 hours
Good	1 day
Fair	7 days
Poor	1 month
Very Poor	Does not drain

The FHWA Design Manual (1992) also includes the table below that suggests values based on 85% saturation [Techniques for Pavement Rehabilitation-A Training Course Manual (1987)].

Pavement Rehabilitation Guidance for Time to Drain

Quality of Drainage	Time to Drain (85% of saturation)
Excellent	Less than 2 hours
Good	2 to 5 hours
Fair	5 to 10 hours
Poor	Greater than 10 hours
Very Poor	Much greater than 10 hours

The stated time-to-drain parameters obviously represent the drainage capability of the subbase and are essential for sub-drainage design purposes.

The time-to-drain parameters can be estimated by using one of the following methods:

1. The FHWA procedures [FHWA Notebook (1992)]
2. The SUBDRAIN computer program

The FHWA Procedure

In the FHWA design procedure, drainage times are determined by using various graphs and equations or by running the program DAMP. DAMP is a computer program created by the FHWA that will perform the time to drain calculations. Both methods are based on formulas published by Casagrande and Shannon in 1951 [McEnroe (1994)]. The methods were derived from a simplified one-dimensional analysis in which the phreatic surface (water table) was considered parallel to the slab slope. However, the FHWA introduced an additional coefficient into their analysis and used experimental data to determine its values for various conditions to better represent the actual shape of the surface.

The SUBDRAIN Program [McEnroe (1994)]

SUBDRAIN is a computer program that simulates the subsurface drainage of a flat, longitudinal grade section of roadway. A one-dimensional flow model, in which the primary direction of flow occurs in the transverse direction, represents the drainage of the subbase layer. The program employs the Brooks-Corey equation to the soil-water retention behavior during the drainage process. The initial condition is complete saturation and the subbase receives no inflow during

the drainage period. The input data include the geometry of the pavement and subbase sections. Additionally, the hydraulic properties of the subbase, i.e., the coefficient of permeability and the Brooks-Corey constants (λ, θ_r, ψ_a) are required. The program's output includes the degree of saturation and the degree of drainage at the end of each time step until the subbase is 90% drained. The program also computes the time to 85% saturation and the time to 50% drainage.

The FHWA method uses a constant called the effective porosity, or *drainable porosity*, n_d, to represent the water retention characteristic of the subbase material. The drainable porosity can be obtained from the following equation previously described:

$$n_d = 0.0355\, k^{0.235}$$

where k is the permeability of the subbase measured in m/day. Unlike the FHWA method, SUBDRAIN was developed based on water retention (Brooks-Corey) and flow through porous media, which are not empirically derived. By introducing additional parameters into the model, SUBDRAIN can provide reasonable measurements of pavement drainability. However, the more complicated parameters necessitate careful scrutiny in preparing the input data.

Chapter 2 Soil Properties

Introduction

This research project's primary goal is to study the typical soil conditions in Florida and their drainage characteristics. The soil samples used in this study were provided by the FDOT from various sites. The collected soil samples represent typical subbase materials used in conjunction with rigid pavements. Essential lab tests were performed to obtain basic soil properties, which in turn allowed for the determination of other more detailed characteristics.

Sources of Samples

The soil samples from the six different sources represent the typical subbase material for construting rigid pavement in Florida. The FDOT also provided some basic properties of the samples as shown in Table 2-1.

Table 2-1. Descriptions of obtained samples

Soil #	Description	FDOT Permeability (cm/s)	Sieve Analysis (% Fines)	Modified Proctor		Opt. Water Content (%)
				(pcf)	(g/cm^3)	
1	72280-3424 004H	N/A	9.82	106.61	1.709	9.31
2	Test Pit Tan Sand	6.1375×10^{-4}	4	108.7	1.743	10.9
3	Beck Pit Subgrade	3.278×10^{-3}	2	104.5	1.675	13.6
4	Goldhead	4.317×10^{-4}	6	108.2	1.735	9.2
5	GrovePark / Whitehurst	2.804×10^{-5}	13	119.2	1.911	9.2
6	Middleburg-Clay Co.	4.873×10^{-5}	9	109.9	1.762	11.2

Basic Properties

Sieve Analysis

Sieve analyses were performed on the six soil samples using U.S. standard sieves. The procedure followed ASTM D422 with the sieve series listed below:

Sieve No.	Sieve size (mm)
4	4.75
10	2.00
20	0.85
30	0.59
40	0.42
70	0.21
100	0.149
200	0.075
Pan	0

The weight of soil retained on each sieve was measured and was input into a worksheet to compute the percentage of soil finer through each sieve. The details of the worksheet data are shown in the Appendix. The relationship between the %finer and sieve size for each of the samples was plotted to create grain size distribution curves, shown in Fig. 2-1.

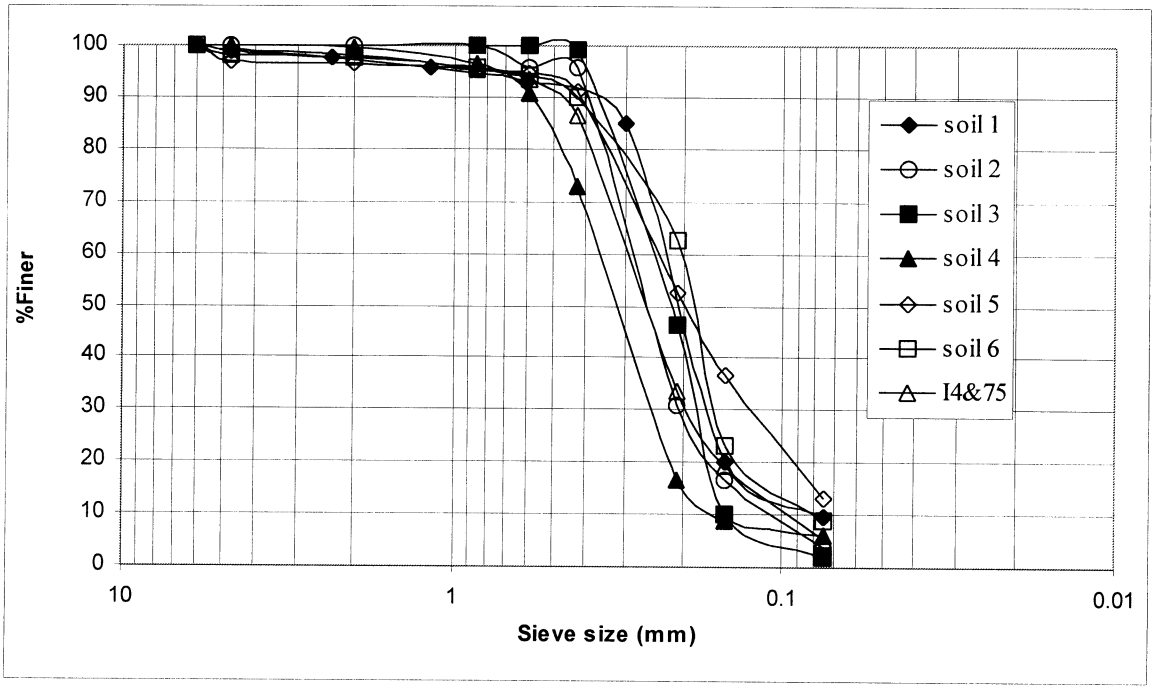

Figure 2-1. Grain size distribution curves of six Florida soil samples.

Soil Classification

Several organizations have developed soil classification systems based on specifications relevant to their intended purpose. For example, the textural classification system developed by the U.S. Department of Agriculture lists the soils after their principal components: sandy clay, silty clay, etc. On the other hand, the AASHTO classification system classifies soils into seven major groups, specifically for use as highway materials. This classification system is based on grain size, on the percentage of material in each grain size class, plasticity, etc. Finally, the Unified Soil Classification System uses two letters as symbols to classify soils into two broad categories:

1. Coarse-grained soils having gravel or sand less than 50% (by weight) passing the #200 sieve.
2. Fine-grained soils—silt or clay—with at least 50% (by weight) passing the #200 sieve.

In addition, the system applies Atterberg limits and the coefficient of uniformity to further classify soils into particular groups. Many engineers, however, still use a convenient method based on the particle size distribution. The particle-size distribution is a plot of %finer (by weight), versus diameters (in mm), based on results from the sieve analysis tests. This widely used method classifies soils, based on particle sizes, as sand, silt, or clay, noted at the top of the plot (Fig.2-2). By visually matching the particle size distribution curves of the six samples (Fig.2-1) to Fig.2-2, all of the samples are classified as medium to fine sand.

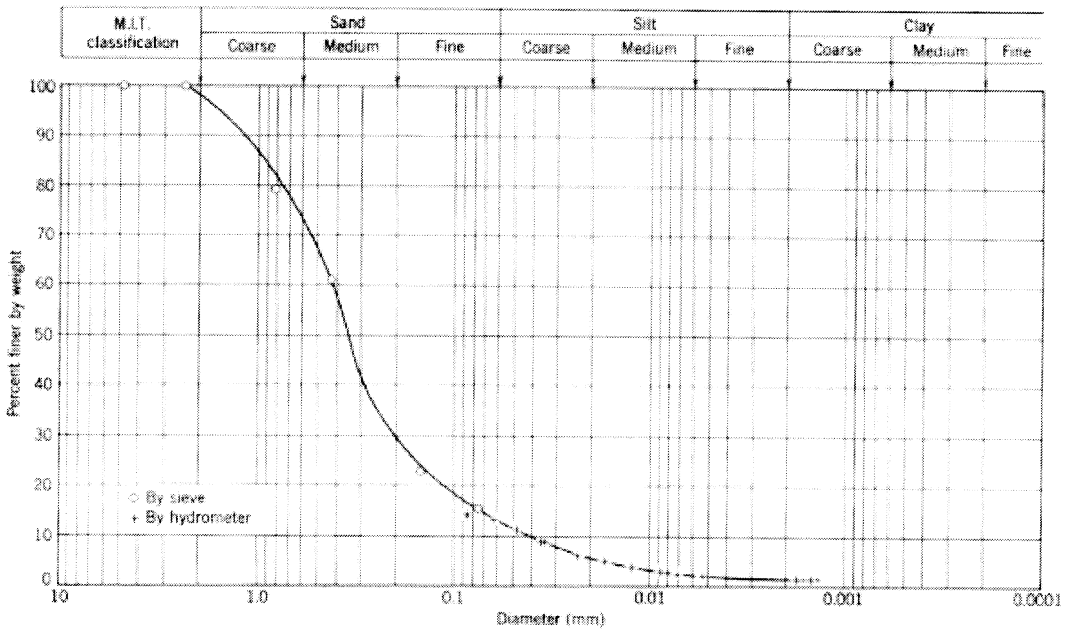

Fig. 3.3 Particle size distribution curve (From Lambe, 1951).

Figure 2-2. Particle size distribution curve (From Lambe and Whitman 1969)

Coefficient of Permeability with %fines Sensitivity

The coefficient of permeability of a saturated granular soil is primarily a function of the grain-size distribution, the void ratio and the roughness of the mineral particles. The empirical equation cannot accurately determine the permeability value a given grain size distribution plot. To examine the effect of %fines on the permeability of various materials, permeability tests were performed on samples of each soil type. Particles passing through the #200 sieve were separated from each sample, producing material lacking particles smaller than 0.075mm. Subsequently, a pre-determined amount of #200 material was added to each same sample to obtain samples with fixed amount of fines. The designated %fines used for studying fine particle effects were 0%, 5%, 10%, 15% and 20%. Each prepared sample was compacted in an ASTM permeability device using a hand-tamper and a vacuum was applied to remove the air from the sample. Because the six samples were classified as medium to fine sands, constant head tests were performed for permeability, following the ASTM D2434 standard procedure. Test data of the samples was input into a prepared spreadsheet to calculate the dry density and the permeability of each sample. All of the spreadsheet data are included in the Appendix. The summary of the results can be seen in Figs. 2-3 and 2-4(a through f).

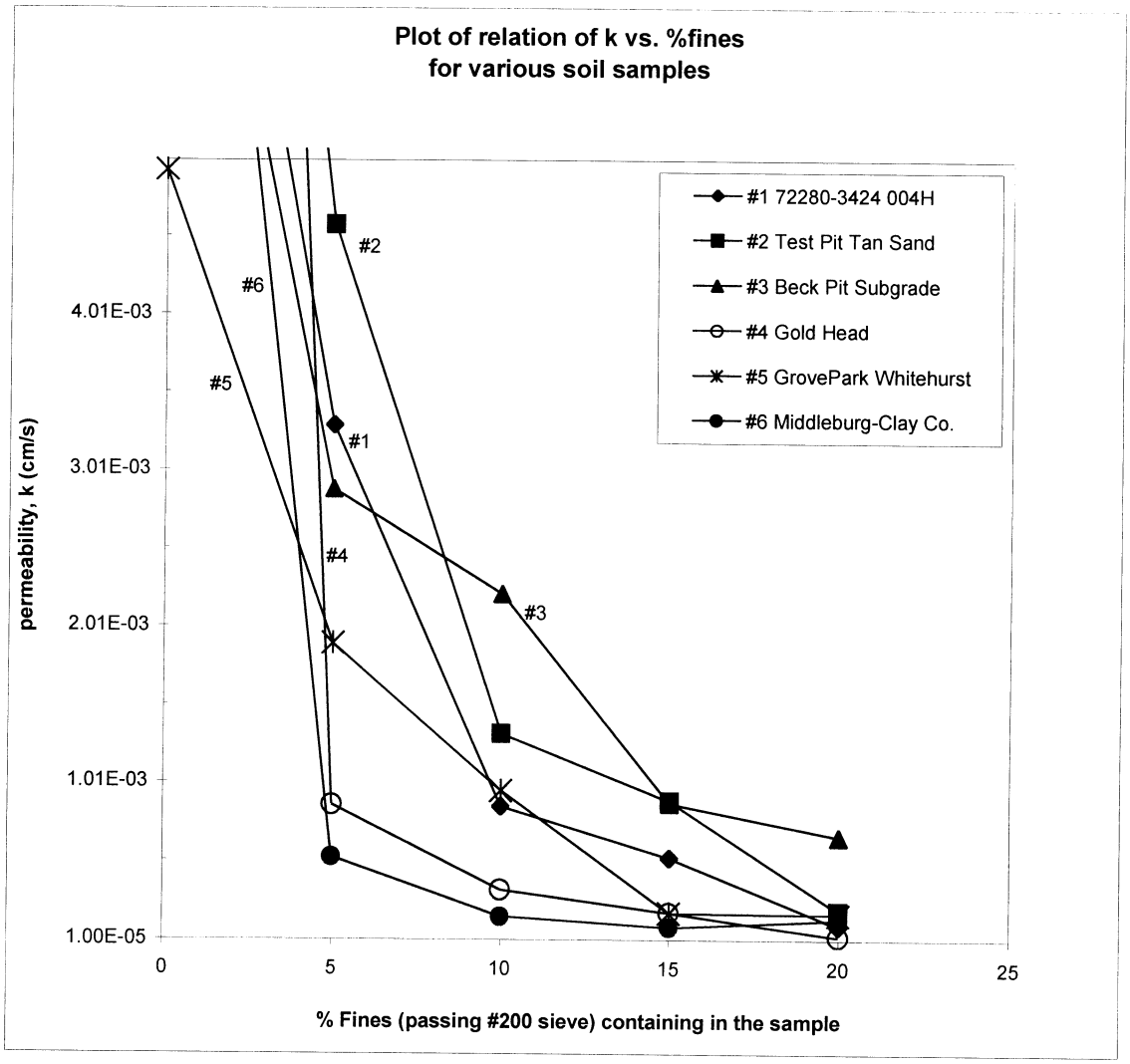

Figure 2-3. Permeability values from test results of samples with various %fines.

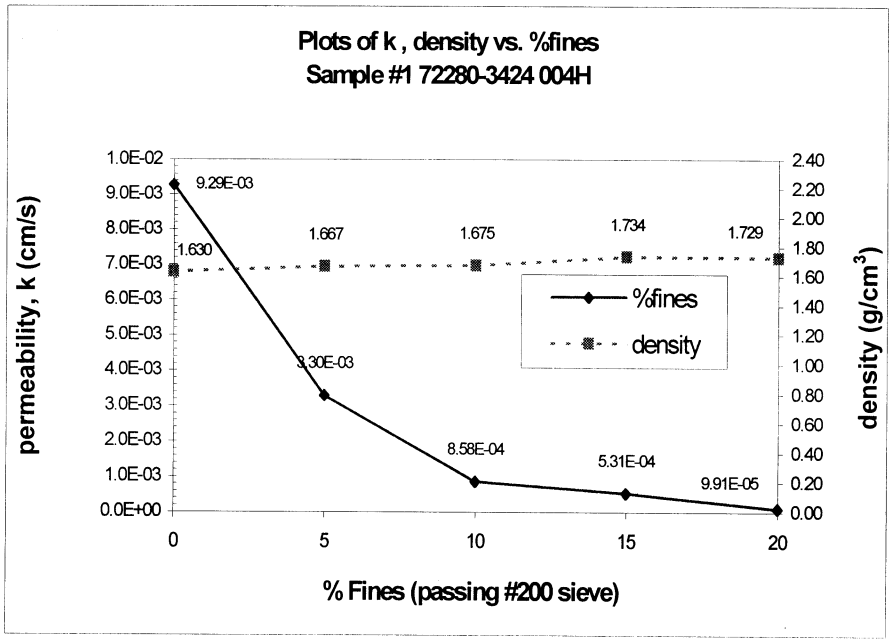

Figure 2-4(a). Permeability and density values for sample # 1.

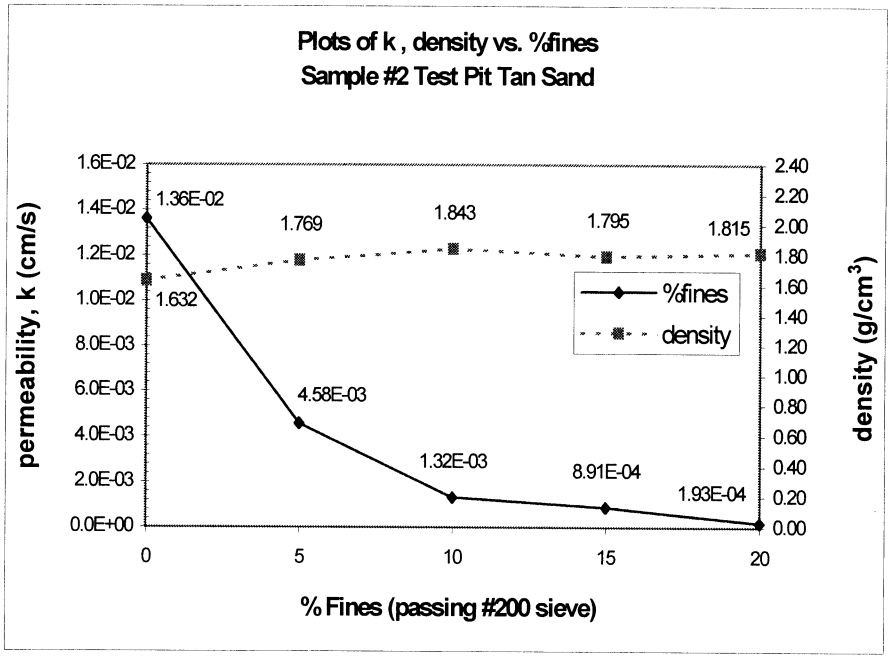

Figure 2-4(b). Permeability and density values for sample # 2.

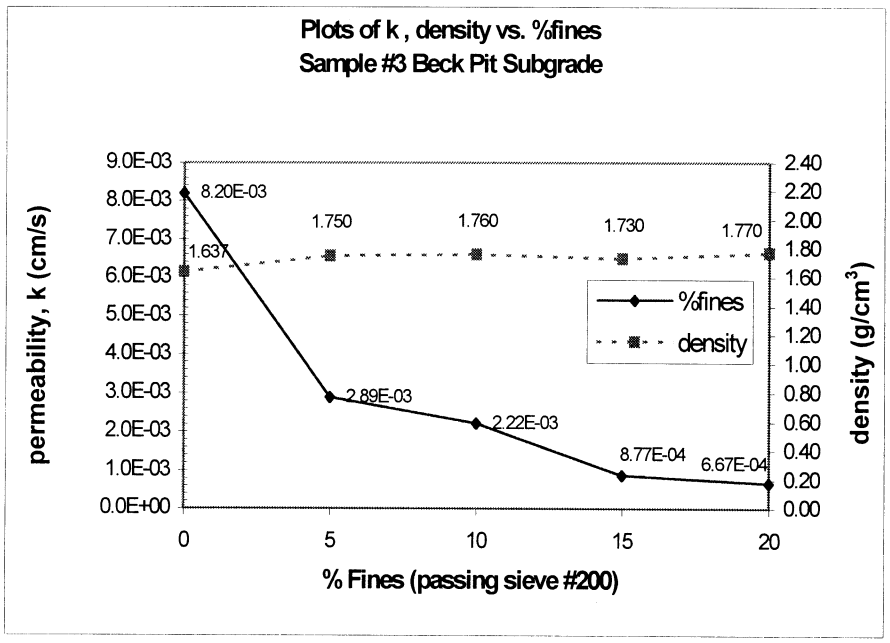

Figure 2-4(c). Permeability and density values for sample # 3.

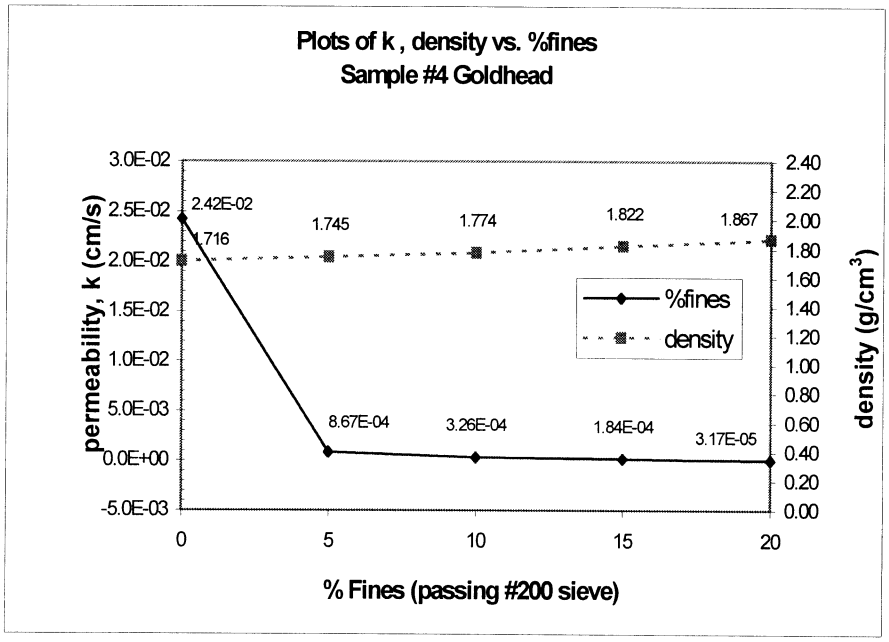

Figure 2-4(d). Permeability and density values for sample # 4.

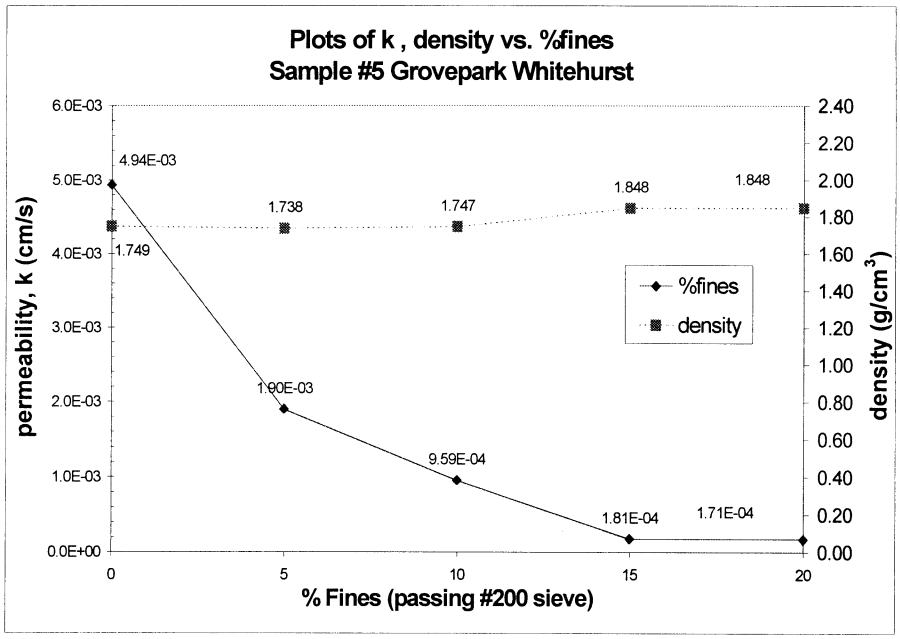

Figure 2-4(e). Permeability and density values for sample # 5.

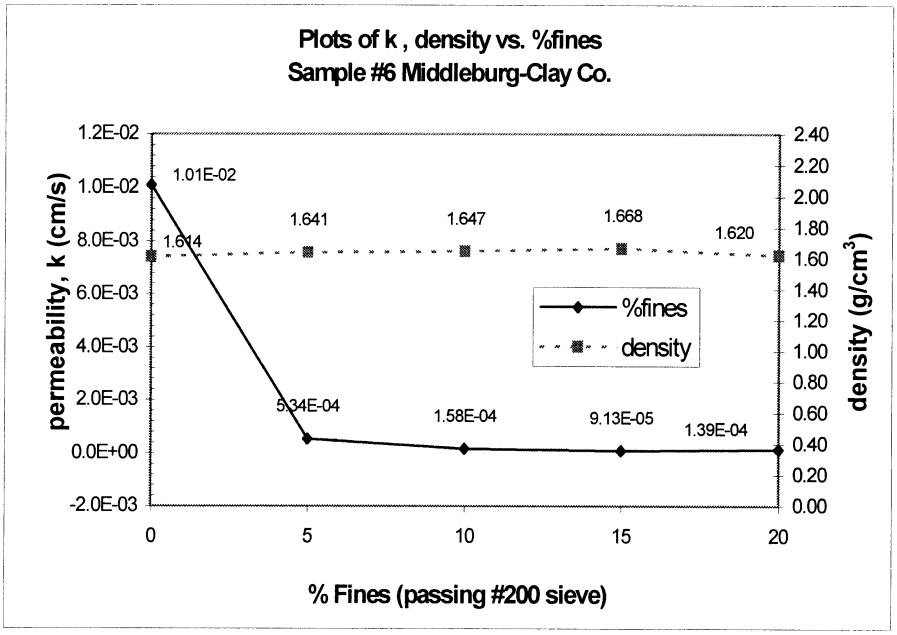

Figure 2-4(f). Permeability and density values for sample # 6.

Density and Permeability versus %Fines

1. The effect of %fines on the dry density of the samples.

The six samples were compacted in the cylinder containers using hand-tamping efforts. The density of the samples prepared by hand effort [Figs. 2-4(a through f)] is within reasonable variance of the density of the samples in Table 2-1. The energy of the compaction effort, however, varied slightly for each sample, thus affecting the dry density. Considering the relationship between the %fines and the dry density (γ_d) of each sample, the density tends to increase slightly as the %fines increase. This is true because the fine particles fill the voids between the larger particles, resulting in greater sample densities.

2. The effect of %fines on permeability.

The addition of fine material to the samples increased their densities, thus reducing the effective pore volumes. As a result, a reduction in permeability was observed. In the '% fines vs. permeability' plots for the six samples, the permeability declines rapidly as the % fines increased from 0% to 5%. However, further reduction is minor between 5% to 20% fines. Therefore, for the soils tested, once 5% fines content is reached, further reduction in k appears minimal.

The average permeabilities, density values, and standard deviations of the six samples are summarized in Table 2-2 and Fig. 2-5.

Table 2-2. Average permeability and density of the six samples and their standard deviations.

% Fines	0		5		10		15	
	AVG.	STDEV.	AVG.	STDEV.	AVG.	STDEV.	AVG.	STDEV.
γ dry, (g/cm^3)	1.663	0.055	1.719	0.051	1.741	0.071	1.766	0.067
k (cm/s)	1.25E-02	7.53E-03	2.45E-03	1.62E-03	1.02E-03	7.84E-04	4.82E-04	3.81E-04

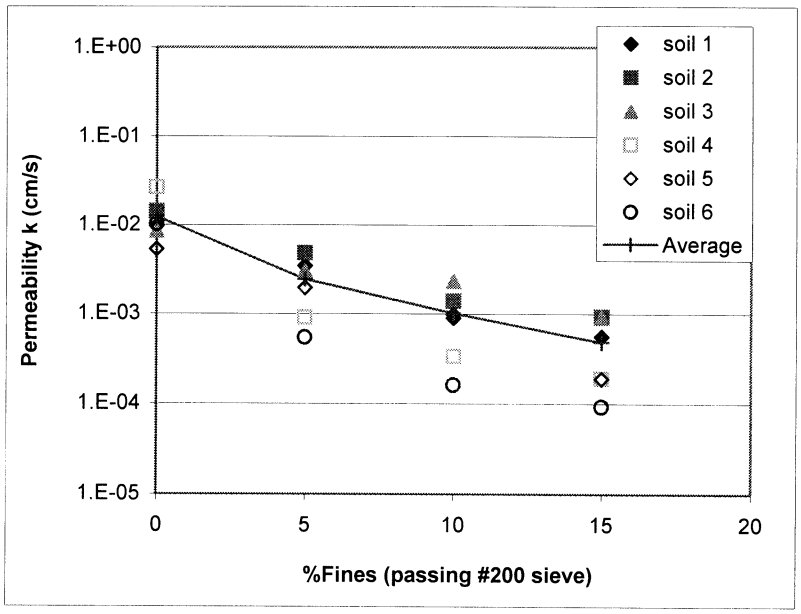

Figure 2-5. Average permeability of the six samples vs. %fines content.

Water-retention Properties

The SOILPROP program (Brooks-Corey) was executed to estimate the water-retention parameters of the six samples. The output lists the saturated volumetric water content θ_s (equivalent to porosity n, i.e., volume of voids divided by total volume), residual volumetric water content θ_r, pore-size distribution index λ and air-entry head ψ_a. The input includes the grain-size distribution from a sieve analysis and the bulk density, or dry density, corresponding to each %fines level. The input was obtained from the same data used in the permeability versus %fines tests. In general, SOILPROP first fits the VG (van Genuchten) soil-water retention parameters. It then converts them into equivalent Brooks-Corey parameters (Ref. from SOILPROP manual p.11). The conversions were performed using the optimum match point, based on the method of Lenhard, et al (1989). Following this conversion, an average was found for different %fines content of all samples. The final results include the average values of the Brooks-Corey parameters (θ_s, θ_r, λ, ψ_a), the average dry density, and the average permeability

from the constant head permeability test for each %fines. The results are summarized in Table 2-3 and Figs. 2-6 and 2-7.

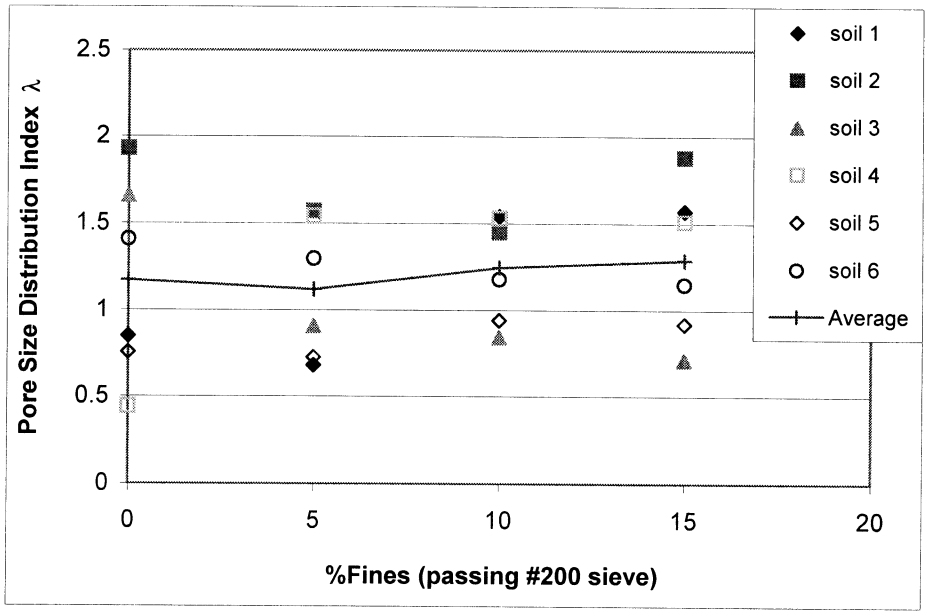

Figure 2-6. Pore-size distribution index vs. %fines from SOILPROP.

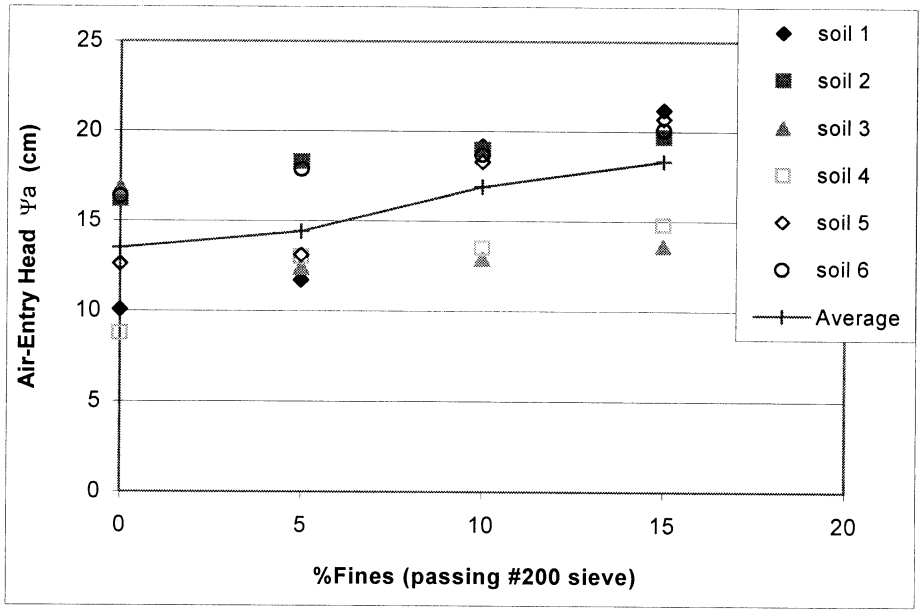

Figure 2-7. Air-entry head vs. %fines from SOILPROP.

Table 2-3. Summary of averages and standard deviations of the six samples vs. %fines.

% Fines	0		5		10		15	
	AVG.	SD.	AVG.	SD.	AVG.	SD.	AVG.	SD.
γ dry, (g/cm^3)	1.663	0.055	1.719	0.051	1.741	0.071	1.766	0.067
k, (cm/s)	1.25E-02	7.53E-03	2.45E-03	1.62E-03	1.02E-03	7.84E-04	4.82E-04	3.81E-04
θ_s	0.373	0.021	0.352	0.019	0.345	0.028	0.333	0.027
θ_r	0.002	0.004	0.002	0.002	0.014	0.019	0.026	0.019
λ	1.175	0.579	1.121	0.401	1.248	0.306	1.291	0.439
Air-entry head ψ_a, (cm)	13.49	3.52	14.40	2.91	16.93	2.91	18.35	3.28

As can be seen from the data, as the % fines increase, the air-entry head also increases, resulting in a higher capacity rise in the soil.

As described in SOILPROP user's manual, the estimation of these parameters saves time and effort by eliminating the need to perform laboratory calibration tests. However, without these tests, the accuracy of the parameters is reduced. Rawls, Brakensiek and Miller (1983) determined average values for the soil-water characteristic parameters by testing approximately 1,200 types of soil (5,000 horizons) from 34 states. Their data include the following: detailed profile descriptions, particle-size distribution, bulk density, total porosity, clay mineralogy, chemical data, and 5 to 10 water retention values covering a range of matrix potentials from 160 to 15,300 cm. The average soil-water parameters in their report were presented in the Green-Ampt assumption format, as shown in Table 2.4.

The Green-Ampt parameters were calculated from the estimated Brooks and Corey constants as follows:

The wetting front capillary pressure ψ_f, $\psi_f = \frac{2\lambda + 3}{2\lambda + 2}\left(\frac{\psi_a}{2}\right)$

The Green-Ampt effective porosity θ_e, $\theta_e = \phi - \theta_r$

where ϕ equals the total porosity and is also equivalent to θ_s, the saturated volumetric water content. This equivalency between the total porosity ϕ and the saturated volumetric water content θ_s is reasonable since all the available pores are filled with water.

$$\therefore \theta_e = \theta_s - \theta_r$$

This equation represents the maximum amount of drainable water that can be removed by a large suction head. The other symbols were previously described in the Brooks-Corey equation.

The Brooks-Corey parameters from SOILPROP were transformed into the Green-Ampt-parameter format in order to compare the SOILPROP results with the recorded database. The basic and transformed values are summarized in Table 2.5. The transformed Green-Ampt values from SOILPROP are within the range of recorded values from the Rawls, Brakensiek and Miller study. This correlation indicates that the SOILPROP program does a reasonably good job of estimating the required input values for Subdrain. Note that the values of θ_e in Table 2.4 and the values of N_e and n_d in Tables 1-2 and 1-3 are different. This is due to the fact that N_e / n_d values are based on gravity drainage conditions, while the θ_e values are determined via the application of a large suction head.

The soil properties obtained from the laboratory tests and from the software runs will be used as input data for further analyses in subsequent chapters.

Table 2.4. Green-Ampt parameters according to Rawls, Brakensiek and Miller (1983).

Soil Class	Porosity, ϕ	Green-Ampt Effective Porosity, θ_e	Wetted front capillary pressure, ψ_f (cm)	Permeability, k (cm/s)
Sand	0.437 (0.374-0.500)	0.417 (0.354-0.480)	4.95 (0.97-25.36)	3.27×10^{-3}
Loamy sand	0.437 (0.363-0.506)	0.401 (0.329-0.473)	6.13 (1.35-27.94)	8.3×10^{-4}
Sandy loam	0.453 (0.351-0.555)	0.412 (0.283-0.541)	11.01 (2.67-45.47)	3.0×10^{-4}

The numbers in parentheses below each parameter are ± one standard deviation of the parameter value.

Table 2.5. Water retention parameters from SOILPROP and Green-Ampt transformed values.

Properties	Average values from SOILPROP			
	0% Fines	5% Fines	10% Fines	15% Fines
γ dry, (g/cm^3)	1.663	1.719	1.741	1.766
k, (cm/s)	1.25E-02	2.45E-03	1.02E-03	4.82E-04
θs, ϕ	0.373	0.352	0.345	0.333
θr	0.002	0.002	0.014	0.026
λ	1.175	1.121	1.248	1.291
Air-entry head ψ_a, (cm)	13.49	14.40	16.93	18.35
Green-Ampt transformed values				
$\theta_e = \phi - \theta_r$	0.372	0.350	0.331	0.308
wetting front capillary ψ_f, (cm)	8.30	8.90	10.35	11.18

Soil Properties Summary

1. The soil samples obtained from the FDOT are classified as fine to medium sand. They will be used to represent typical Florida subbase material in subsequent chapters.
2. The hydraulic properties, such as the permeability and the water-retention properties (θ_r, λ, ψ_a) of these samples were found to depend on grain-size distribution and dry density.
3. The grain-size distributions of the samples are similar to each other. The only major variation is in the %fines. With the same level of compactive effort, the dry density depends to a large extent on the %fines in the sample.
4. The soil properties of the samples prepared with different %fines compositions show that there is a threshold amount of fines (for the samples tested ~ 5%) in which the permeability remains relatively constant up to 20%.

Chapter 3 Joint Infiltration of Rigid Pavement Systems

Introduction

For this study, joint infiltration is based on the water entering only through longitudinal and transverse joints. It uses common units of $ft^3/day/ft$ or $cm^3/day/cm$, and its maximum value occurs during steady state conditions. An average rate is typically used in highway sub-drainage design to determine the amount of water that must be removed expeditiously. A section is designed to consequently drain the infiltrated water through the subbase layer to the side drains and out through the collecting pipe. The average joint infiltration rate is then applied to determine the amount of water draining from beneath the pavement. This figure is needed to determine both the geometry and necessary material properties of the subbase layer, and to design the size and layout of the side drain and collecting pipe. A reasonable joint infiltration rate will not only lead to effective sub-drainage which protects the pavement from water-induced distress, but also economizes pavement costs. A typical rigid pavement section is shown below.

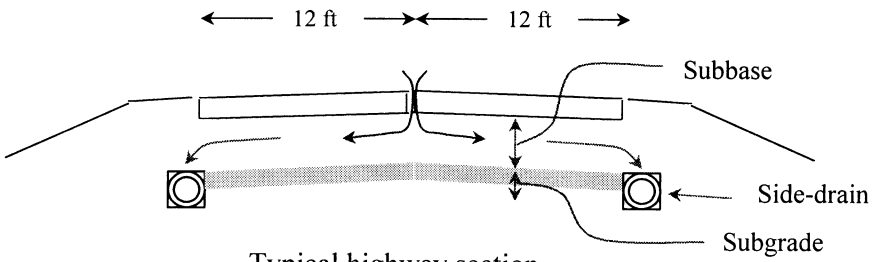

Typical highway section

Methods For Determining a Joint Infiltration Rate

The following three methods for determining joint infiltration rates were used in this study:

1. *conventional equation*
2. *SEEP/2D computer program*
3. *MODFLOW computer program*

These three methods were used to obtain the joint infiltration rates based on input data which includes a 12-ft drainage path, a 10-in. thick pavement, a subbase with $1x10^{-3}$cm/s permeability and 0% subgrade slope, and variety of subbase thicknesses ranging from 0.5-ft to 3-ft. Figure 3-1 shows the typical output plot from SEEP/2D. Figure 3-2 presents all three methods and indicates that the results for a subbase thickness range between 0.5-ft and 2-ft produces similar rates. Also from the plot, SEEP/2D produces slightly lower infiltration rates than the other two for thicknesses greater than 1.5-ft. The rates shown in this figure and throughout this section are based on a 12-ft sectional model. In actuality, the longitudinal joint is at the middle of a 2-lane, 24-ft pavement. Thus, water can drain to either side, which doubles the infiltration rate. Since SEEP/2D is more user friendly and can account for various input parameters, it was used for the parametric sensitivity analyses.

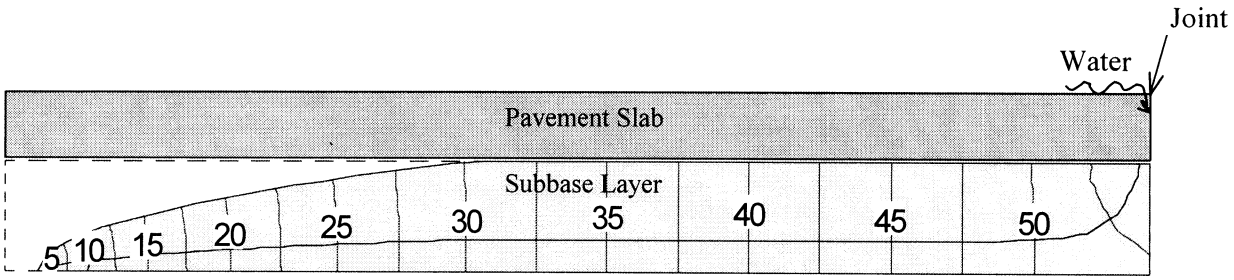

Figure 3-1. Flow net and two-dimensional section from SEEP/2D. The numerical notations express the equipotential head values in cm.

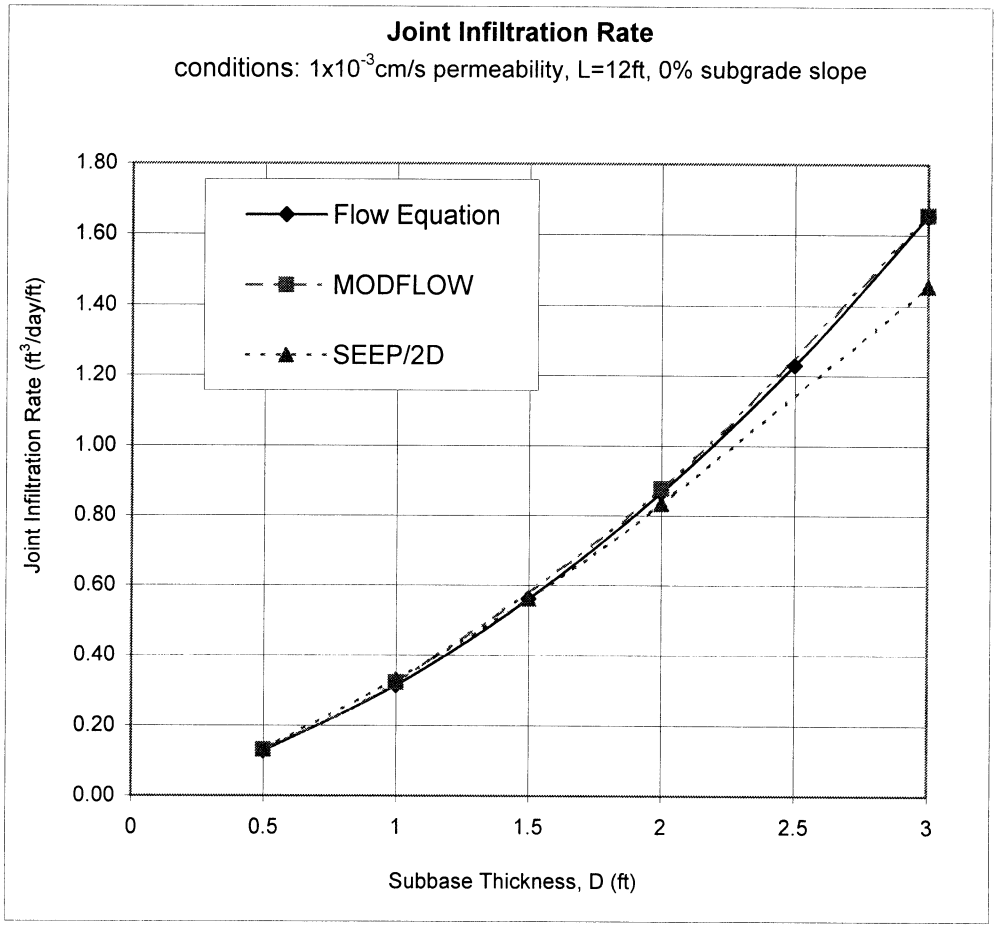

Figure 3-2. Joint Infiltration rates from the three methods: confined/unconfined flow equations, SEEP/2D and MODFLOW.

Parametric Sensitivity on Joint Infiltration Rate

The joint infiltration rate is dependent upon the sectional geometry and the material properties of the subbase. Analyzing parametric sensitivity helps explain the effect that each of the parameters has on the joint infiltration rate. This study was performed by determining the joint infiltration rate corresponding to variations in a single parameter while all others are held constant. The relationship between the joint infiltration rate and each parameter is observed and analyzed in the following sections.

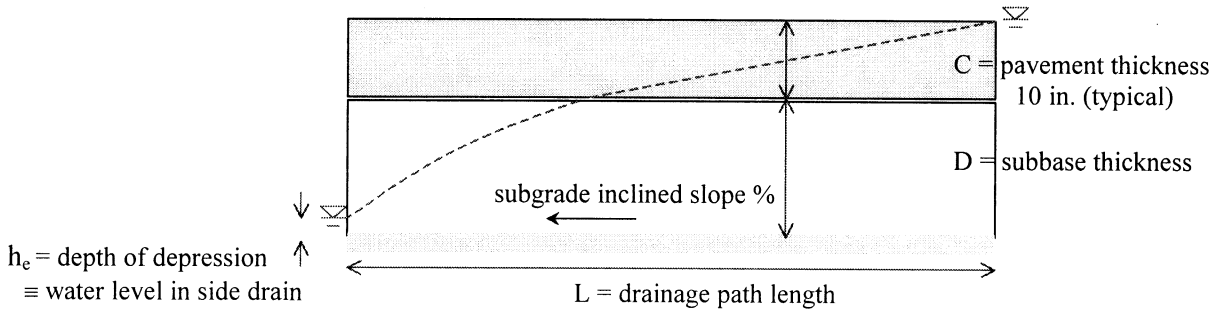

Joint Width

A small cracked slab model with no underlying soil was constructed to determine the amount of water that could flow through a small opening. The width of the joint was varied by adjusting two threaded rods at both ends of the slab, as shown in the drawing on the next page. It was found that a 1-mm wide opening producing a joint infiltration rate of 39 ft^3/day/ft was required before water began accumulating above the joint. The addition of an underlying coarse sand layer resulted in an inflow rate of 22 ft^3/day/ft before standing water was observed. Finally a kaolinite clay layer was used as a subbase material and no water entered the joint. These test values indicate that the width of the joint has a minor effect on the amount of water flowing

through the joint. Of course, a wider joint will produce correspondingly larger flows; however, it appears that even differences of several millimeters will not produce a 0.7 ft^3/day/ft joint infiltration rate (the recommended value specified by the FHWA). Thus, it is reasonable to assume that the underlying material characteristics and the sectional geometry are the principal factors in determining the joint infiltration rate.

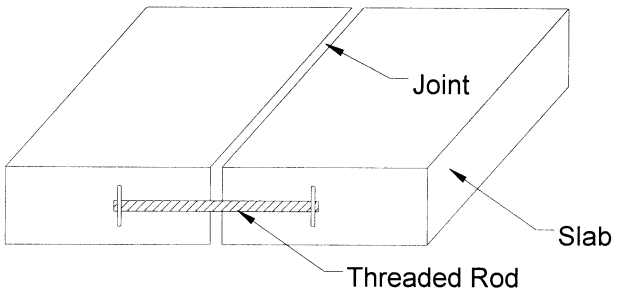

Above: Representation of the cracked slab adjustable joint width model

Permeability of Subbase

In the combined flow equation for a subbase with a 0% subgrade slope,

$$Q = \frac{k}{2L}(2CD + D^2 - h_e^2)$$

According to this equation, the infiltration rate (Q) is linearly proportional to the permeability of the subbase material. This relationship may also be interpreted from the plot in Figure 3-3. Frequently the infiltration rate and the permeability are referred to in the combined form of "*q/k*" to reduce the parameters to a common form. This linear relationship is valid only for steady-state flow conditions. The drainage time analysis (mentioned previously), is a non-steady-state flow condition, and hence permeability is no longer linearly proportional to the drainage time. The detail of this relationship will be discussed in Chapter 4.

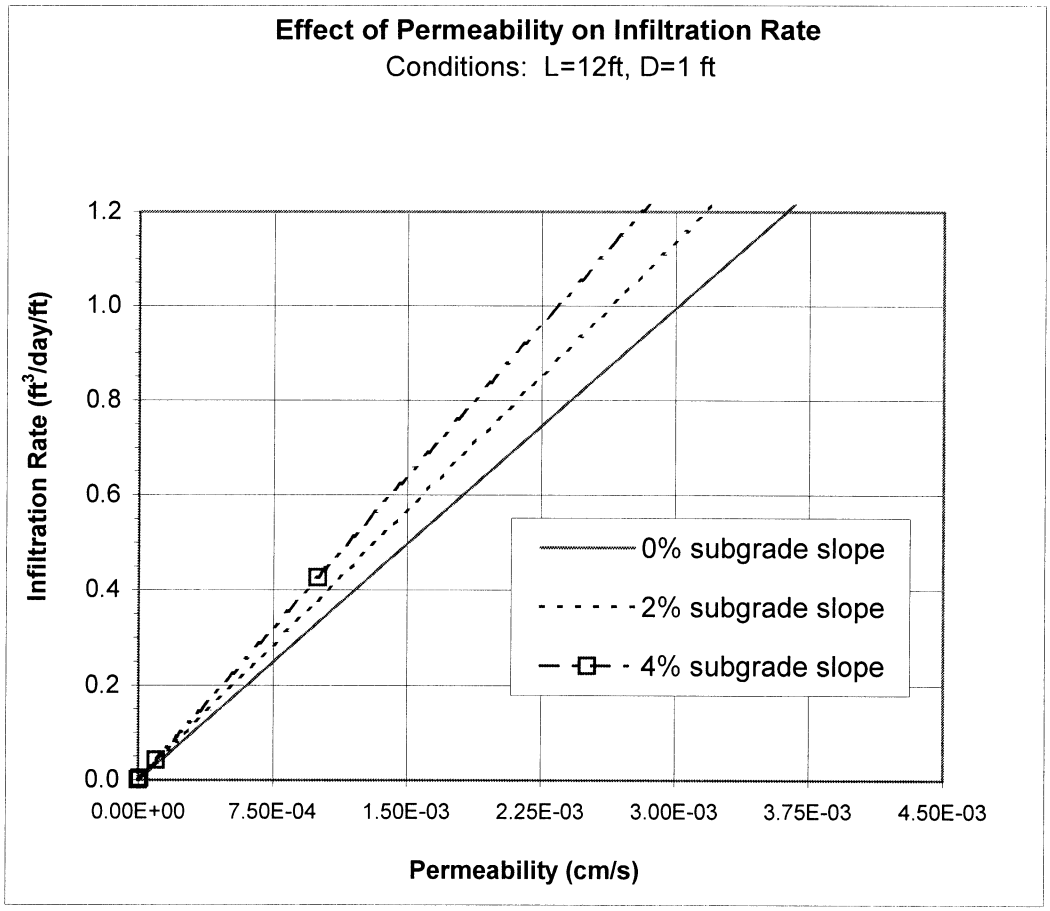

Figure 3-3. Effect of permeability on joint infiltration rate for three subgrade slopes.

Subgrade Slope

This analysis was performed by varying the subgrade slope from 0% to 4% while maintaining the following parameters constant: $1x10^{-3}$ cm/s permeability, 12-ft drainage distance, and 1-ft or 2-ft subbase thickness. A linear relationship was found between changes in infiltration rate (ΔQ) and changes in the subgrade slope (Δs), with $\Delta Q/\Delta s = 0.0365$ ft^3/day/ft/% and $\Delta Q/\Delta s = 0.0238$ ft^3/day/ft/% for 2-ft and 1-ft subbase thicknesses, respectively. The results are depicted in Fig. 3-4.

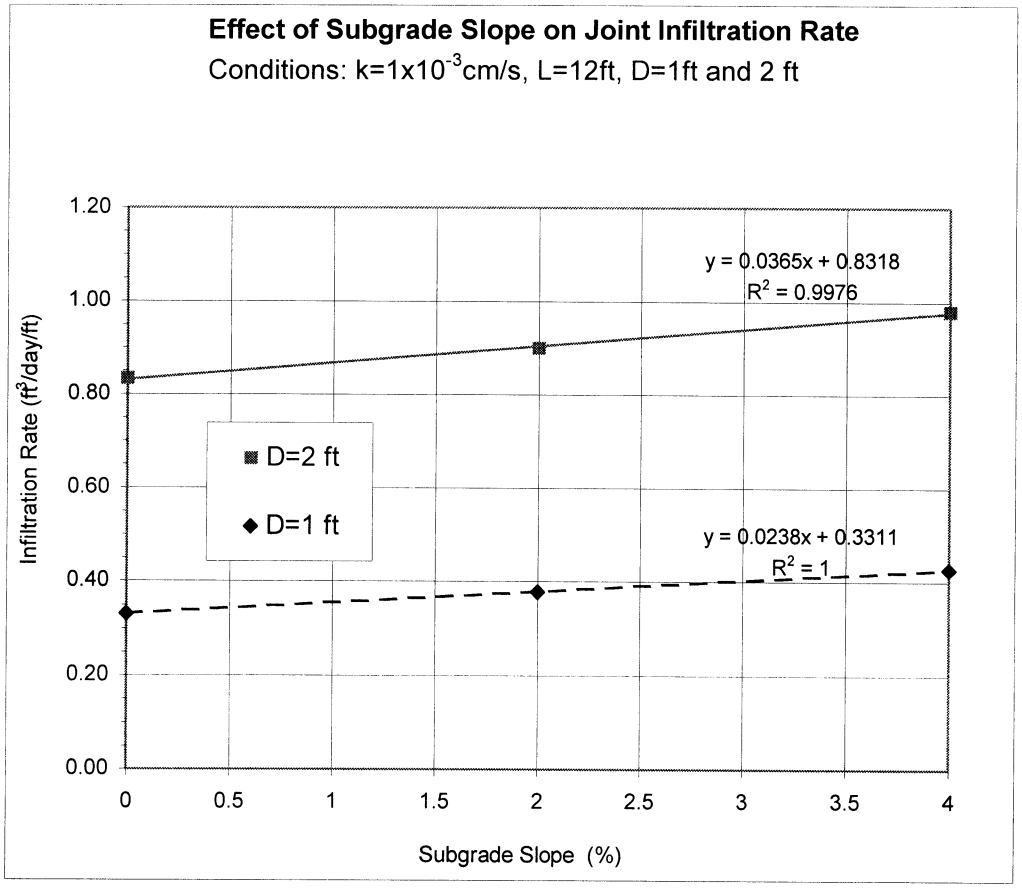

Figure 3-4. Joint infiltration rate as a function of the subgrade slope.

Subbase Thickness

Figure 3-5 is a plot of joint infiltration versus subbase thickness with other parameters held constant, (e.g., 12-ft drainage path, 10-in. thick pavement, $1x10^{-3}$cm/s permeability and 2% subgrade slope). The plot reveals the parabolic relationship between the infiltration rate (Q) and of the subbase thickness (D). Moreover, the flow equation,

$$Q = \frac{k}{2L}(2CD + D^2 - h_e^2),$$

confirms this relationship and its parabolic shape. (Eq'n referenced from derivation on page 8)

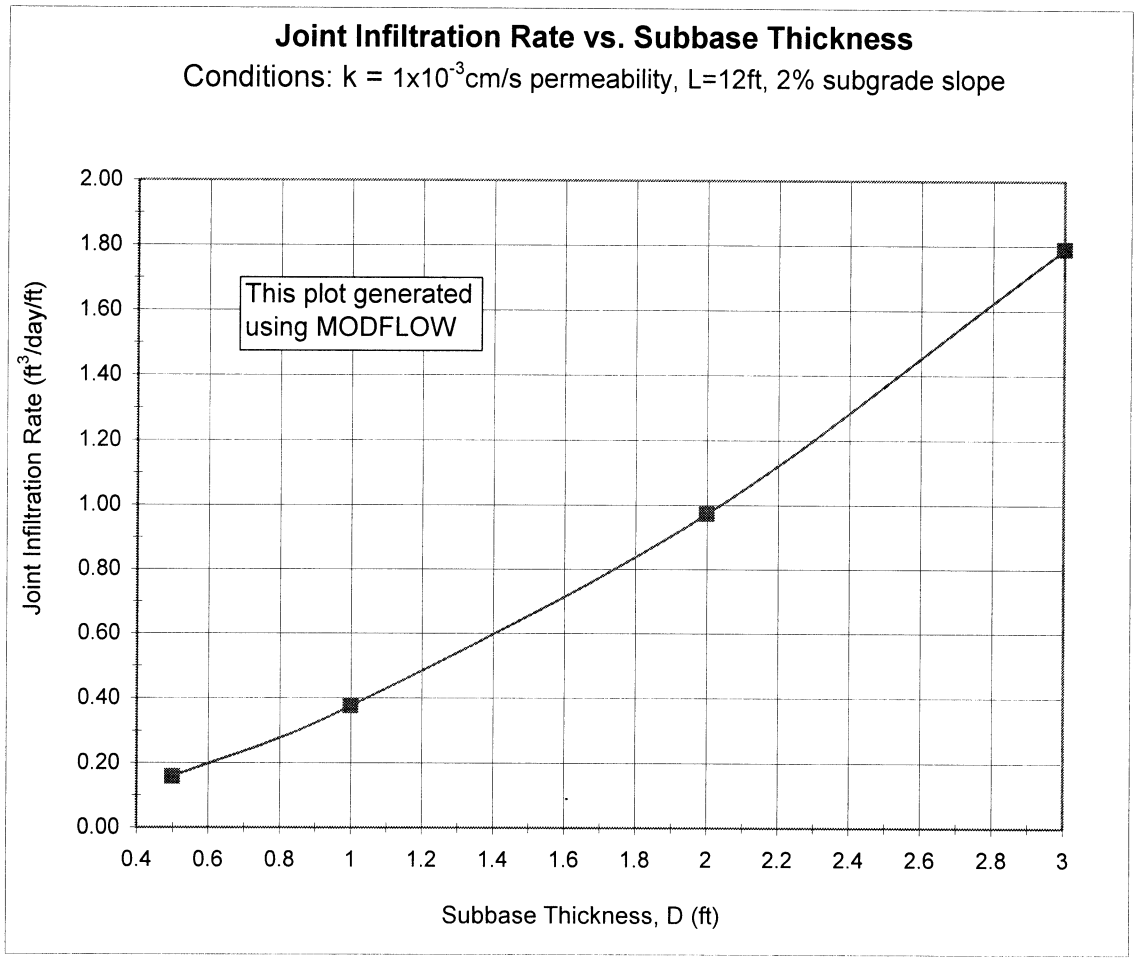

Figure 3-5. Joint infiltration rate as a function of subbase thickness.

Drainage Length

The joint infiltration rates stated in previous sections are analyzed based on a 12-ft wide portion of slab. Therefore, the drainage distance is 12 feet. This is true a for two-lane roadway, which contains two 12-ft wide slabs gently sloping away from the centerline where they meet. For pavement containing three or four traffic lanes, a section consists of two portions of 12-ft wide slabs. Water infiltrates through the joint at the centerline and at the joints between lanes. Therefore, the modeled section must include these two portions of pavement in the steady-state analyses. The results will then include the joint infiltration rates of both joint locations. In this study, the joint infiltration rates of single slab and multi-slab portions were analyzed by two-dimensional MODFLOW. The results are tabulated in Table 3-1.

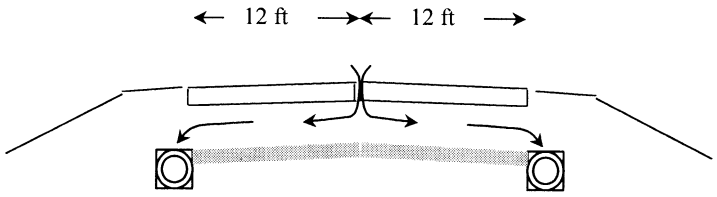

Two-lane Section

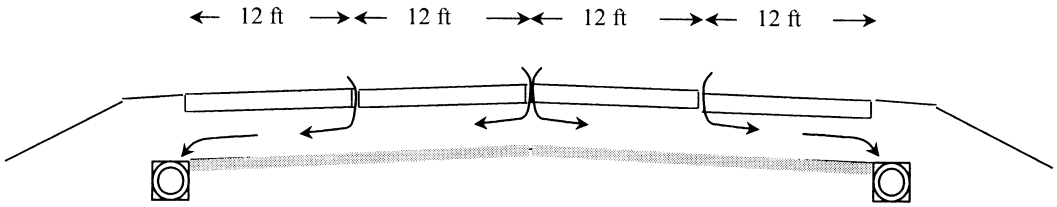

Four-lane Section

Table 3-1. Joint infiltration rates as the result of multi-slab sections.

	Joint infiltration rate	Conditions
12-ft width 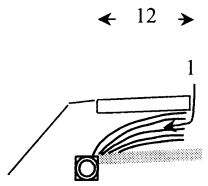	# 1. = 0.942 ft^3/day/ft	2.5x10^{-3}cm/s permeability 1-ft subbase thickness 2% subgrade slope 10-in. slab thickness
24-ft width 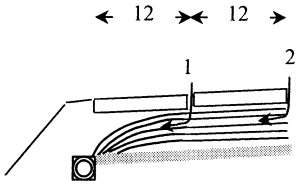	# 1 = 0.942 ft^3/day/ft # 2 = 0.139 ft^3/day/ft	
36-ft width 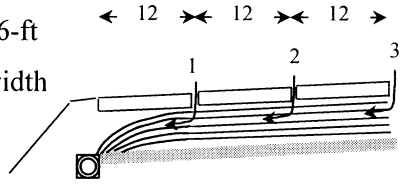	# 1 = 0.942 ft^3/day/ft # 2 = 0.139 ft^3/day/ft # 3 = 0.139 ft^3/day/ft	

The joint infiltration rate of the outermost slab (slab 1) is typical for all three cases. Therefore, the drainage distance due to the addition of slabs has no effect on the joint infiltration rate of the outer one. However, the infiltration rates of the interior slabs (2 and 3) are equivalent but at a reduced rate, a rate based on Darcy's equation with the subgrade slope as the gradient. The flow in sections 2 and 3 are lower than 1, because 1 has a shorter distance to the outlet therefore the gradient in 1 is greater.

Darcy's equation: $Q = k\,i\,A$

$Q = (2.5\text{x}10^{-3}\text{cm/s})(0.02)(30\text{cm}) = 0.0015\ \text{cm}^3\text{/sec/cm}$

$Q = (0.0015)(24\text{x}3600/30.48^2) = \underline{0.1395}\ \text{ft}^3\text{/day/ft}$

where i = Δ H / L, k = permeability, and A = subbase thickness times a unit width

Flow Characteristics of Joint Infiltration

1. Flow Pattern of Infiltrated Water

In actual situations, water can infiltrate through both longitudinal and transverse joints. The two-dimensional simplifications—SEEP/2D and the conventional equation—were only concerned with joint infiltration through longitudinal joints, wherein the effects of transverse joint infiltration was neglected. This assumption is workable on a continuous reinforced concrete pavement or on a jointed reinforced concrete pavement with wide transverse-joint spacing. The graphical output from MODFLOW in Figure 3-6 shows flow directions and equipotential lines for the total head of infiltrated water from both longitudinal and transverse joints to the subbase layer. Note that the arrows only show the flow direction, and do not represent the magnitude of the flow velocity. Pavement sections of 3.6-m x 6.0-m (trans. x long.) joint spacing and 3.6-m x 9.0-m (trans. x long.) joint spacing were modeled. The pavement consists of a 0.30-m subbase, 0.25-m pavement, 0% subgrade slope, and a $1x10^{-3}$ cm/s subbase permeability.

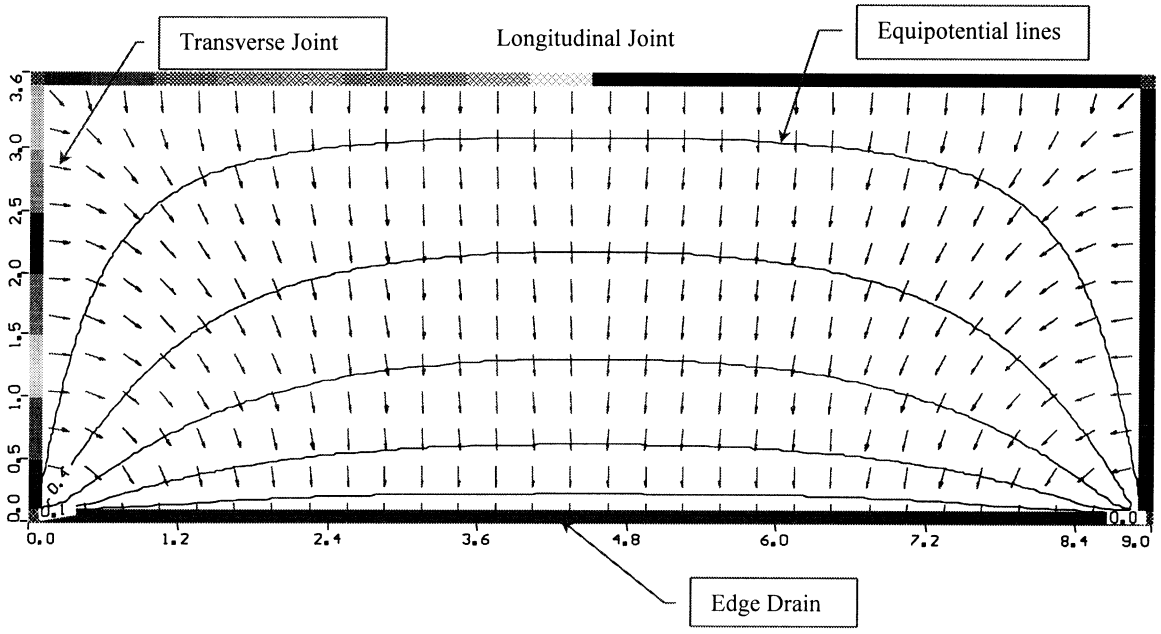

Figure 3-6. Plan view of seepage directions and equipotential lines in the subbase layer.

Considering transverse joint infiltration, the infiltration rate tends to be higher than for the longitudinal joint. This is reasonable because the transverse joint has a shorter average drainage distance than the longitudinal joint. Infiltrating water, therefore, travels from a transverse joint to the side drain in shorter time period than from a longitudinal joint. Results from MODFLOW in Figure 3-7 shows that the transverse joint infiltration rate is indeed higher. The transverse rate ranges from a high of 2.6 ft^3/day/ft at the outside edge of pavement to a low of 0.04 ft^3/day/ft at the innermost point of the pavement. Figure 3-7 also shows that the longitudinal joint infiltration rate increases progressively from 0.04 ft^3/day/ft at the joint-intersection point to 0.3 ft^3/day/ft at the mid-span point. Note that 0.3 ft^3/day/ft is close to the joint infiltration rate from the two-dimensional model (MODFLOW = 0.32 ft^3/day/ft, Flow equation = 0.315 ft^3/day/ft). The flow is lowest at the joint intersection because it has the longest distance to travel and is affected by both the transverse and longitudinal flow.

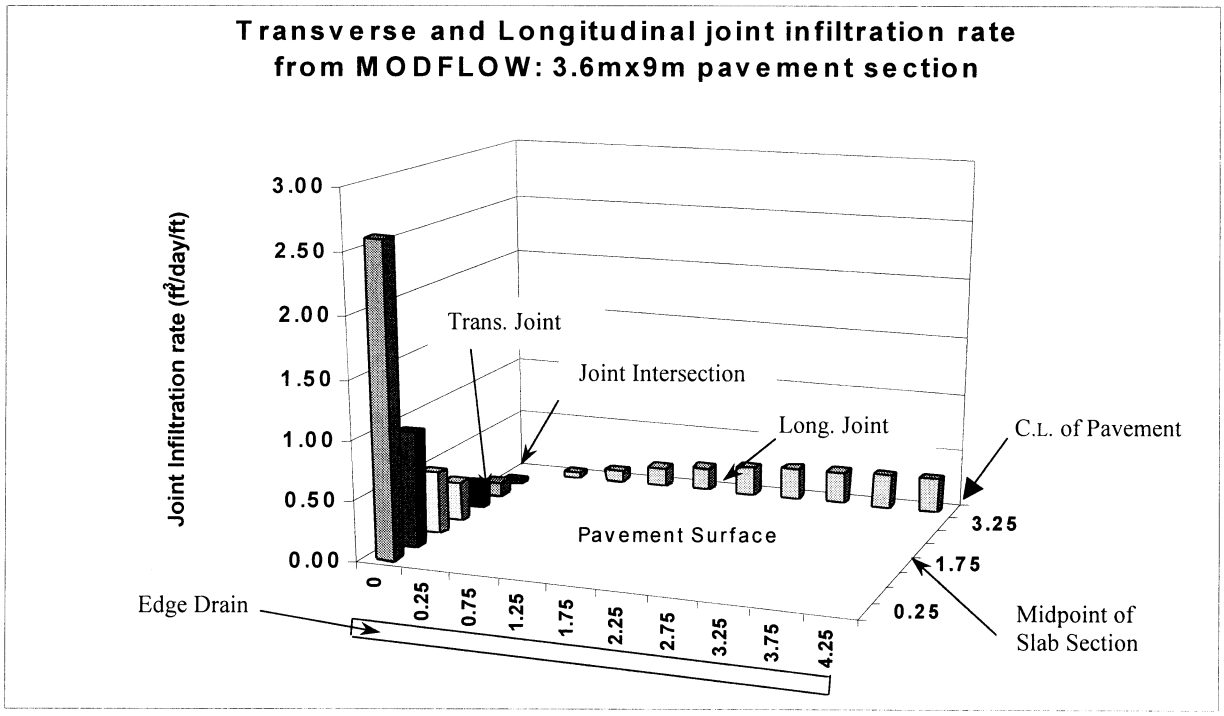

Figure 3-7. Joint infiltration rates at points along the transverse and longitudinal joints.

In long transverse joint spacing, the longitudinal joint infiltration rate converges, from the lowest rate at the joint-intersection point, to a steady rate somewhere in the middle part of the longitudinal joint. The magnitude of the longitudinal infiltration rate is a function of the distance from the joint-intersection point. The maximum longitudinal infiltration rate is approximately equal to the joint infiltration rate computed from the two-dimensional solution.

2. Degree of Saturation Area Under Pavement

Figure 3-8 shows a graphical output containing the equipotential lines based on the following pavement section properties input into MODFLOW:

- Pavement thickness = 0.25 m
- Subbase thickness = 0.30 m
- Constant water head through pavement joint and subbase = 0.25 m + 0. 30 m = 0.55 m
- Subgrade slope = 0%
- Pavement dimensions = 3.6 m x 6.0 m
- Permeability of subbase material = $1x10^{-3}$ cm/s

Since the top level of the subbase material is located at the 0.30-m elevation point (zero elevation at the subgrade level), the 0.30-m equipotential line in Figure 3-8 is the separating line between the saturated (100% saturated) zone and the partially-saturated zone. As can be seen, the saturated zone comprises more than 70% of the total pavement area, and shows that the area immediately surrounding the longitudinal and transverse joints are indeed saturated. This condition makes the transverse joint the most susceptible area to pumping distress. This evidence confirms the initially stated assumption of a fully saturated subbase.

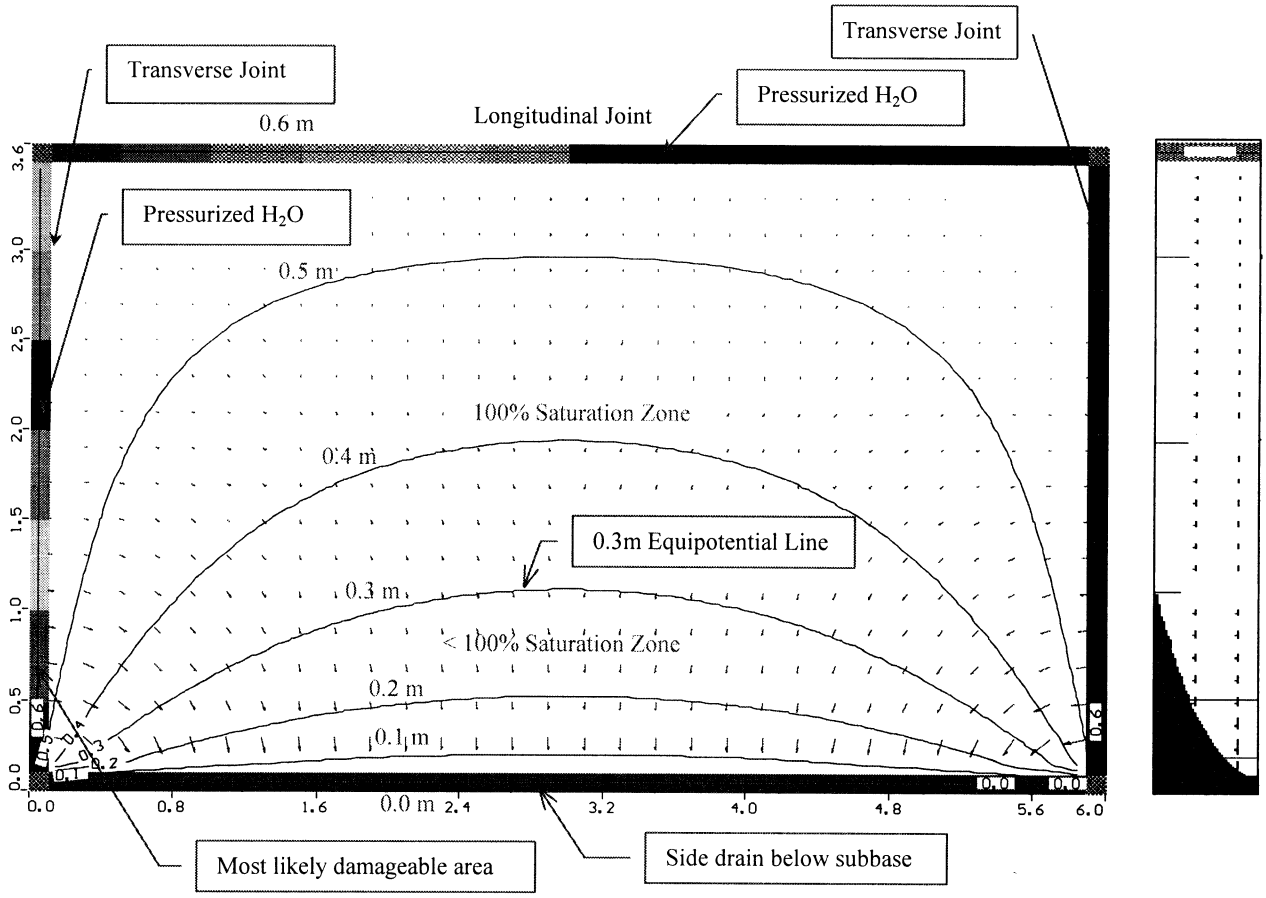

Figure 3-8. Flow velocity vectors and equipotential lines from 0 m to 0.6 m. Plan view: magnitude-scaled velocity vector. Sectional view: transverse cross section at the mid-span.

Concrete Joint Infiltration Field Test

To quantify the infiltration rate of water through concrete joints during a rainfall was one of the objectives of this project. Thus to effectively measure the amount of water flowing into an actual jointed pavement was the next task at hand. A field test for measuring the joint infiltration rate was developed with the idea of simulating infiltration caused by precipitation. By using the concept of the double-ring infiltrometer, a novel joint infiltration test was created to accurately measure the amount of water flowing into a joint. The device is shown in Figue 3-9. To conduct a test, first the selected pavement joint was prepared by a hot glue gun to separate the joint into three partitions as indicated. The lengths of the partitions are set at 18 in. for the left and right ones and 6 in. for the middle partition. Water from the Marriot tank is then applied to each joint section in order to flood the three partitions. Note: A marriot tank produces a constant pressure regardless of the level of water in the tank. The inflow rate of the water into the middle partition is measured using a rotameter flow meter. The two 18-in. side partitions act as water boundaries to keep the water in the middle partition flowing only through the middle projected area. Without these boundary sections, the water from the middle section would flow into the joint and spread out in all directions through the soil mass beneath the joint. This test was designed to test both longitudinal and transverse joints that have edge or side drain systems beneath their shoulders. In order to better analyze the flow and drainage properties of the subbase material it is recommended that a few items be added to the field test: the ability to monitor the water stored in the soil (the water level or piezometric pressure), the obtainment of information on the pavement and subbase geometry, and the testing of the soil's hydraulic properties.

Several infiltration field tests were performed at various sites in Florida. The results of these field tests are tabulated in Table 3-2.

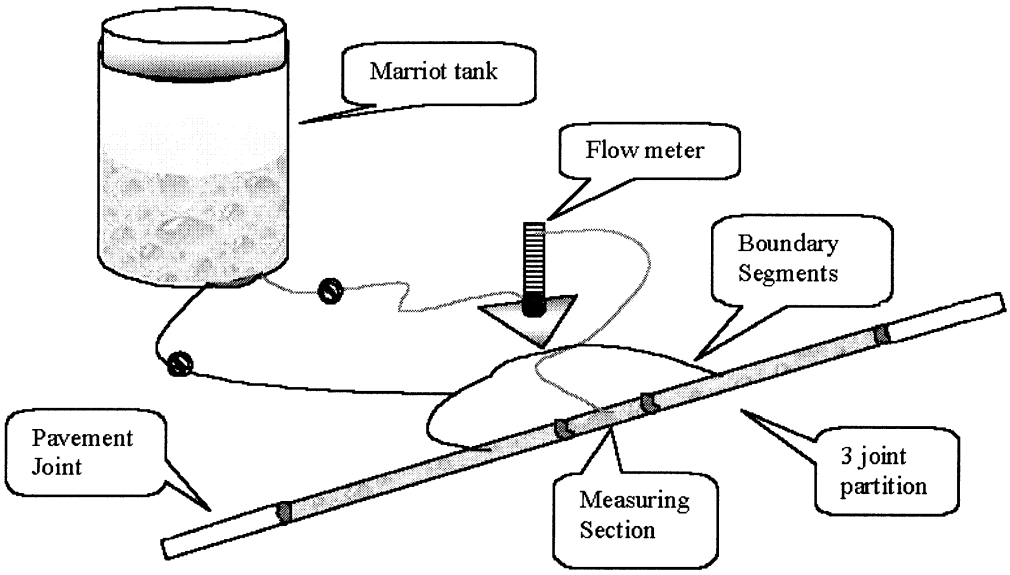

Figure 3-9. Diagram of the joint infiltration field testing device.

Table 3-2. Summary of joint infiltration field test results.

Location	Date of Test	Weather	Time	Joint type	Infiltration Tate (ft3/day/ft)
UF Campus Road	May 20, 1998	Mild	10-2 PM	Transverse	0.186
SR-24 in Waldo, FL. Location #1	Jun 5, 1998	Hot	1-4PM	Transverse	0.516
SR-24 in Waldo, FL. Location #2	Jun 11, 1998	Hot	2:30 PM-4:30 PM	Transverse	0.196 - 0.215
Construction area on I-4 at I-75 junction, Tampa FL. 3 measured parts on the same joint	Aug 27, 1998	Hot	4-5 PM	Transverse	0.61 0.13 0.135
I-75 Northbound between Exit 48 and 49 on 3 locations (#1,#2,#3)	Sep 17, 1998	Mild	2:30 PM 2:30 PM 4-5 PM 5-5:30 PM	Longitudinal Transverse Longitudinal Longitudinal	0.103 (#1) 0.365 (#1) 0.055 (#2) 1.139 (#3)

Compared to the values obtained with MODFLOW, the trend and order of magnitude appeared reasonable.

Relationship Between Infiltration Rate vs. Temperature Effect on Concrete

A typical rigid pavement such as a concrete slab undergoes curling due to changes in temperature. The curling of the slab also affects the infiltration rate through its joint.

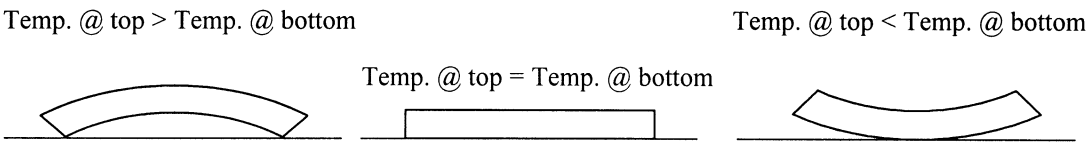

To understand the curling deflection due to temperature difference, an experiment was performed at the FDOT State Materials Lab in Gainesville, Florida. Several spans of jointed concrete pavement equipped with LVDTs and temperature-sensing devices were constructed. The LVDTs were attached at the transverse joints to read the vertical deflections. The temperature-recording devices recorded the temperatures at the top and bottom of each span of pavement. The vertical displacements and temperature readings were recorded periodically during a 24-hr cycle. A sample of the recorded data is shown in Fig.3-10. During the daytime (11am-7pm), the temperature at the top of the slab is significantly higher than at the bottom. At night (11pm-7am), the opposite situation exists. The difference in temperatures forces the pavement to deflect, or as in this case, curl (depicted in the diagram above). As expected, a transition period occurs between night and day. During these periods, the shape of the pavement is not deflected because the temperatures at the top and bottom of the slab are equal.

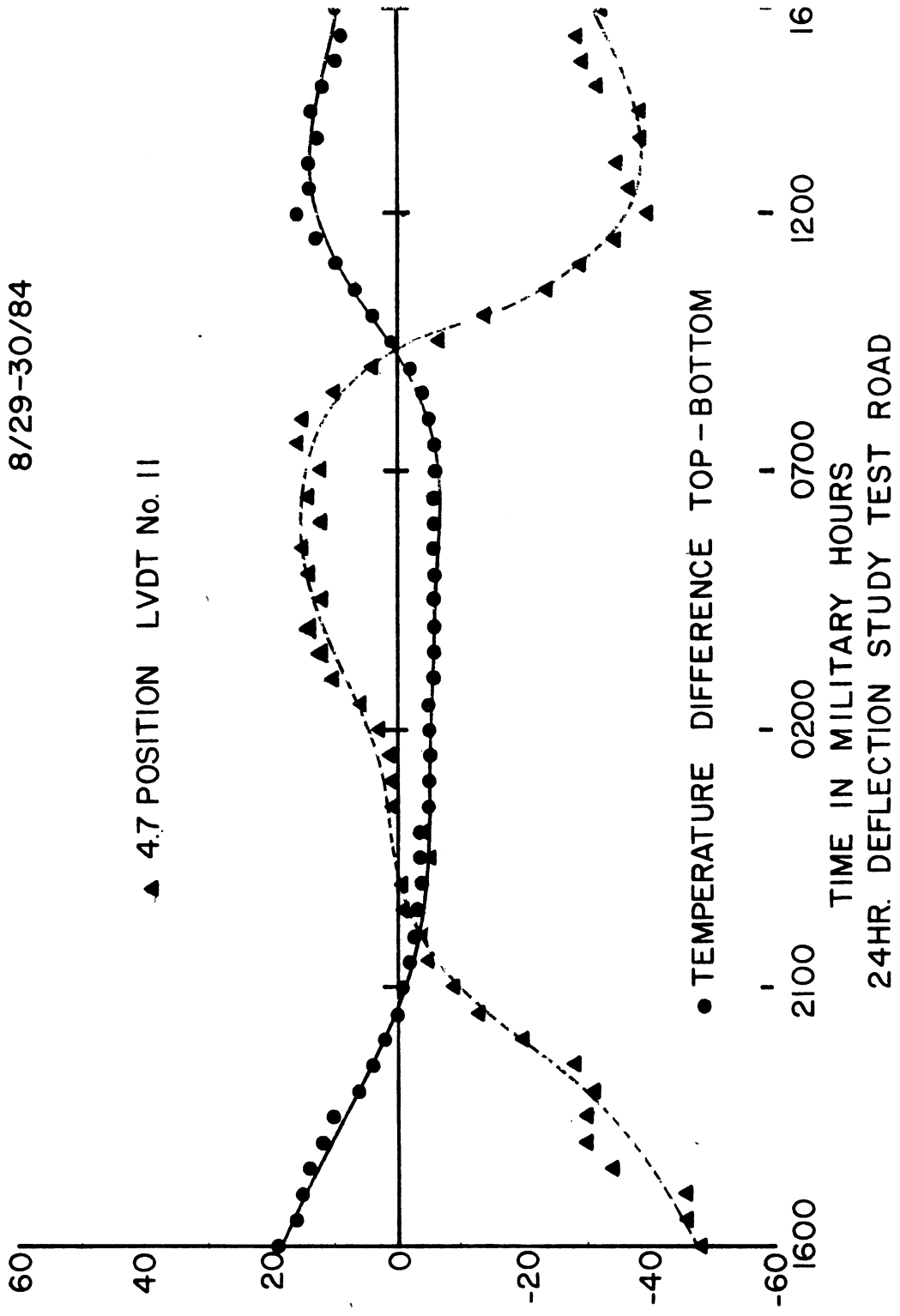

Figure 3-10. Temperature differences and vertical deflections of a tested slab.

[LVDT (deflection sensors) are located at the transverse joint]

Experiment

Once the slab curls upward, more of the base soil's surface area is exposed and more water can then penetrate into the soil. In order to measure this effect on the infiltration rates, a joint infiltration field test was performed on an existing pavement. The test site was a construction area at the junction of I-4 at I-75 near Tampa, Florida. The joint infiltration field tests were performed at three critical times: 5am, 10am and 2pm. These times were chosen to represent the three optimum curling shapes. The five-part test (two testing partitions and three control partitions) was set up on a transverse joint and two data sets were obtained (one data set from each testing partition). The test layout and results are summarized below.

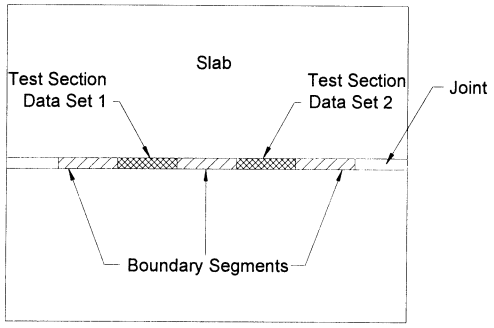

Time	Data Set 1	Data Set 2
5 AM	2.62 ft^3/day/ft	0.92 ft^3/day/ft
10 AM	1.55 ft^3/day/ft	0.45 ft^3/day/ft
2 PM	1.28 ft^3/day/ft	0.33 ft^3/day/ft

Conclusion

The joint infiltration rate was a maximum at 5 AM when the pavement edges were curled up, creating a gap beneath the joint. The infiltration rate had decreased by 10 AM when the slab was level. Finally, the rate reached its minimum value at 2 PM when the pavement edges were curled downward, effectively closing the transverse gap. Voids created by the curling action permit more water to seep directly into the subbase. The greater the amount of free surface area, the

more water that is free to contact the subbase, creating a higher joint infiltration rate. It is also possible that in highways with side drains installed the water may also infiltrate into the transverse joint and seep through the temporary void directly to the side drain at the shoulder of the pavement. This could carry additional fine materials with it exacerbating the situation. The difference in the magnitude of the values between the two data sets may be explainable by variations in the amount of voids directly underneath the test sections.

Realistic Behavior vs. Design Assumption

The joint infiltration rate, from a general point of view, depends on the physical properties of the subbase and the cross-sectional geometry of the pavement system. However, the joint infiltration field test data reveal that other factors influence the rate of joint infiltration. The curling gap due to daily temperature changes, which occurs under a transverse joint, has been verified through testing to have an effect on the joint infiltration rate. Other unverified factors likely to influence the joint infiltration rate include the following:

- Discontinuities of the subbase course, e.g., soil cracks and roots will result in a higher infiltration rate.
- Partially saturated conditions in the subbase will make the unsaturated permeability less than the saturated permeability and will lead to a lower joint infiltration rate. This is because the entrapped air blocks the flow.

These factors cause the field infiltration rate to differ from the estimated infiltration rate, which is obtained from design procedures. They are difficult to monitor and determine. For design purposes, some minor factors are disregarded and assumptions are created to account for the neglected conditions, e.g., assuming a 100% saturation area below the phreatic surface in order to use the saturated permeability value in the calculations.

Joint Infiltration Summary

1. The joint infiltration rate can be determined by applying seepage theory at a steady state to the pavement section.
2. The joint infiltration rate depends on the sectional geometry and the soil property factors. The uncertain factors are disregarded from the analysis, i.e., the slab deflection at the transverse joint due to the temperature gradient.
3. Parametric sensitivity and the corresponding effects on the joint infiltration rate are as follows:
   - Minor joint width fluctuation has a minimal effect.
   - Permeability of subbase ↑, joint infiltration ↑ linearly
   - Subgrade slope ↑, joint infiltration ↑
   - Subbase thickness ↑, joint infiltration ↑ ↑
4. The joint infiltration rate quantitatively ranges from the maximum value at the transverse joint, which has the shortest distance to the side-drain, to the minimum value at the longitudinal-transverse joint intersection. The value at the center portion of the longitudinal joint is approximately equivalent to the value determined by the two-dimensional method.
5. The 0.7 ft^3/day/ft joint infiltration rate recommended by FHWA is an *averaged* value which is applied to calculate the amount of water infiltrating from both the transverse and the longitudinal joints. This amount of infiltrated water is then used to determine the subbase thickness.
6. The joint infiltration rate is equivalent to the rate of water that is drained out through the side drain. If no side drain is present then it is equal to the water that seeps out from the sides of the highway embankment. It also indicates the drainage capability of the pavement section. The joint infiltration rate tends to be proportional with the drainage capability of the

pavement system. The higher the joint infiltration rate, the better the drainability of the pavement.

7. The question of whether the 0.7 ft^3/day/ft is applicable to Florida conditions can be satisfied by evaluating the drainage capability of a pavement section and its properties corresponding to this recommended joint infiltration rate.

Chapter 4 Pavement Subdrainage

Introduction

Providing a good subdrainage system for pavements is important to protect them from pumping deterioration. The minimum degree of saturation and the corresponding drainage time are the best measure of the drainability of the pavement system. The water that drains from the subbase layer depends on both the physical properties of the subbase material and the cross-sectional geometry of the pavement. Capillary force may also play a role in that a fine-grained subbase may remain fully saturated even with gravity at work.

As stated previously, drainage time is an essential parameter used to measure the drainage capacity of the system. The time to 85% saturation (T_{85}) and the time to 50% drainage (T_{50}) are widely used as the drainage time measurements. The time to 85% saturation is more meaningful than the time to 50% drainage as a measure of the drainage quality. The FHWA provides recommendations for the time to drain, based on the quality of sub-drainage system. The FHWA recommends a method for drainage time estimation, based on Casagrande and Shannon's procedure (The FHWA Drainable Pavement Systems: notebook 1992). A new method implemented in SUBDRAIN was developed by the Kansas DOT [McEnroe (1994)] using the basic principles of water retention and flow through porous media. McEnroe (1994) evaluated the FHWA method with SUBDRAIN and found that the FHWA method tends to overestimate the amount of drainage from fine-grained material and greatly underestimates the amount of drainage from coarse-grained materials. Thus in this chapter, SUBDRAIN will be used to evaluate several drainage scenarios.

Factors Affecting Pavement Drainabilty

The average minimum degree of saturation and the drainage time are the essential parameters indicating the drainability of a pavement sub-drainage system. In this report, the time to 85% saturation is considered the predominant drainage time parameter because it is more effective than the time to 50% drainage in terms of comparing the drainage times of different pavement systems. This is because the time to 50% drainage is a relative value dependent on both the depth of the subbase and the completed drainage level of each soil sample. However, the time to 85% saturation is simply an indicator of the location of the phreatic level in the subbase. For example:

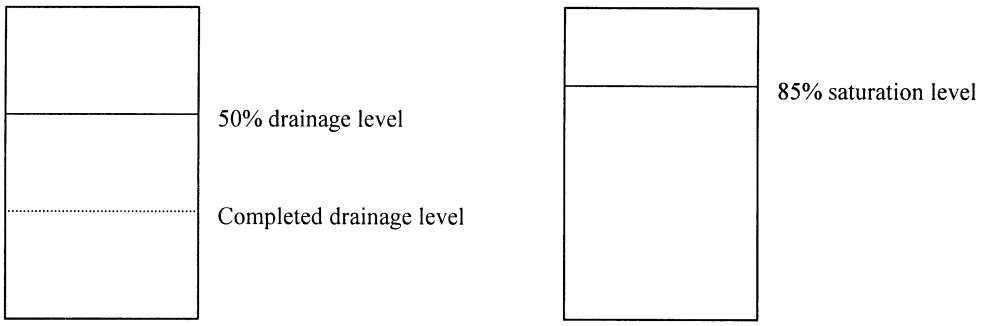

Time to 50% drainage

Time to 85% saturation

The average minimum degree of saturation and the drainage time depend not only on the hydraulic properties of the subbase layer, but also on the cross-sectional geometry of the pavement system. This section looks at time to 50% drainage, time to 85% saturation, and drainage to a finite depth (using the phreatic level) as a function of the cross-sectional geometry of the subbase and pavement system.

The hydraulic properties required include the permeability, the water-retention constants (Brooks-Corey parameters: λ, θ_r, ψ_a), and the porosity. Each hydraulic parameter has its own specific

meaning. However, in a coarse-grained soil (gravel or sand) with a low clay composition, all of the hydraulic parameters listed above depend primarily on the bulk density, the type of material and the grain-size distribution. For this parametric sensitivity study, it was felt that grouping several parameters together would be more beneficial. Thus, both the grain-size distribution and the bulk density of the material were modified. Then the hydraulic parameters corresponding to the assigned material properties were obtained. This process led to a more practical result. Hence the procedure involved the addition of %fines into each of the six samples. Then the actual laboratory tests and the results from SOILPROP were applied to determine the average hydraulic properties of the compacted samples as described in Chapter 2.

The cross-sectional geometry of the pavement system includes the subbase thickness, slope, and the distance of the drainage path. This distance is the maximum distance water must travel through the subbase to reach a side drain, as indicated in Fig. 4-1.

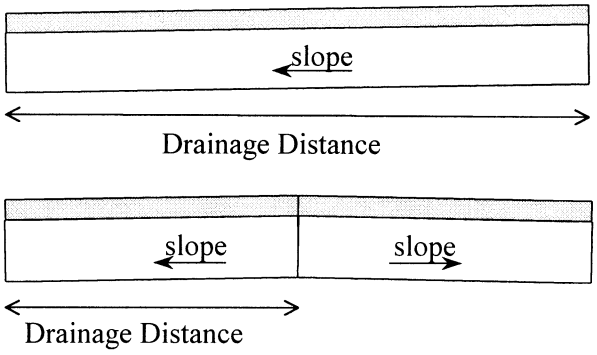

Figure 4-1. Diagram shows how to determine the distance of a drainage path.

Characteristic Drainage Curve

A characteristic drainage curve shows the progression of drainage in terms of average degree of saturation vs. elapsed time. Figures 4-2 and 4-3 show examples of this type of curve, which is developed from typical highway sections and material properties. The curves indicate how much and how fast gravity action drains water from the subbase layer. The drainage parameters, such as the average minimum degree of saturation, the time to 85% saturation and the time to 50% drainage, can be determined from the plot. The SUBDRAIN program provides an output option for plotting this drainage curve. In addition, the average degree of saturation and the % drainage for each time step can be obtained. Plots in Figs.4-2 and 4-3 were generated using this option.

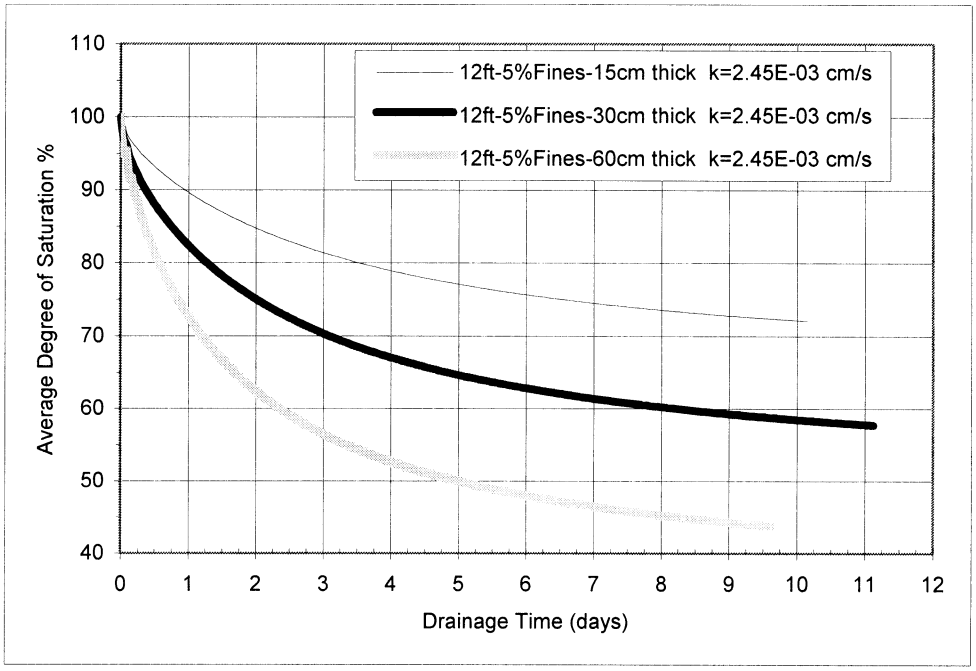

Figure 4-2. Characteristic drainage curves of the 12ft-standard sectional geometry. The subbase layer contains 5%fines composition and three different thicknesses.

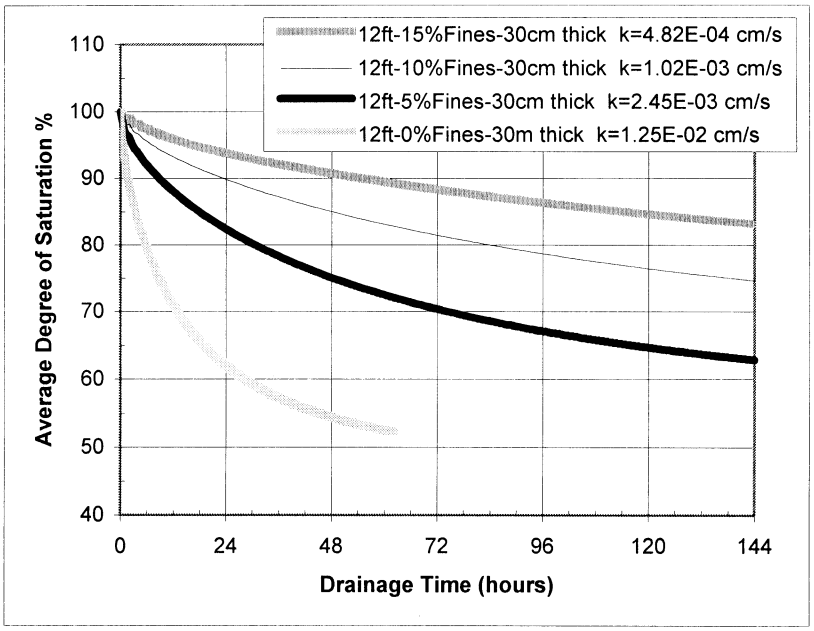

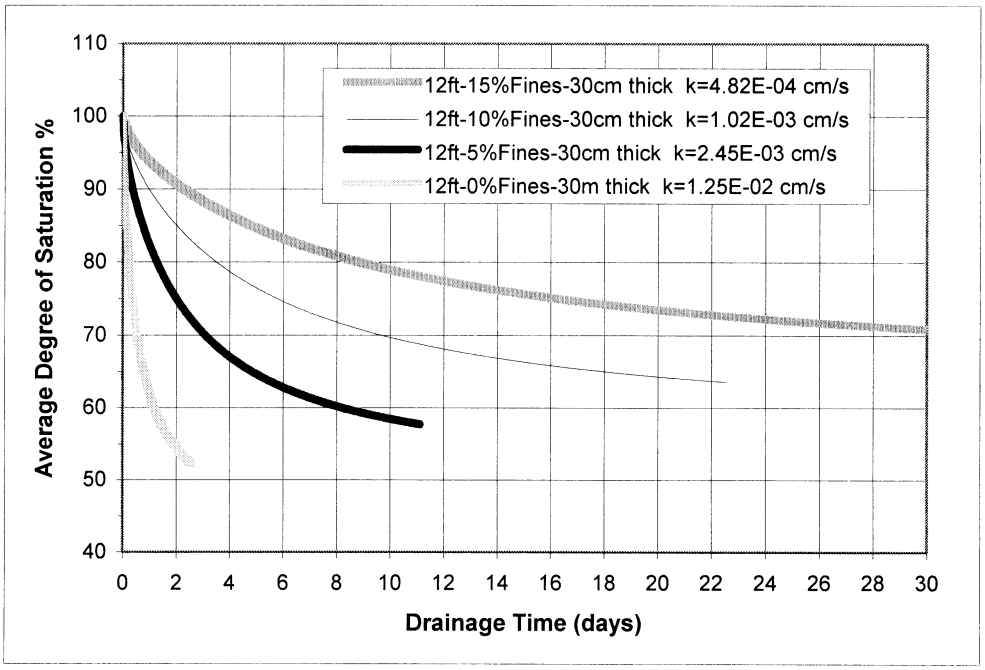

Figure 4-3. Characteristic drainage curves of the 12ft-standard sectional geometry. The subbase layer contains a 30-cm thickness and 0%-15% fines composition.

Average Degree of Saturation and Phreatic Level in Subbase

The average degree of saturation indicates the amount of water retained in the subbase. This value can be obtained directly from drainage analysis. However, this indicator is still difficult to imagine in terms of how much water remains in the subbase. The phreatic level, or saturation level, is a better indicator of where the water actually is relative to the pavement surface. SUBDRAIN calculates the average degree of saturation from the sectional geometry of a pavement section and from the water retention properties of the material. The equations for average minimum degree of saturation at any distance x from the side drain are as follows:

$$S_{\min}(x) = \frac{1}{d}\int_{mx}^{mx+d} s(z)dz$$

$$s(z) = s_r + (1 - s_r)\cdot\left(\frac{\psi_a}{w+z}\right)^{\lambda} \quad < 1.0 \quad \text{if } z > \psi_a - w$$

$$s(z) = 1 \qquad \text{if } z \le \psi_a - w$$

where $S_{\min}(x)$ is average minimum degree of saturation at a distance x from the side drain, s(z) is the degree of saturation at a vertical position z from the bottom of the subbase layer, m is the subgrade slope, d is the subbase thickness, w is the depth of depression in the side drain, s_r is the residual degree of saturation, and ψ_a is the air-entry head.

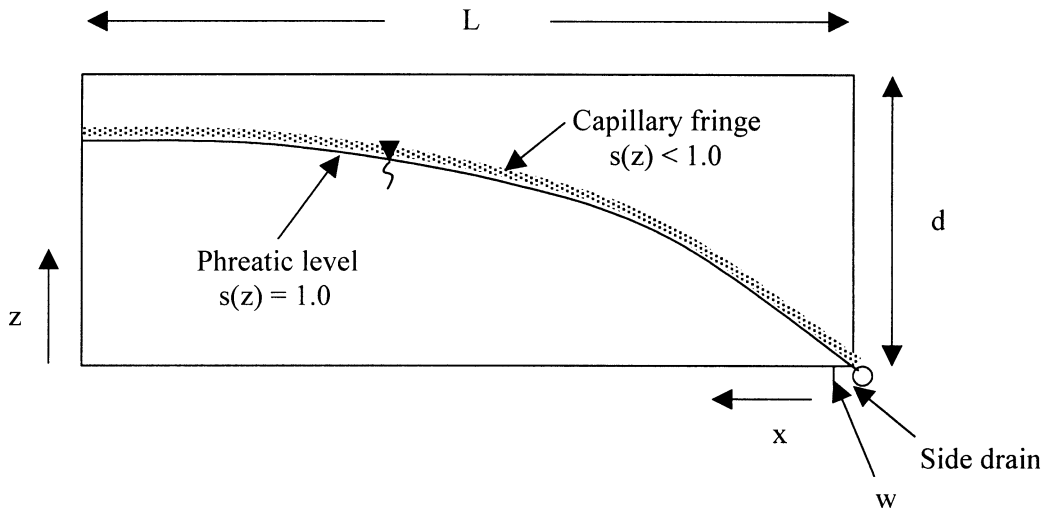

The phreatic level (saturation level) corresponding to any average degree of saturation can be estimated by applying the following assumption to the SUBDRAIN equations:

during the draining process and at a distance x from the side drain, the immediate air-entry head (ψ_a) at this state will be equal to $w + m \cdot x + Y$, where Y is the distance from the bottom of the subbase to the phreatic level and is always greater than 0.

The relation between the average degree of saturation, *S(x)*, and the corresponding phreatic level, *Y*, can be obtained by substituting $w + m \cdot x + Y$ for ψ_a into the $S(x) = \frac{1}{d}\int_{mx}^{mx+d} s(z)dz$ equation:

$$S(x) = \frac{1}{d}\left[\int_{mx}^{mx+Y} 1.0dz + \int_{mx+Y}^{mx+d} s_r + (1-s_r)\cdot\left\{\frac{w+mx+Y}{w+z}\right\}^{\lambda} dz\right]$$

where only *S(x)* and *Y* are variables in the equation. The other terms are constants obtained from the sectional geometry and material properties and can be inserted into the equation. One half of the drainage distance, L, is selected to replace the x variable, in order to represent the average value for the entire sectional width. Solution of the *S(x)* and *Y* relationship equation can be solved mathematically. Graphical results of an example are shown in Fig.4-4. Note that even a small degree of saturation can be related to different water level conditions. For example, the 85% average degree of saturation means the phreatic surface is located 18 cm below the pavement for the 30-cm thick subbase, but 32 cm for the 60-cm thick subbase. The importance of this may signify that one needs only to drain to 95 % or 98 % to prevent pumping. The analysis of the subbase drainage to a depth away from the concrete slab may be a better method of determining subbase design, more testing and analysis needs to be performed in order to verify the validity of the theory. A more in-depth analysis of the phreatic level is presented in the appendix.

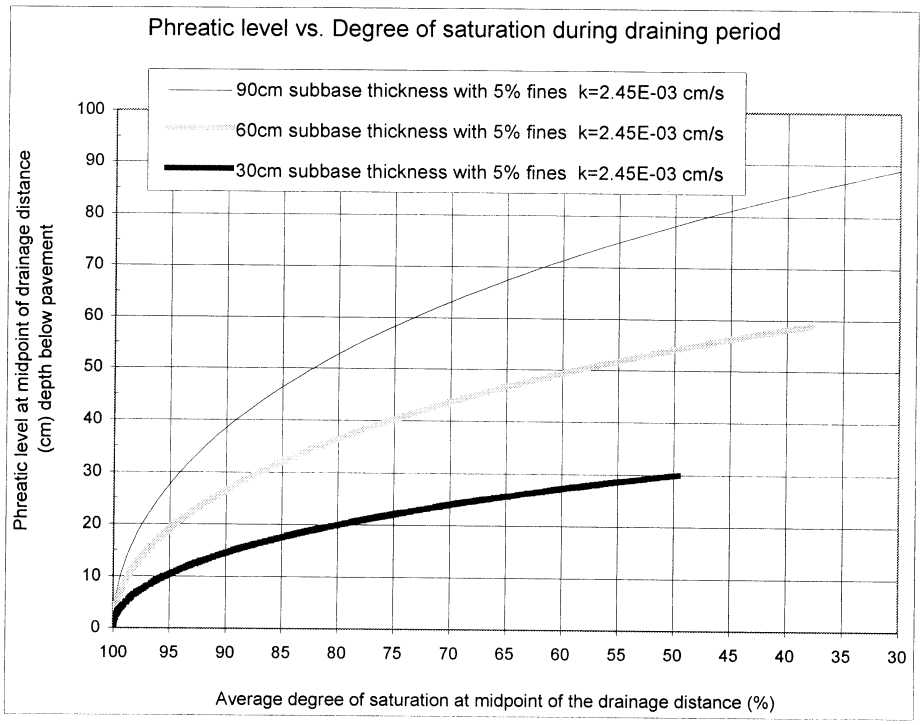

Figure 4-4(a). Relationship of the average degree of saturation at the midpoint of the drainage distance and the phreatic level in the subbase. Conditions: 2% subgrade slope, 12-ft drainage distance and hydraulic properties from material with 5% fines composition.

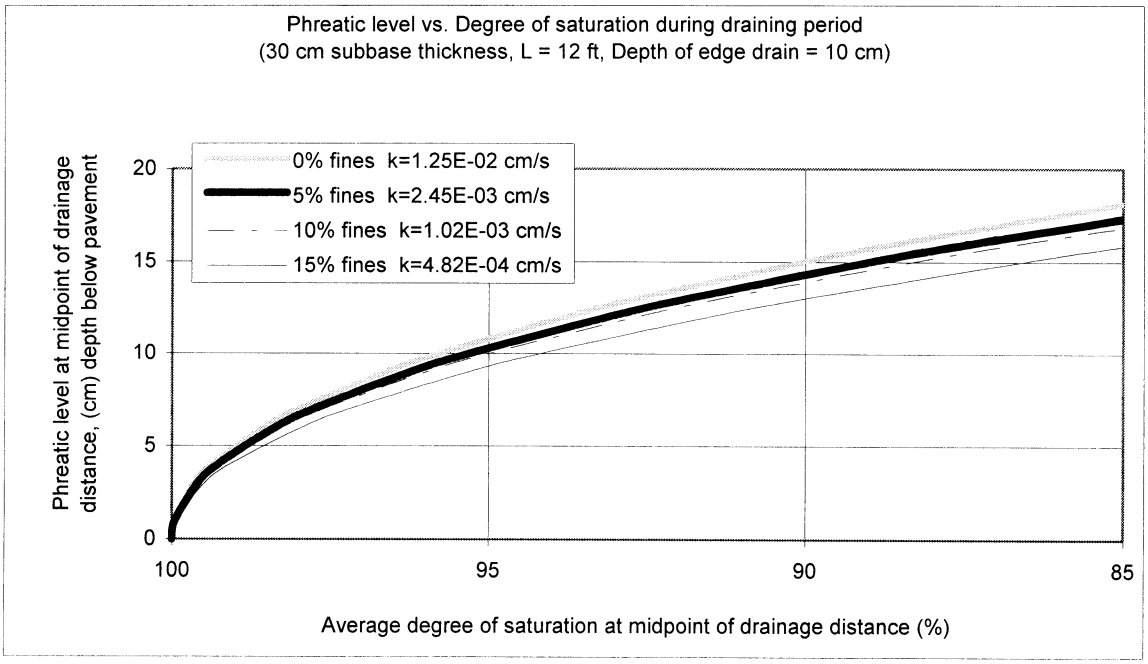

Figure 4-4(b). Relationship of the average degree of saturation at the midpoint of the drainage distance (6 ft) and the phreatic level in the subbase Conditions: 2 % subgrade slope, 12-ft drainage distance, and hydraulic properties from soils with 0%, 5%, 10%, 15% fines composition.

Parametric Sensitivity of Pavement Drainability for Typical Florida Conditions

1. Hydraulic Properties by Varying the %Fines

The average hydraulic properties of the typical Florida material corresponding to each %fines were obtained as described in Chapter 2. The average hydraulic properties (k, θ_s, λ, θ_r, ψ_a) and the cross-sectional geometry of the pavement system were input into SUBDRAIN to determine the drainage parameters.

Standard cross-sectional geometry:

- Distance of drainage path = 3.6 m. or 12 ft.
- Slope of subgrade = 2%
- Depression depth of water in side drain = 10 cm. or 4 in.
- Pavement thickness = 25 cm. or 10 in.

Drainage output from SUBDRAIN includes:

- Average minimum degree of saturation
- Time to 85% saturation, T_{85}
- Time to 50% drainage, T_{50}
- Table of degree of saturation and percent of drainage corresponding to each elapsed time.

Increasing the %fines results in a progressive reduction of the material's permeability. The other material properties, which include the bulk density, the residual volumetric water content, θ_r, the pore-size distribution index, λ, and the air-entry head, ψ_a, increase slightly with increasing %fines (Chapter 2).

Figs.4-5 and 4-6 indicate that average minimum degree of saturation appears to increase proportionally with %fines. This is reasonable since capillary tension is directly related to the size of the flow channels. The addition of fines reduces the size hence greater suction. Also, the time to 85% saturation increases progressively with the addition of %fines. The average minimum degree of saturation (undrainable water percentage) indicates the volume of water that cannot be drained from the subbase by gravitational forces, and the time to 85% saturation shows how quickly the water can be removed from the subbase layer. Therefore, adding more %fines into the material composition will result in a slower drainage response and in a greater amount of water stored in the subbase. Materials containing high %fines will experience reduced drainability, and pumping distress will become more critical.

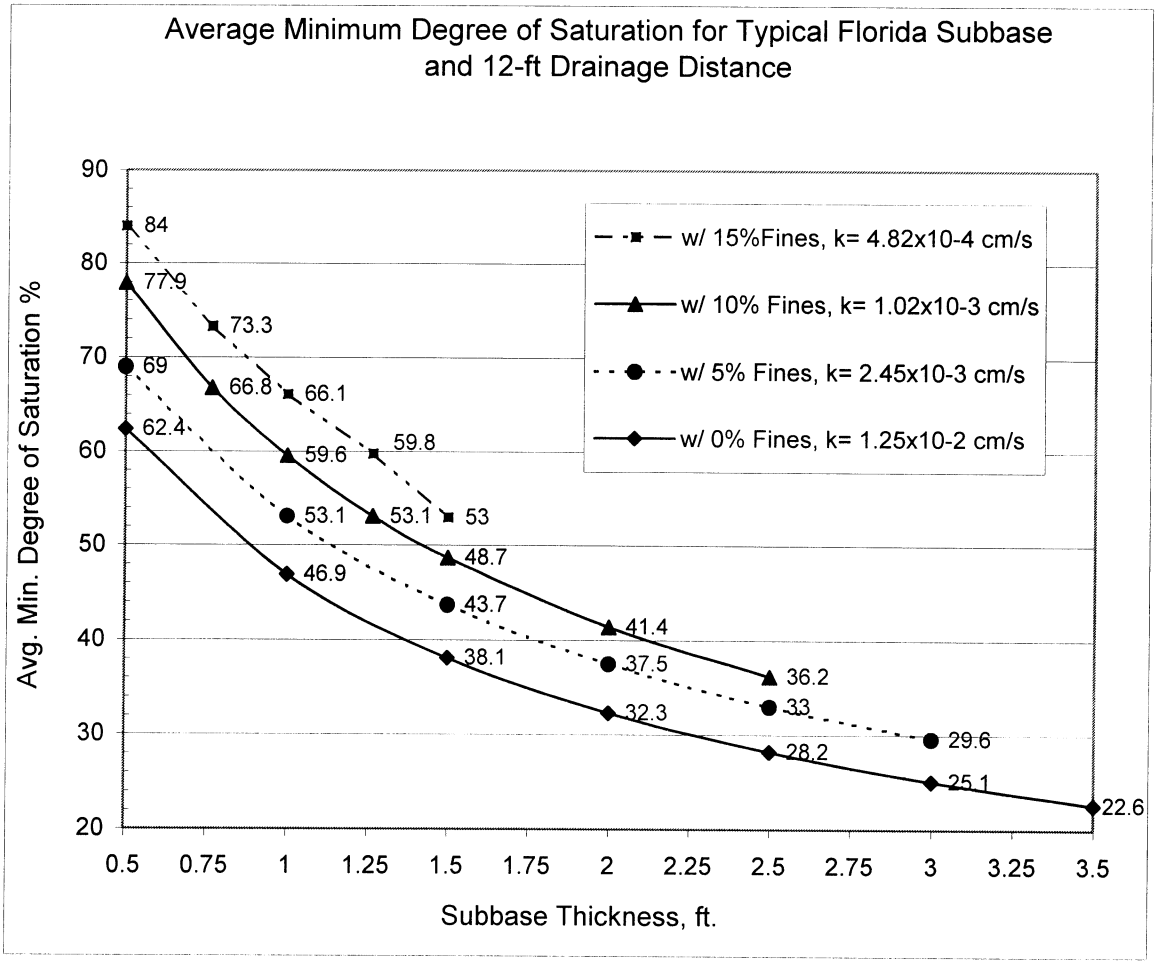

Figure 4-5(a). Effect of the subbase thickness and the %fines on the average minimum degree of saturation for a12-ft drainage length.

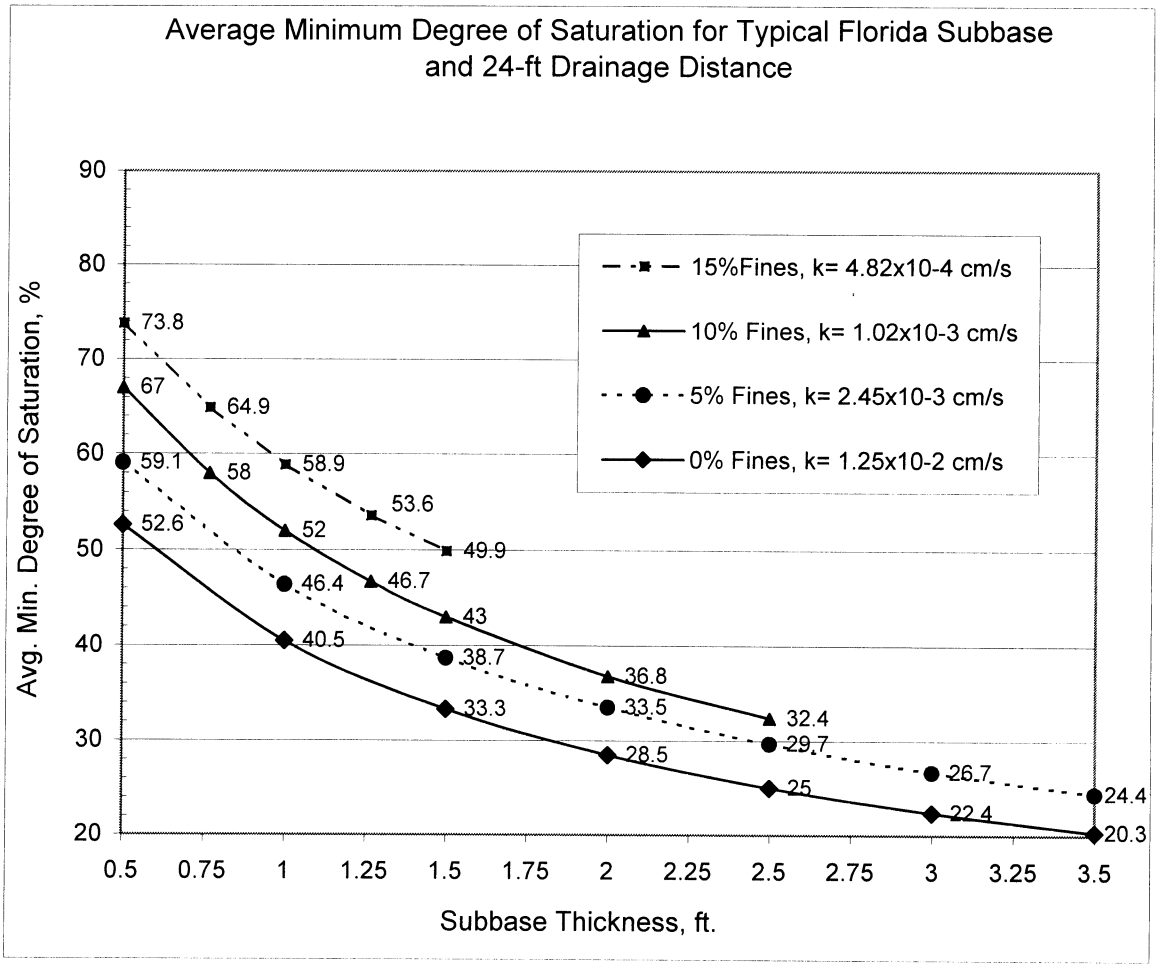

Figure 4-5(b). Effect of the subbase thickness and the %fines on the average minimum degree of saturation for a 24-ft drainage length.

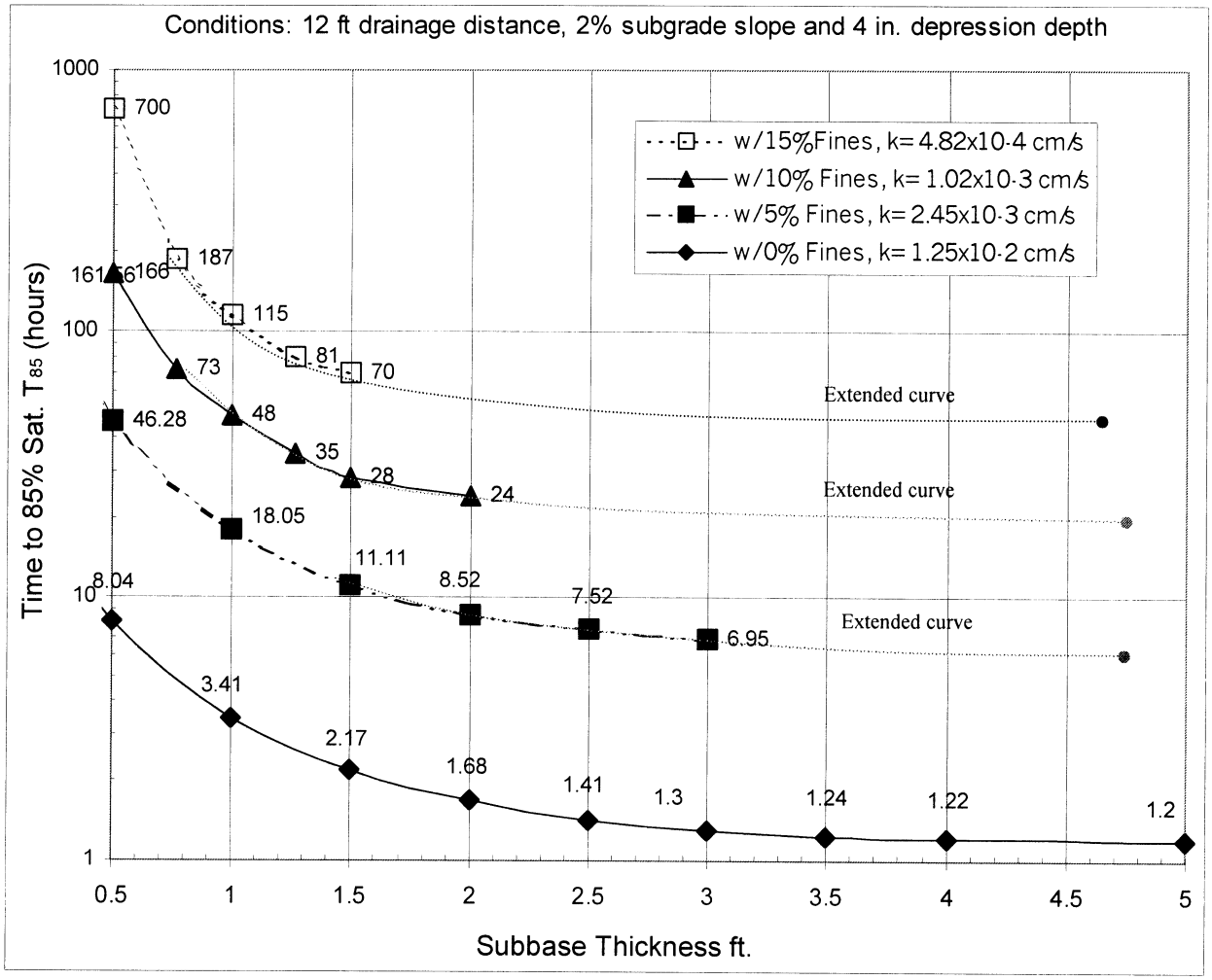

***Note:** Extended curves have a small downward slope, although they appear asymptotic

Figure 4-6(a). Time to 85% saturation as a function of the subbase thickness and %fines composition for a 12-ft drainage length.

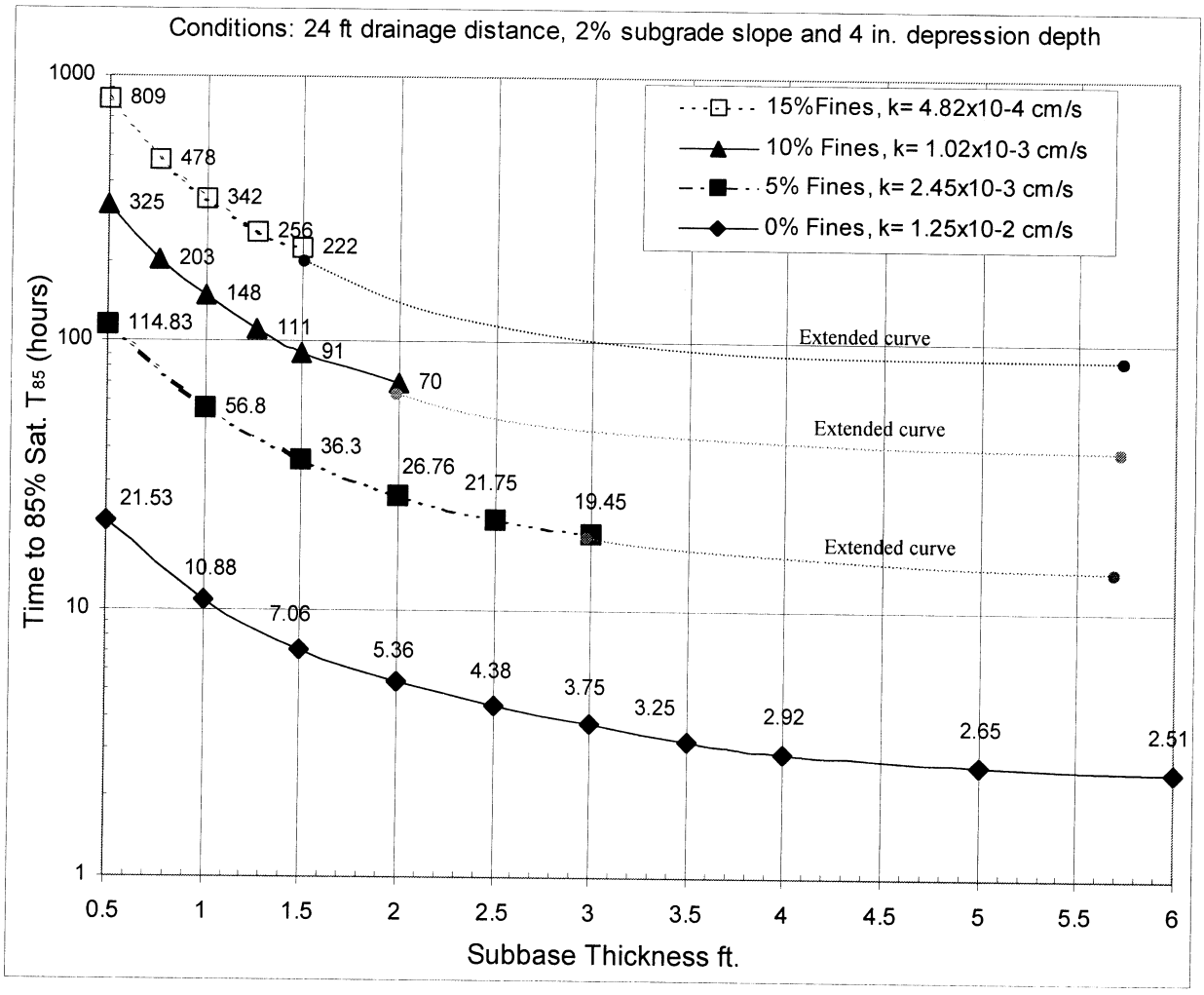

***Note:** Extended curves have a small downward slope, although they appear asymptotic

Figure 4-6(b). Time to 85% saturation as a function of the subbase thickness and %fines composition for a 24-ft drainage length.

2. Cross-sectional Geometry of Pavement System

The Subbase Thickness

Figures 4-5 and 4-6 are the results of varying the subbase thickness and the %fines composition from the SUBDRAIN analyses, using a 12-ft and 24-ft standard sectional geometry. They reveal that the subbase thickness has a significant effect on both the average minimum degree of saturation and the time to 85% saturation.

The average minimum degree of saturation decreases with an increasing subbase thickness. In addition, an incremental change in subbase thickness causes the time to 85% saturation to also decrease. Figures 4-5 and 4-6 indicate that increasing the subbase thickness from 0.5 ft to 1.5-2.0 ft can reduce the time to 85% saturation significantly. However, increasing the thickness more than 2.0 ft has less of an effect on the drainage time reduction. In addition, the time to 85% saturation tends to converge to a large thickness value.

The Slope of Subgrade

Subgrade slopes ranging from 0.1% to 5% were considered in this study. The material properties were taken from the 5% and the 10% fines composition material. The other factors were kept constant (12-ft drainage distance and 1-ft subbase thickness). Figure 4-7 depicts the results based on these conditions. This points out that the steeper the subgrade slope, the lower the minimum degree of saturation and the shorter the drainage time. This evidence is similar to the action of a subgrade slope on the joint infiltration rate: the steeper the slope, the higher the joint infiltration rate. This means that the water can flow out faster and in larger quantities.

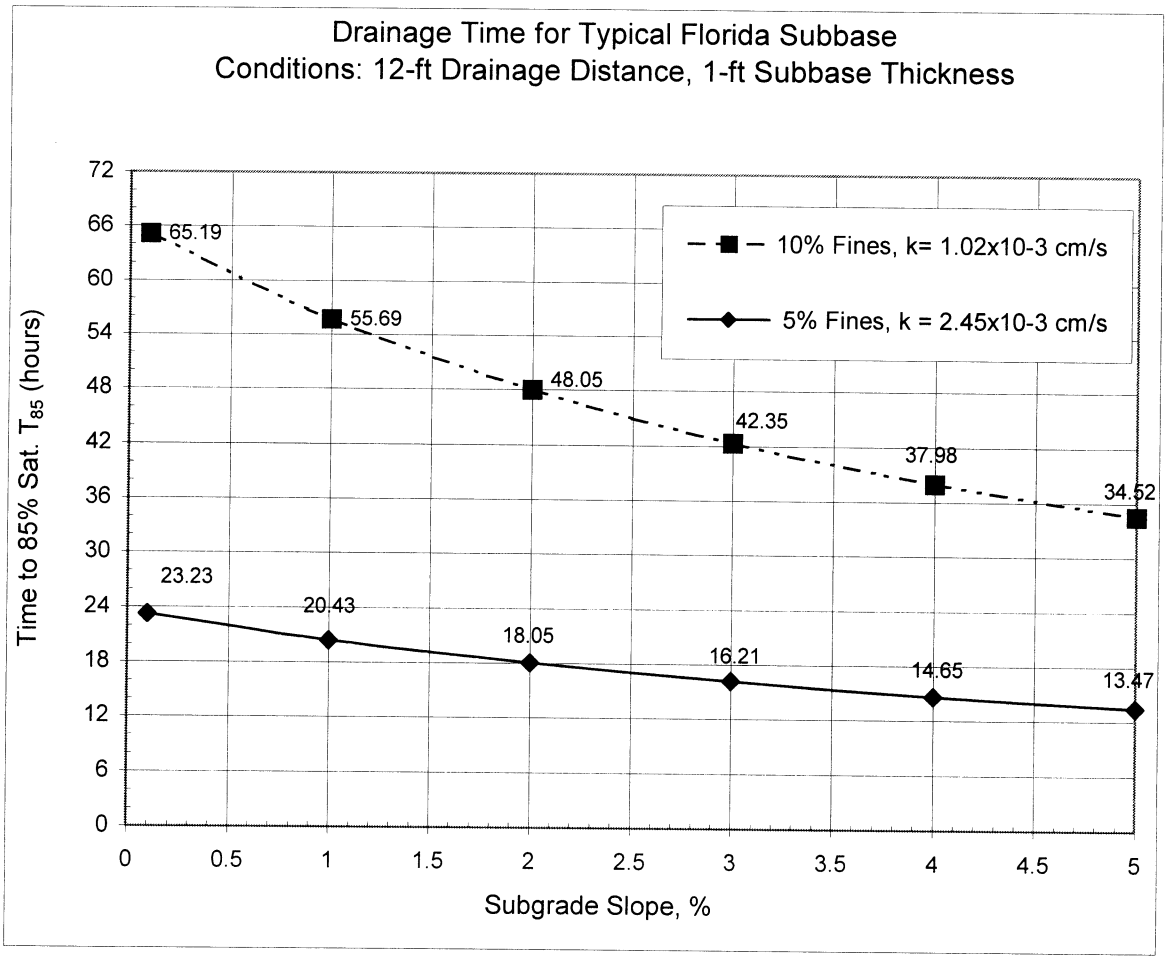

Figure 4-7. Effect of the subgrade slope on the time to 85% saturation.

The Length of Drainage Path Influence

The drainage distance referenced in the previous sections presented the 12-ft drainage path, which is compatible with a two-lane pavement's crest point at the centerline. For pavements having three or four traffic lanes, the drainage distance will be 24 ft. The effects of drainage distance focused on the minimum degree of saturation and the time to 85% saturation for the 12-ft and 24-ft drainage distance. The other factors were kept constant in each analysis. Figure 4-8 shows that the time to 85% saturation of the 12-ft drainage distance is less than that of the 24-ft distance.

However, the relationship between the minimum degree of saturation and the drainage distance is different from the drainage time relationship. The minimum degree of saturation for the 12-ft drainage distance is higher than the minimum degree of saturation for the 24-ft condition (see Fig.4-9). This is because increasing of the drainage distance will impede the drainage rate of water, which results in a longer time for 85 % saturation to occur. With the same subgrade slope, the 24-ft section has the higher gravity head than the 12-ft section. Increasing the gravitational force can result in more water being drained from the subbase. This causes the percentage of water retained in the 24-ft section to be less than that in the 12-ft section.

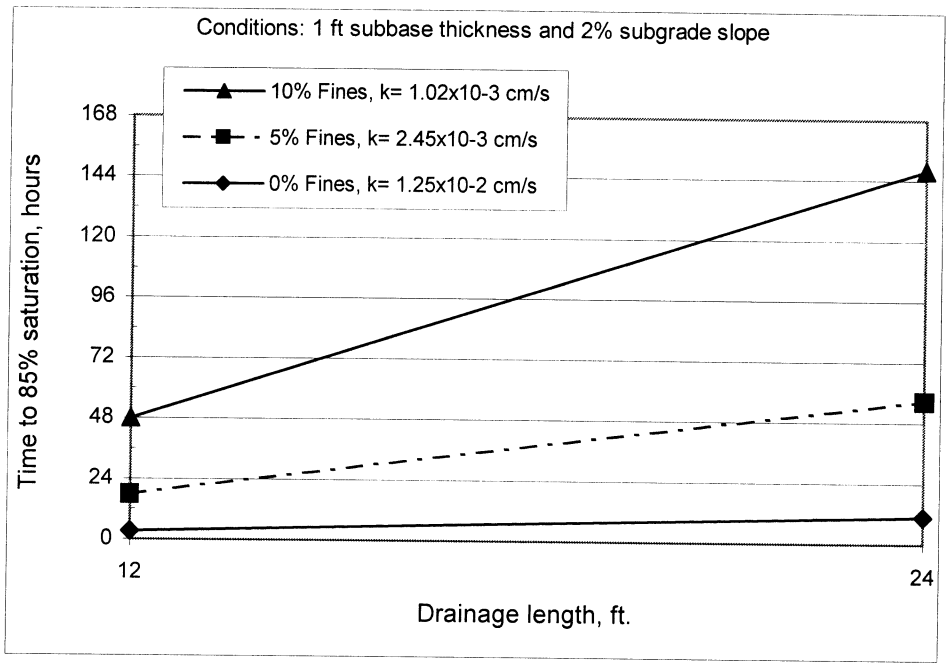

Figure 4-8. Time to 85% saturation for 12-ft and 24-ft drainage lengths.

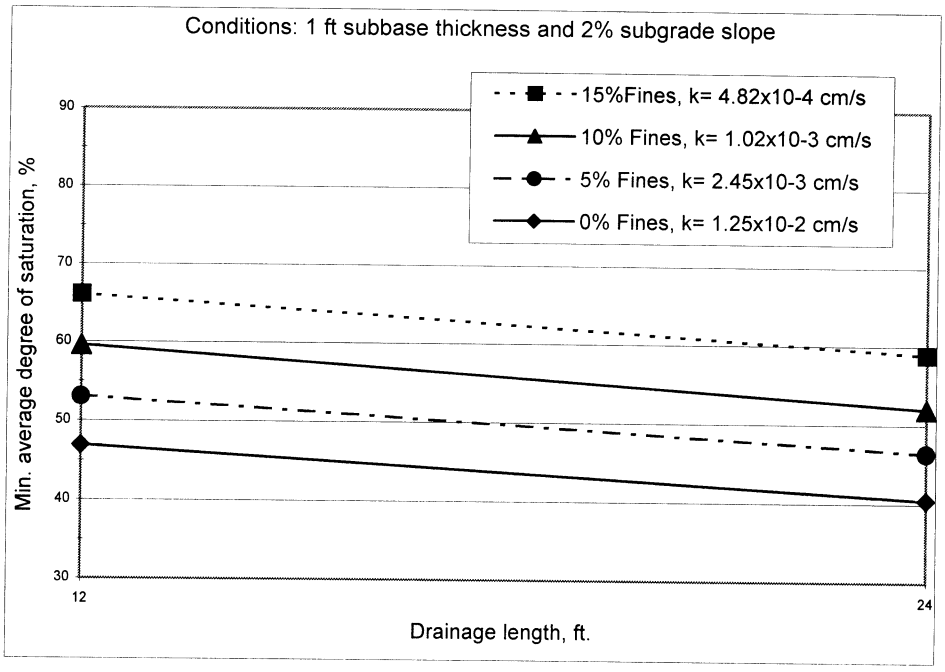

Figure 4-9. Minimum average degree of saturation vs. the 12-ft and 24-ft drainage distance.

Pavement Subdrainage Summary

1. The time to 85% saturation ($T_{85\%Sat}$) and the minimum average degree of saturation are two parameters that indicate the drainability of a pavement section.

2. A relationship between the phreatic level and an average degree of saturation provides a good indicator of the amount of water retained in the subbase. This relationship can lead to a design approach based on drainage of the subbase to a finite depth.

3. From the parametric sensitivity analysis:
   - The addition of %fines produces a longer time to reach 85% saturation and an increased minimum average degree of saturation.
   - Adding subbase thickness will result in a significant reduction in $T_{85\%Sat}$ and the minimum average degree of saturation.
   - A steeper subgrade slope will slightly lessen both $T_{85\%Sat}$ and the minimum average degree of saturation.
   - A longer drainage distance (more traffic lanes) will increase the drainage time, but the miimum average degree of saturation will decrease.

4. Based on the FHWA drainage quality guidelines, a pavement section and its soil properties can be evaluated by obtaining values from graphs of $T_{85\%Sat}$. Examples of these calculations are described in the next chapter.

Chapter 5 Verification of Joint Infiltration

Joint Infiltration of Pavements That Meet FHWA Time to Drain Criteria

Sectional Properties That Can Meet the Recommended Quality of Drainage

The FHWA and AASHTO suggested values of drainage times can be used as a guideline to determine a subbase thickness and its material properties for a specified highway section.

The process begins with determining the hydraulic properties of the material based on its soil-composition and density. The sectional geometry of the pavement is generally fixed by typical values, such as 12-ft/24-ft drainage distance, 2% subgrade slope and 4 in. assumed depression depth in the side drain. The subbase thickness is the only unknown sectional variable.
The material properties and the cross-sectional geometry of the pavement are the input conditions for SUBDRAIN (or any other analytical method) to determine the drainage parameters for various subbase thicknesses. The output is then presented in terms of the time to 85% saturation vs. subbase thickness. The required thickness can be obtained from this plot by simply reading the thickness corresponding to the suggested drainage time.

The Corresponding Joint Infiltration Rate

The above process identifies both the cross-sectional geometry and the subbase properties required for an adequate quality of drainage. The FHWA *Drainage Pavement Systems* notebook (1992) provided an example for determining the subbase thickness from a standard joint infiltration rate, subbase properties and pavement geometry. Therefore, the average joint infiltration rate of a section can be determined by back-calculation using the same processes as in the FHWA example.

This corresponding joint infiltration rate can then be compared to the FHWA recommended value in order to evaluate whether the suggested value is applicable to Florida conditions. Examples for determining the subbase thickness and the average joint infiltration rate are described in the following sections.

Procedure:

Obtain the time to 85% saturation ($T_{85\%Sat.}$) plot as a function of the unknown factor. (Basically, the drainage distance, the depression depth and the subgrade slope are fixed.) The unknown factor is either the subbase thickness or the subbase material properties.

Enter the plot with the recommended $T_{85\%Sat.}$ for a desired level of drainage quality, i.e., five hours for good quality and 10 hours for a fair quality. Then, read off the corresponding variable (subbase thickness or %fines composition) from the plot.

With the sectional geometry and soil properties known, the joint infiltration rate (I_C) can be determined by using the FHWA methods (see next section) to back-calculate an average rate. It also can be estimated by using two-dimensional analysis to determine its value for both the longitudinal and transverse joint.

Determining the Subbase Thickness by the Joint Infiltration Rate

FHWA Method # 1

This method treats the subgrade slope as a uniform gradient and is similar to employing Darcy's equation.

Pavement infiltration:

$$q_d = q_i L = k S_R D \qquad \text{(which resembles Darcy's } Q = k\, i\, A\text{)}$$

where,

q_d is the subbase discharge, $ft^3/day/ft$

q_i is the pavement infiltration rate, $ft^3/day/ft^2$

L is the drainage length

k is the subbase permeability

S_R is the slope of the subgrade

D is the subbase thickness

Joint infiltration rate:

$$q_i = I_C \left[\frac{N_C}{W} + \frac{W_C}{W \cdot C_S} \right]$$

where,

I_C is the joint infiltration rate, $ft^3/day/ft$

N_C is the number of longitudinal contributing joints = no. of lanes in the draining direction +1

W_C is the length of the transverse contributing joints

W is the width of the subbase

C_S is the spacing of the transverse joints

FHWA Method # 2

Apply a chart for estimating the flow. This method seems to be more rational than method #1, since it includes the effect of drawdown on the hydraulic gradient near the edge drain. The average joint infiltration rate (I_C) is then calculated using the previous equation,

$$q_i = I_C\left[\frac{N_C}{W} + \frac{W_C}{W \cdot C_S}\right]$$

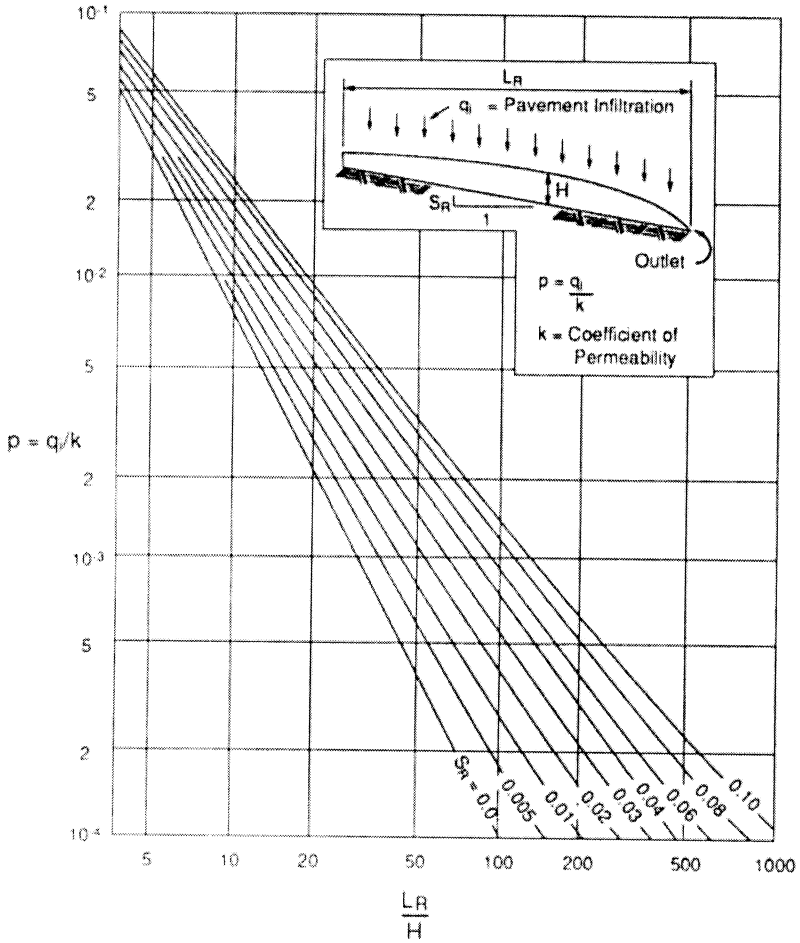

Figure 5-1. Chart for estimating the depth of flow [from FHWA *Drainable Pavement System* Notebook (1992)].

Example 1

Given a pavement section, find the subbase thickness required to yield a fair to good level of drainage.

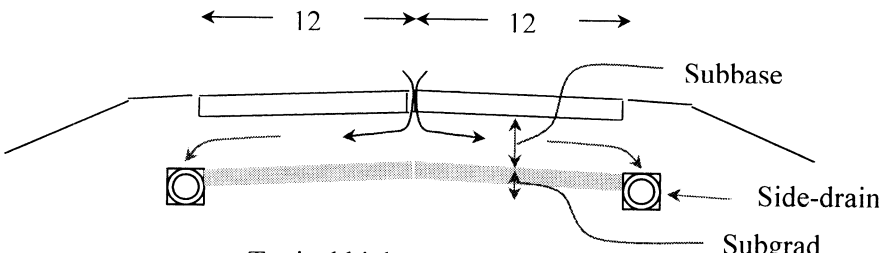

Typical highway section

Given:

- Spacing of transverse joints, $C_S = 20$ ft
- Drainage distance, $L = 12$ ft.
- Subgrade slope, $S_R = 2\%$
- Depression depth in side drain, $w = 4$ in.
- Hydraulic properties of subbase materials

Hydraulic properties	0% fines composition	5% fines composition
Permeability k, cm/s	1.25×10^{-2}	2.45×10^{-3}
Dry density γ_{dry}, g/cm^3	1.663	1.719

For 0% fines Subbase Material

From Fig.4-6a (repeated on page 88), a subbase thickness of 0.8 ft is needed to provide good drainage quality.

Method # 1

$$q_i = k\, S_R\, D / L$$

$$q_i = (1.25 \times 10^{-2}\text{cm/s} \times 24 \times 3600/30.48)(0.02)(0.8)/(12) \quad (\text{ft}^3/\text{day}/\text{ft}^2)$$

$$q_i = 0.04724\ \text{ft}^3/\text{day}/\text{ft}^2$$

Also, $$q_i = I_C \left[\frac{N_C}{W} + \frac{W_C}{W \cdot C_S} \right]$$

$$q_i = I_C \left[\frac{2}{12} + \frac{12}{12 \cdot 20} \right]$$

$q_i = I_C$ (0.217)

I_C = (0.04724 $ft^3/day/ft^2$)/(0.217) = <u>0.22 $ft^3/day/ft$</u>

Method # 2

L/H = (12)/(0.8) = 15

From the chart (Figure 5-1), $q_i/k = 6.5 \times 10^{-3}$

$q_i = (6.5 \times 10^{-3})(1.25 \times 10^{-2}$cm/s x24x3600/30.48) $ft^3/day/ft^2$

q_i = 0.23 $ft^3/day/ft^2$ (compared to 0.04724 $ft^3/day/ft^2$ from method # 1)

I_C = (0.23 $ft^3/day/ft^2$)/(0.217) = <u>1.06 $ft^3/day/ft$</u>

Two-dimensional Method

From the plot of infiltration rate vs. subbase thickness (Figure 3-5),

(I_{C1}/k_1) = (0.27 $ft^3/day/ft$)/(1.0×10^{-3}cm/s) for a 0.8 ft subbase thickness

$I_C = (I_{C1}/k_1)(k)$ = [(0.27 $ft^3/day/ft$) / (1×10^{-3}cm/s)] (1.25×10^{-2}cm/s) = <u>3.375 $ft^3/day/ft$</u>

For 5% fines Subbase Material

From Fig.4-6(a), the subbase thickness for the 5%-fines material will exceed 4 ft in order to achieve a "good" drainage quality. However, a fair quality can be attained using a thickness of 1.6 ft.

Method # 1

$q_i = (2.45 \times 10^{-3}$cm/s x24x3600/30.48)(0.02)(1.6)/(12) $ft^3/day/ft^2$

q_i = 0.01852 $ft^3/day/ft^2$

Also, $$q_i = I_C \left[\frac{2}{12} + \frac{12}{12 \cdot 20} \right]$$

$q_i = I_C$ (0.217)

I_C = (0.01852 $ft^3/day/ft^2$)/(0.217) = <u>0.09 $ft^3/day/ft$</u>

Method # 2

$L/H = (12)/(1.6) = 7.5$

From the chart (Figure 5-1), $q_i/k = 2\text{x}10^{-2}$

$q_i = (2\text{x}10^{-2})(2.45\text{x}10^{-3}\text{cm/s x}24\text{x}3600/30.48)\ \text{ft}^3/\text{day/ft}^2$

$q_i = 0.139\ \text{ft}^3/\text{day/ft}^2$

$I_C = (0.139\ \text{ft}^3/\text{day/ft}^2)/(0.217) = \underline{0.64\ \text{ft}^3/\text{day/ft}}$

Two-dimensional Method

From the plot of infiltration rate vs. subbase thickness (Figure 3-5),

$(I_{C1}/k_1) = (0.72\ \text{ft}^3/\text{day/ft})/(1\text{x}10^{-3}\text{cm/s})$ at 1.6 ft subbase thickness

$I_C = (I_{C1}/k_1)(k) = [(0.72\ \text{ft}^3/\text{day/ft}) / (1\text{x}10^{-3}\text{cm/s})]\ (2.45\text{x}10^{-3}\text{cm/s}) = \underline{1.76\ \text{ft}^3/\text{day/ft}}$

Supporting Graph # 1

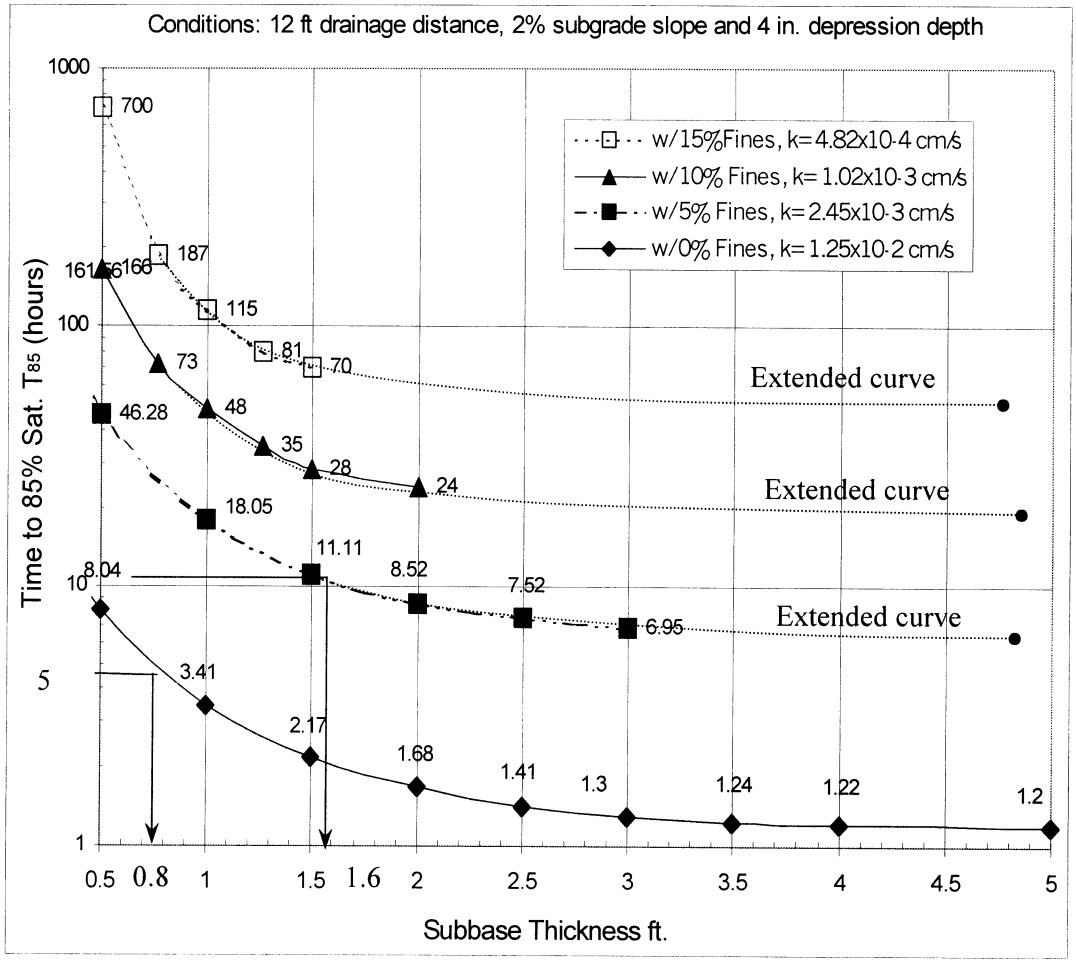

***Note:** Extended curves have a small downward slope, although they appear asymptotic

Figure 4-6(a). Used to determine the subbase thickness for a given time to 85% saturation.

Supporting Graph # 2

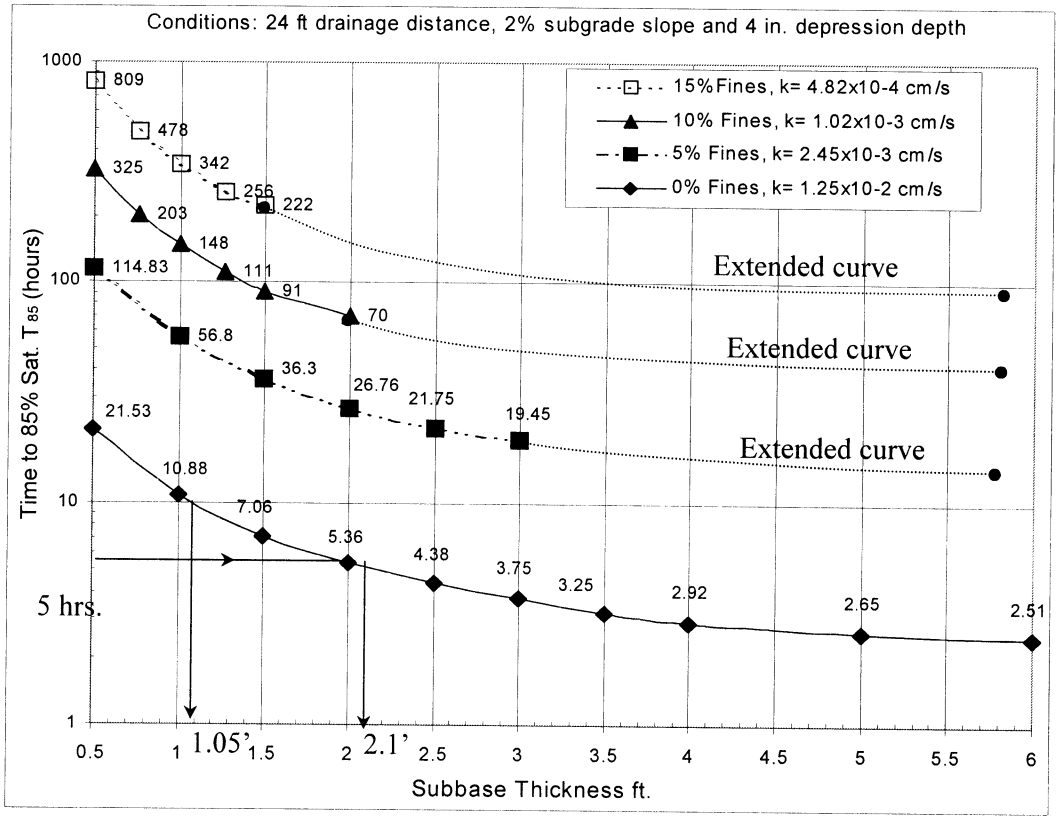

***Note:** Extended curves have a small downward slope, although they appear asymptotic

Figure 4-6(b). Used to determine the subbase thickness for a given time to 85% saturation.

Supporting Graph # 3

This figure is used to find the joint infiltration rate of the longitudinal joint for a given subbase thickness. It was developed based on the two-dimensional analyses.

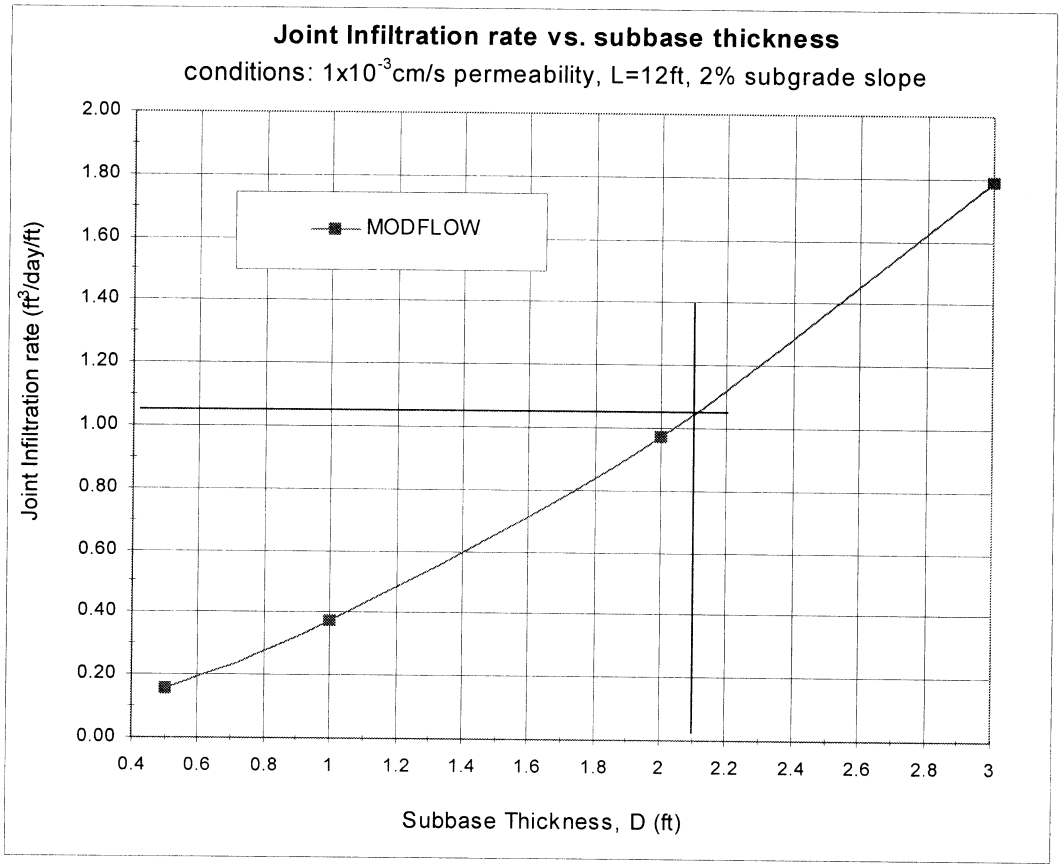

Figure 3-2(b). Joint infiltration rate as a function of subbase thickness.

Example 2

Given a four-lane pavement section, find the subbase thickness required to provide fair to good drainage quality and the corresponding joint infiltration rate for the section.

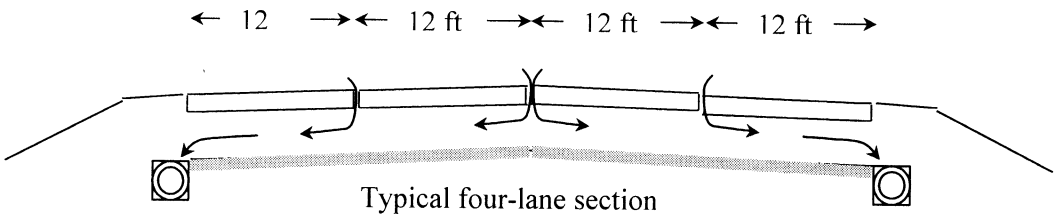

Typical four-lane section

Given:

- Spacing of transverse joints $C_S = 20$ ft
- Drainage distance, $L = 24$ ft.
- Subgrade slope, $S_R = 2\%$
- Depression depth in side drain, $w = 4$ in.
- Hydraulic properties of subbase materials

Hydraulic properties	0% fines composition	5% fines composition
Permeability k, cm/s	1.25×10^{-2}	2.45×10^{-3}

From the plot of time to 85% saturation (T_{85}),

- For $T_{85} = 5$ hr (good drainage quality), the subbase with 0% fines should be 2.1 ft thick.
- For $T_{85} = 10$ hr (fair drainage quality), the subbase with 0% fines should be 1.05 ft thick.
- The 5% fines subbase needs more than 6 ft of thickness to obtain at least a fair quality of drainage. Based on the plot, the 10% fines and 15% fines materials cannot achieve a fair quality of drainage.

The FHWA methods were used to determine the corresponding joint infiltration rate (I_C).

Method # 1

For good drainage quality, subbase thickness = 2.1 ft

$q_i = k\, S_R\, D / L$

$q_i = (1.25\text{x}10^{-2}\text{cm/s x24x3600/30.48})(0.02)(2.1)/(24)$ $\text{ft}^3/\text{day}/\text{ft}^2$

$q_i = 0.062\ \text{ft}^3/\text{day}/\text{ft}^2$

$$q_i = I_C \left[\frac{N_C}{W} + \frac{W_C}{W \cdot C_S} \right]$$

$$q_i = I_C \left[\frac{3}{24} + \frac{24}{24 \cdot 20} \right]$$

$q_i = I_C\,(0.175)$

$I_C = (0.062\ \text{ft}^3/\text{day}/\text{ft}^2)/(0.175) = \underline{0.35\ \text{ft}^3/\text{day}/\text{ft}}$

For fair drainage quality, subbase thickness = 1.05 ft

$q_i = (1.25\text{x}10^{-2}\text{cm/s x24x3600/30.48})(0.02)(1.05)/(24)$ $\text{ft}^3/\text{day}/\text{ft}^2$

$q_i = 0.031\ \text{ft}^3/\text{day}/\text{ft}^2$

$q_i = I_C\,(0.175)$

$I_C = (0.031\ \text{ft}^3/\text{day}/\text{ft}^2)/(0.175) = \underline{0.18\ \text{ft}^3/\text{day}/\text{ft}}$

Method # 2

$L/H = (24)/(2.1) = 11.4$ and $(24)/(1.05) = 22.9$

From the chart (Figure 5-1), $q_i/k = 1\text{x}10^{-2}$ for $L/H = 11.4$

$q_i/k = 4\text{x}10^{-3}$ for $L/H = 22.9$

For T_{85} = 5 hr, subbase thickness = 2.1 ft.

$q_i = (1\text{x}10^{-2})(1.25\text{x}10^{-2}\text{cm/s x24x3600/30.48}) = 0.354\ \text{ft}^3/\text{day}/\text{ft}^2$

Also, $$q_i = I_C \left[\frac{3}{24} + \frac{24}{24 \cdot 20} \right]$$

$q_i = I_C\,(0.175)$

$I_C = (0.354\ \text{ft}^3/\text{day}/\text{ft}^2)/(0.175) = \underline{2.02\ \text{ft}^3/\text{day}/\text{ft}}$

For T_{85} = 10 hr, subbase thickness = 1.05 ft.

$$q_i = (4\text{x}10^{-3})(1.25\text{x}10^{-2}\text{cm/s x}24\text{x}3600/30.48) = 0.142\ \text{ft}^3/\text{day/ft}^2$$

Also, $$q_i = I_C \left[\frac{3}{24} + \frac{24}{24 \cdot 20} \right]$$

$$q_i = I_C\,(0.175)$$

$$I_C = (0.142\ \text{ft}^3/\text{day/ft}^2)/(0.175) = \underline{0.81\ \text{ft}^3/\text{day/ft}}$$

Two-dimensional Method

The longitudinal joint infiltration rate at the joint next to the pavement shoulder can be obtained by reading the plot of infiltration rate vs. subbase thickness. The value at the centerline joint of the pavement can be determined by Darcy's $q = k\,i\,A$ equation, treating i as the subgrade slope and A as the subbase thickness (D *or* H) times a unit width (1 ft).

From the plot of infiltration rate vs. subbase thickness (Figure 3-5),

(I_{C0}/k_0) = (1.05 ft^3/day/ft)/(1x10^{-3}cm/s) at the 2.1 ft subbase thickness

$I_{C1} = (I_{C0}/k_0)(k_1)$ = (1.05 ft^3/day/ft)(1.25x10^{-2}cm/s)/(1x10^{-3}cm/s)

I_{C1} = <u>13.1 ft^3/day/ft</u> for the joint next to the pavement shoulder

And $I_{C2} = k\,S_R\,H$

I_{C2} = (1.25x10^{-2}x24x3600/30.48)(0.02)(2.1)

I_{C2} = <u>1.49 ft^3/day/ft</u> for the centerline joint

Also,

(I_{C0}/k_0) = (0.4 ft^3/day/ft)/(1x10^{-3}cm/s) at the 1.05 ft subbase thickness from the plot

$I_{C1} = (I_{C0}/k_0)(k_1)$ = (0.4 ft^3/day/ft)(1.25x10^{-2}cm/s)/(1x10^{-3}cm/s)

I_{C1} = <u>5.0 ft^3/day/ft</u> for the joint next to the pavement shoulder

And I_{C2} = (1.25x10^{-2}x24x3600/30.48)(0.02)(1.05) = <u>0.74 ft^3/day/ft</u> for the centerline joint

Example 3

Design the subbase thickness using the 0.7 ft^3/day/ft joint infiltration rate.

This example will illustrate the calculations necessary to determine the subbase thickness using the FHWA methods #1 and #2.

$$q_i = I_C \left[\frac{N_C}{W} + \frac{W_C}{W \cdot C_S} \right]$$

where, I_C = 0.7 ft^3/day/ft

C_S = 20 ft

For a 12-ft lane draining in one direction,

$W = W_C$ = 12 ft

$$q_i = 0.7 \left[\frac{2}{12} + \frac{12}{12 \cdot 20} \right] = 0.152 \text{ ft}^3\text{/day/ft}^2$$

Method # 1

Determine the permeable base discharge rate (q_d) = q_i x L = (0.152 ft^3/day/ft^2)(12 ft)

q_d = 1.824 ft^3/day/ft

and $q_d = k S_R H$

For material with 0% fines,

k = 1.25x10^{-2}cm/s.

H = (1.824 ft^3/day/ft) / (1.25x10^{-2}cm/s x24x3600/30.48) / (0.02) = <u>2.57 ft</u>

Method # 2

Apply the chart for estimating the maximum depth of flow (Fig. 5-1).

$p = q_i / k$ = (0.152 ft^3/day/ft^2)/(1.25x10^{-2}cm/s x24x3600/30.48) = 4.3 x10^{-3}

L_R/H = 21 (from chart, Figure 5-1)

H = 12 ft/21 = <u>0.57 ft</u>

By following the above calculations, the subbase thickness for the other conditions (24-ft drainage distance, 5%-15% fines materials) can be determined.

Summary of Results from Examples

12-ft drainage distance

2% subgrade slope

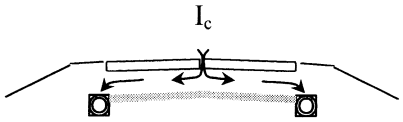

Good quality of drainage	Fair quality of drainage
0% fines material: 0.8-ft thick subbase I_c = 0.22 ft^3/day/ft (FHWA method#1) I_c = 1.06 ft^3/day/ft (FHWA method#2) I_c = 3.375 ft^3/day/ft (2D analysis) 5%, 10% and 15% fines material: either exceeds 6-ft thickness or could not be achieved	5% fines material: 1.6-ft thick subbase I_c = 0.09 ft^3/day/ft (FHWA method#1) I_c = 0.64 ft^3/day/ft (FHWA method#2) I_c = 1.76 ft^3/day/ft (2D analysis) 10% and 15% fines material: either exceeds 6-ft thickness or could not be achieved

24-ft drainage distance

2% subgrade slope

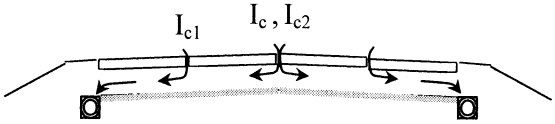

Good quality of drainage	Fair quality of drainage
0% fines material: 2.1-ft thick subbase I_c = 0.35 ft^3/day/ft (FHWA method#1) I_c = 2.02 ft^3/day/ft (FHWA method#2) 2D analysis: I_{c1} = 13.1 ft^3/day/ft for the outer joint I_{c2} =1.49 ft^3/day/ft for the centerline joint 5%, 10% and 15% fines material: either exceeds 6-ft thickness or could not be achieved	0% fines material: 1.05-ft thick subbase I_c = 0.18 ft^3/day/ft (FHWA method#1) I_c = 0.81 ft^3/day/ft (FHWA method#2) 2D analysis: I_{c1} = 5.0 ft^3/day/ft for the outer joint I_{c2} = 0.74 ft^3/day/ft for the centerline joint 5%, 10% and 15% fines material: either exceeds 6-ft thickness or could not be achieved

The corresponding subbase thicknesses based on the 0.7 ft^3/day/ft joint infiltration rate are listed in the following table:

%fines composition in material	Subbase thickness			
	12-ft drainage distance		24-ft drainage distance	
	FHWA method #1	FHWA method #2	FHWA method #1	FHWA method #2
0%	2.57 ft	0.57 ft	4.15 ft	1.0 ft
5%	13.1 ft	1.71 ft	21.17 ft	3.2 ft
10%	31.47 ft	2.86 ft	50.84 ft	5.1 ft

Summary

1. Material with %fines < 5% qualifies as a subbase that can achieve a good drainage quality for a typical two- or four-lane pavement section. In addition, a reasonable subbase thickness is required to reach the desired level of drainage quality. However, material with % fines ≥ 5% is unlikely to provide even a fair quality of drainage. It is important to note that there are many existing pavements in Florida that are performing well with higher % fines (10-12 %) and a permeability of approximately 1 x 10^{-4} cm/sec. Some possible explanations include vertical drainage occuring in the subgrade (i.e. subgrade is permeable), better joint sealent, and more importantly, the fact that the water may not have to drain to 85% to prevent pumping. More research on these effects are needed to completely understand how they relate to the overall performance of a pavement system.
2. The joint infiltration rate has shown to be related to pavement drainability. Pavements with a high joint infiltration rate have a shorter time to 85% saturation and a lower minimum average degree of saturation. The opposite scenario is true for a pavement with a low joint infiltration rate.

3. One can relate the joint infitration approach to the time-to-drain approach, by back-calculating a subbase section that satisfies the recommended time to drain. However, the FHWA provides two methods for determining the subbase thickness using a standard joint infiltration rate. These methods provide significantly different results from one another.

Based on the FHWA method #1, which is similar to Darcy's equation, the joint infiltration rate of the section that qualifies as a good quality of drainage is less than the 0.7 ft^3/day/ft.
For the FHWA method #2, which includes the effect of the drawdown of the hydraulic gradient near the edge drain, a pavement section with a good drainage quality has a joint infiltration rate higher than 0.7 ft^3/day/ft. This is because the joint infiltration is an indirect indicator of the quality of drainage that a subbase design will yield. Therefore, the suggested joint infiltration rate for designing a subbase is not typical for every pavement condition. The suggested value should be predetermined based on the time to drain and the method of design in order to obtain a sufficient section. The method based on the time to drain yields a more accurate result. This is because the time to drain is a more direct drainage characteristic. However, more work due to the requirement of water-retention properties and the more complicated design process is a drawback to this method.

Chapter 6 Conclusions and Recommendations

Subbase Soil Properties

The Florida subbase materials used in this research are classified as medium to fine sand. Their grain-size distribution curves are approximately the same range but vary in %fines composition. As a subbase material, their hydraulic properties such as permeability, porosity and water-retention characteristics are directly related to the %fines content.

Joint Infiltration

Joint infiltration rate indicates the inflow and outflow rate of water through the subbase layer, and is not uniform. It varies in magnitude with the joint type (longitudinal or transverse) and location of the joint with respect to the edge drain within the same line of joint. The suggested uniform value by FHWA is an average value for designing the pavement sub-drainage system including the subbase thickness.

A parametric sensitivity study on the joint infiltration rate concluded the following:

- Joint width has minimal effect.
- Permeability of subbase ↑, joint infiltration ↑ linearly.
- Subgrade slope ↑, joint infiltration ↑.
- Subbase thickness ↑, joint infiltration ↑ ↑.

Pavement Sub-drainage

The drainability of a pavement system is the measurement of the volume of and rate at which infiltrated water is removed from the subbase after precipitation has ceased.

The parametric sensitivity analysis on pavement drainability concluded the following:

- If %fines in the subbase material ↑, drainability ↓.
- If subbase thickness ↑, drainability ↑.

- If subgrade slope ↑, drainability ↑.
- If drainage length ↑ or the number of traffic lanes ↑, drainability ↓.

Based on the FHWA recommended time to drain method, results from the analyses reveal that subbases with %fines < 5% can achieve a good drainage quality for a typical two- or four-lane pavement section. In addition, it provides a reasonable subbase thickness to reach the desired level of drainage quality. Meanwhile, material with % fines ≥ 5% is unlikely to provide even a "fair" quality of drainage (as defined by the FHWA). Table 6-1 shows suggested subbase thicknesses based on the time-to-drain approach. For example, a 24-ft wide pavement (12-ft drainage distance) with a 2% subgrade slope requires a subbase thickness of 0.77 ft consisting of 0% fines for good drainage quality. However, the thickness increases to 2.1 ft for a 48-ft pavement width (24-ft drainage distance) under identical conditions. The subbase design method based on the time to drain provided a more realistic model; however, the requirement of water-retention properties and a more complicated design process are drawbacks of this method.

The joint infiltration rate can relate to the pavement drainability. Pavement with a high joint infiltration rate has better drainability in terms of less drainage time and less retained water. The recommended value of 0.7 ft^3/day/ft was found to be too high or too low, depending on which method is applied to calculate the subbase thickness. Using too high of a value will result in an oversized section, while using too low of a value will result in insufficient drainage. The suggested joint infiltration rate for designing a subbase of pavement is not typical for every pavement condition. This value should be predetermined based on the time to drain and the method of design in order to obtain a sufficient and economical section.

Both design approaches reveal that soil properties and sectional geometry of the subbase have major effects on improving sub-drainage quality.

Table 6-1. Suggested subbase thickness based on time-to-drain approach.

%Fines	Subbase thickness (ft) for (conditions: 12 ft drainage distance, 2% subgrade slope)	
	Time to 85% saturation = 5 hrs	Time to 85% saturation = 10 hrs
0	0.77	Less than 0.5 ft
1	0.93	0.56
2	1.21	0.72
3	1.70	0.97
4	2.90	1.22
5	N/A	1.61
6	N/A	2.25
7	N/A	3.8
8	N/A	N/A

%Fines	Subbase thickness (ft) for (conditions: 24 ft drainage distance, 2% subgrade slope)	
	Time to 85% saturation = 5 hrs	Time to 85% saturation = 10 hrs
0	2.17	1.09
1	3.14	1.50
2	5.3	2.00
3	N/A	2.75
4	N/A	6.0
5	N/A	N/A

Note: N/A = the material with the corresponding %fines cannot satisfy the specified time to drain

Further Suggestions

The FHWA recommendations for quality drainage scenarios consider the time duration to reach a certain degree of saturation in the subbase, such as 85% average degree of saturation or 50% drainage. But even the application of the same saturation degree that is used for various subbase design conditions yields different locations of the water level in the subbase. For example, an 85% average degree of saturation locates the phreatic level 18 cm below the pavement for a 30-cm thick subbase, but it will be located 32 cm below the pavement for a 60-cm thick subbase. This raises the important question; will pumping occur if the phreatic level drops 1cm, 2 cm, etc... from the pavement surface? Perhaps, the 18 cm is not a reasonable value and a smaller distance could be used. In addition, the question of the minimum quantity of water needed to enable pumping distress is more likely to be described by the phreatic level in the subbase than by the saturation degree. A more detailed explanation of the analysis of the phreatic level is found in the Appendix. Therefore, a further study on the relationship of pumping and water level in the subbase will be helpful in better understanding the pumping phenomenon and for improving the recommended time to drain.

References

1. AASHTO, 1986, *AASHTO Guide for Design of Pavement Structures*.
2. Brooks R.H. and Corey A.T., 1964, *Hydraulic Properties of Porous Media*, Colorado State University Hydrology Paper 3.
3. Brooks R.H. and Corey A.T., 1964, *Hydraulic Properties of Porous Media and Their Relation to Drainage Design*, Transactions of the American Society of Agriculture Engineers VOL.7 No.1 p.26-28.
4. Cedergren H.R.1987, *Drainage of Highway & Airfield Pavements*.
5. Cedergren H.R.1989, *Seepage, Drainage and Flow Nets.*
6. Das B.M., 1985, *Principles of Geotechnical Engineering*, 3rd edition.
7. Davidson J.L., *Soil Mechanics Laboratory Manual*, Department of Civil Engineering, University of Florida.
8. ERES Consultants,Inc.,1987, *Techniques for Pavement Rehabilitation*, Participant's Notebook, October 1987.
9. FHWA, 1992, *Drainage Pavement Systems*: Participant Notebook March 1992, Pub.No. FHWA-SA-92-008.
10. Hassan H.F., Feng A. and White T.D., 1997, *A Realistic Model for Drainage of Water through a Jointed Concrete Pavement*, Papers: 6th International Purdue Conference on Concrete Pavement, Nov.18-21,1997 p.285-299.
11. Lambe T.W. and Whitman R.V., 1969, *Soil Mechanics*, John Wiley and Sons, Inc.
12. Leonards G.A., 1962, *Foundation Engineering*, Dewatering Chapter by Charles I. Mansur and Robert I. Kaufman.
13. McEnroe B.M., 1994, *Drainability of Granular Bases for Highway Pavements*, Kansas Department of Transportation, Report No. K-TRAN: KU-93-4

14. Mishra S., Parker J.C. and Singhal N., 1989, *Estimation of Soil Hydraulic Properties and Their Uncertainty From Particle Size Distribution Data*, Journal of Hydrology, 108 (1989) 1-18.

15. Moulton L.K., 1980, *Highway Subdrainage Design*, Repot No. FHWA-TS-80-224, Office of Research and Development, Federal Highway Administration.

16. Rawls W.J., Brakensiek D.L. and Miller N., 1983, Green-Ampt Infiltration Parameters From Soils Data, Journal of Hydraulic Engineering ASCE Vol.109 No.1 Jan.1983.

17. Ridgeway H.H., 1976, *Infiltration of Water Through the Pavement Surface*, Transportation Research Record 616, 1976.

18. Software Manual of FASTSEEP

19. Software Manual of VISUALMODFLOW

20. Tinjum J.M., Benson C.H. and Blotz L.R., 1997, *Soil-Water Characteristic Curve for Compacted Clays*, ASCE Journal of Geotechnical and Geoenvironmental Engineering 1997 p.1060-1070.

21. U.S. Army Corps of Engineers, 1965, *Drainage and Erosion Control-Subsurface Drainage Facilities for Airfields*, Technical Manual TM5-820-2, August 1965.

22. *User and Technical Guide of SOIILPROP version2.1*, Environmental Systems & Technologies, Inc. 2701 Ramble Road, Suite2 Blackburg VA 24060.

23. Van Wijk A.J., 1985, *Rigid Pavement Pumping: 1) Subbase Erosion, 2) Economic Modeling*, Report No. FHWA/RD-86-121, September 1985.

24. Van Wijk A.J. and C.W. Lovell, 1985, *Erosion of Subbase Materials Under Rigid Pavements*, Proceedings Third International Conference on Concrete Pavement Design and Rehabilitation, Purdue University, April 23-25, 1985.

Appendix

Combination confined & unconfined flow equations

Unconfined Flow

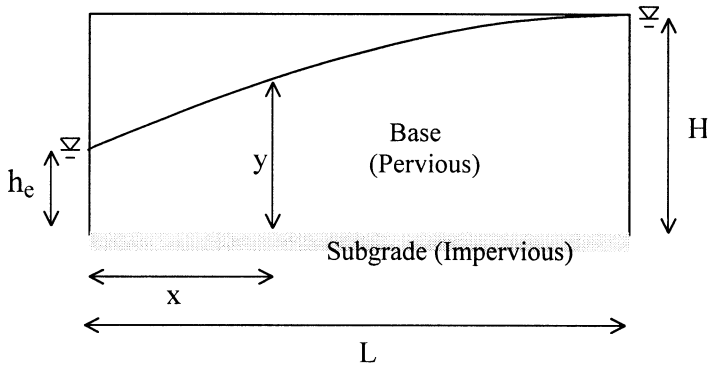

Consider 1 unit width,

From Darcy's Law,

$$Q = kiA$$

$$i = \frac{dy}{dx} \quad \text{and} \quad A = y \cdot 1$$

so $$Q = ky(1)\frac{dy}{dx}$$

or $$y \cdot dy = \frac{Q}{k}dx$$

integrate from $x = 0, y = h_e$ to $x = L, y = H$

$$\int_{he}^{H} y dy = \frac{Q}{k}\int_{0}^{L} dx$$

$$\frac{1}{2}(H^2 - h_e^2) = \frac{QL}{k}$$

$$Q = \frac{k}{2L}(H^2 - h_e^2) \qquad \leftarrow \text{Unconfined Flow Equation}$$

Confined Flow

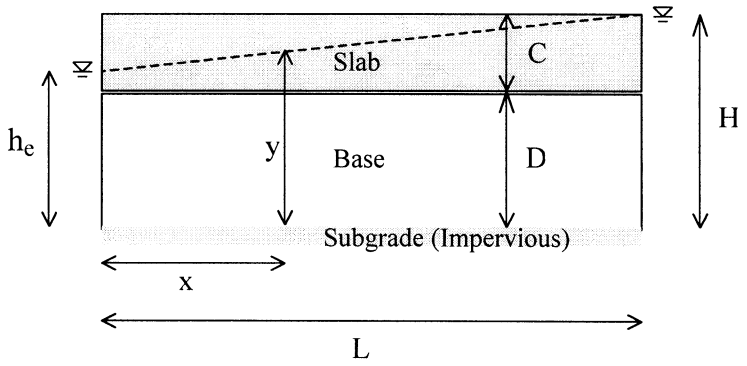

Consider 1 unit width,

Darcy's Law, $Q = kiA$

$$i = \frac{dy}{dx} \quad \text{and} \quad A = D \cdot 1$$

so $$Q = kD(1)\frac{dy}{dx}$$

or $$dy = \frac{Q}{kD}dx$$

integrate both sides

$$\int_{he}^{y} dy = \frac{Q}{kD}\int_{0}^{x} dx$$

$$y - h_e = \frac{Qx}{kD}$$

at $x = L, y = H$,

$$H = \frac{QL}{kD} + h_e$$

$$Q = \frac{kD}{L}(H - h_e)$$ ← Confined Flow Equation

Flow under rigid pavement underlain with impervious subgrade

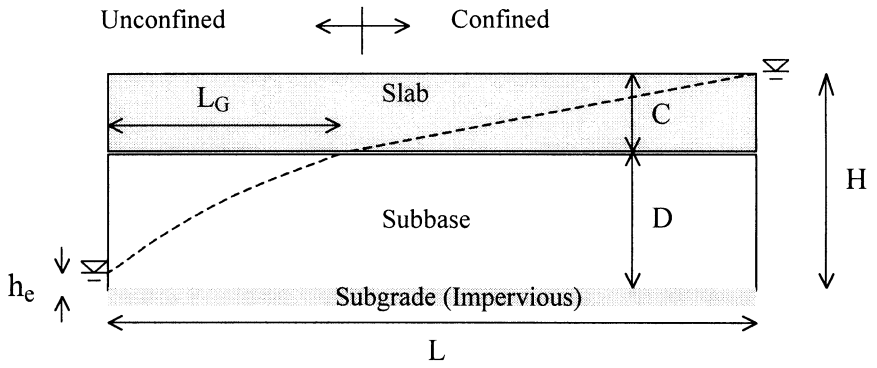

In this case, the flow under the pavement consists of both confined and unconfined flow as shown in the figure above. Therefore, the confined and unconfined flow equations must be combined to develop the flow model.

Confined flow $$Q_1 = \frac{k}{2L_G}(D^2 - h_e^{\,2})$$

Unconfined flow $$Q_2 = \frac{kD}{(L - L_G)}(H - D)$$

But $Q_1 = Q_2$

so that $$\frac{k}{2L_G}(D^2 - h_e^{\,2}) = \frac{kD}{(L - L_G)}(H - D)$$

$$L(D^2 - h_e^2) - L_G D^2 + L_G h_e^2 = 2L_G HD - 2L_G D^2$$

Solving for L_G, $$L_G = \frac{L(D^2 - h_e^2)}{2DH - D^2 - h_e^2}$$

Plug L_G in Q_1 equation,

$$Q = \frac{k(D^2 - h_e^2)(2DH - D^2 - h_e^2)}{2L(D^2 - h_e^2)}$$

$$Q = \frac{k}{2L}(2DH - D^2 - h_e^2) \quad \leftarrow \text{Combined flow equation}$$

Square-Foot Model

The model has 1.152 ft^2 of area and its walls are 20 inches high. At the bottom is a porous stone sealed with silicon gel. Each of the four sides had a porous-stone opening, 4 x 6 inches. The openings on the sides of the box were two inches above the bottom of the container. This was done in order to measure the horizontal and vertical flows within the first one-foot of subbase. This equates to a volume of soil of 1.152 ft^3. Each of the horizontal ports had a collection bin that funneled down into a hose. The vertical catch bin ran into a separate hose. The vertical flow collection bin was open to atmospheric pressure due to tubes inserted in the side of the bin. Two exit hose ports were drilled into the retaining wall on each side of the propagated joint at a height of 3.5 cm.

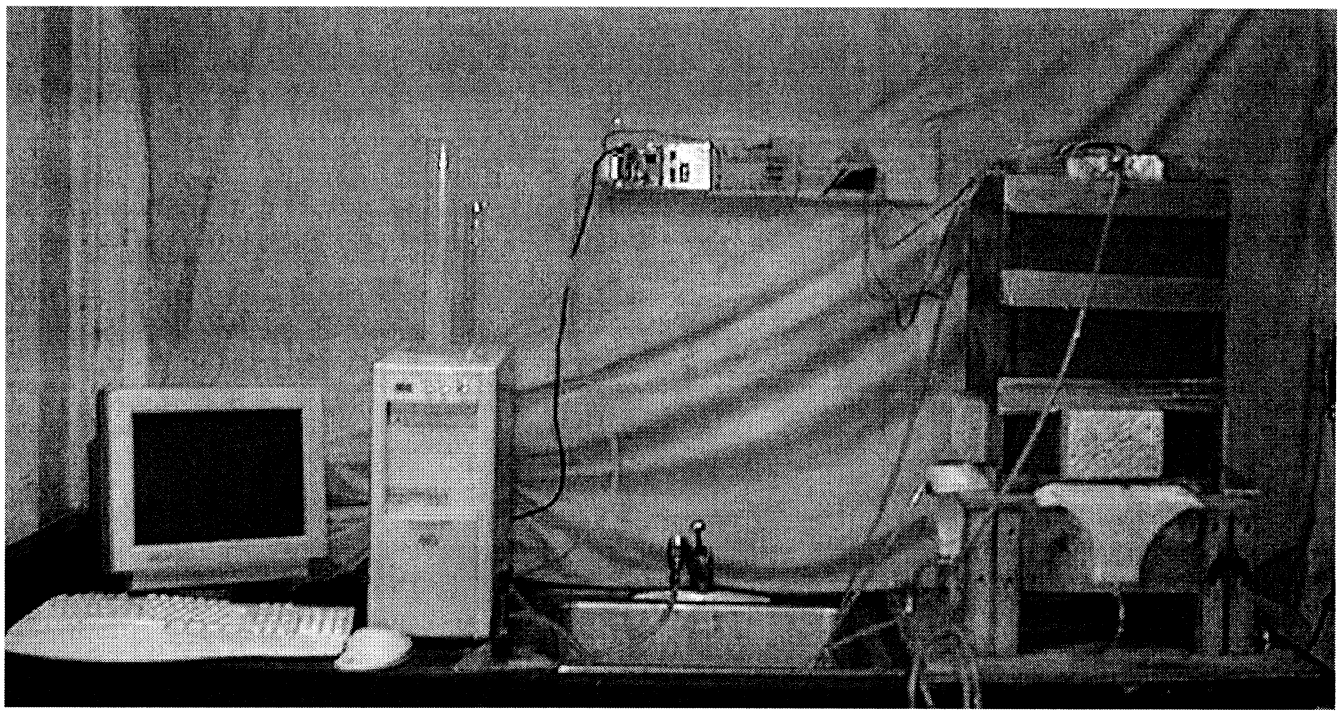

Above: Photo of test setup of the square-foot model

Procedure

The soil sample was to be compacted at the maximum dry unit weight and optimum water content found by the Modified Proctor Hammer test. The mass of soil required to fill one cubic foot was then divided into six lifts and the optimum water content for each lift was added. The soil was compacted in the box per lift. Detectors were placed at the bottom and the top of the one foot soil layer. The FHWA specified flow rate of 0.7 ft^3/day/ft was measured and verified then introduced into the propagated joint of the PCC pavement. The computer timer was then started. Saturation times were recorded by the computer. When the saturation velocity measurements were completed the flow rate was increased until a constant head of 3.5 cm was reached. Both horizontal and vertical flow rates were taken once the system was at steady state. The results of these tests are listed in tables on the next page.

Results

ASTM Results

Sample	Description	FDOT Permeability	Sieve Analysis	Modified Proctor	Opt. Water Content
		cm / s	% Fines	pcf	%
1	72280-3424 004H		9.82	106.61	9.31
2	Test Pit Tan Sand	0.00061375	4	108.7	10.9
3	Beck Pit Subgrade	0.003278	2	104.5	13.6
4	Goldhead	0.0004317	6	108.2	9.2
5	GrovePark/ Whitehurst	0.00002804	13	119.2	9.2
6	Middleburg-Clay Co.	0.00004873	9	109.9	11.2

1 ft^2 Simulator Results - - depth of one foot, soil only.

Sample	Description	Vertical Volume	Vertical Time	Vertical Flow	Horizontal Volume	Horizontal Time	Horizontal Flow
		cc	sec	cu. ft / day / ft	cc	sec	cu. ft / day / ft
1	72280-3424 004H	800	1283	1.90253294	16.75	1283	0.039834283
2	Test Pit Tan Sand	770	1140	2.0608896	62	120	1.576446722
3	Beck Pit Subgrade	680	180	11.5267072	655	537	3.721652922
4	Goldhead	850	960	2.701572	230	2160	0.324894934
5	GrovePark/ Whitehurst	104.7	326.9	0.97723861	0		0
6	Middleburg-Clay Co.	93.18	324.3	0.87668709	0		0

1 ft^2 Simulator Results - - total depth of six inches, 3" of #57 stone with soil added to complete 6"

Sample	Description	Vertical Volume	Vertical Time	Vertical Flow	Horizontal Volume	Horizontal Time	Horizontal Flow
		cc	sec	cu. ft / day / ft	cc	sec	cu. ft / day / ft
1	72280-3424 004H	618.7	377.208	5.00458507	370.2	407.02	2.99450039
2	Test Pit Tan Sand	422.7	727	1.77405341	40.8	727	0.171235816
3	Beck Pit Subgrade	277	125.7	6.72377769	206	137.8	4.561281308
4	Goldhead	289	541.4	1.62872756	0		0
5	GrovePark/ Whitehurst	506.4	552.5	2.79659946	111.4	552.5	0.615207701
6	Middleburg-Clay Co.	140	65.92	6.48006991	80	90.14	2.707954031

SUMMARY

Sample	Description	NO STONE Horizontal Flow	W / #57 STONE Horizontal Flow
		cu. ft / day / ft	cu. ft / day / ft
1	72280-3424 004H	0.039834283	2.99450039
2	Test Pit Tan Sand	1.576446722	0.171235816
3	Beck Pit Subgrade	3.721652922	4.561281308
4	Goldhead	0.324894934	0
5	GrovePark/ Whitehurst	0	0.615207701
6	Middleburg-Clay Co.	0	2.707954031

Observations

Percent Fines. The percent of fines in the subbase affects the soil permeability, thus ability to drain horizontally and vertically. Sample #1 had the largest fines content (9.82%) and the lowest flow rates. Sample #3 had the lowest fines content of two percent. Sample #3 also had the highest flow rates and was the most isentropic in behavior.

Surging. Surging of the outflow was noticed in Sample #1 and Sample #4, which were higher in fines content. Sample #3 had the steadiest outflow observed. As the percent fines increased, so did the occurrence of surging.

Gradation. Compaction was easily achieved with the uniform-graded soils. Samples 2, 3, and 4 were compacted to 100 percent of the Modified Proctor Hammer specifications. Sample #1 was a well-graded soil which was only compacted to 94.5% of what the specifications called for.

Storage. The highest storage capacity was exemplified by Sample #4. The next highest was Sample #1. Both of these samples were on the higher end of fines content spectrum--6 and 9.82% respectively. They also had small horizontal flow rates. The samples seemed to soak the water up but were not able to move the water rapidly.

Conclusion

Localized water under intense pressure with a small vertical flow rate is believed to lead to a larger horizontal flow taking place at the pavement-subbase interface. This high pressure concentration can be attributed to a restriction of flow caused by a high fines content.

The idea for an erosion-free subbase is that the soil should be rigid yet porous enough to drain standing water on the pavement that is entering the joint. The soil would have a medium to high storage capacity. It would drain the water at a rate fast enough to discourage any deterioration of the subgrade. The soil would be isentropic. Isentropic behavior is the condition where flow rate is nearly equal (or of the same order of magnitude) in all directions. This is desired in order to plume the water over a larger surface area within the subbase to deter a concentration of water in one area--lessening the possibility of erosion and void production. Distribution over a larger surface area would also mean less of a pressure gradient during pumping action.

This preliminary investigation has concluded that efficient drainage is possible for Florida conditions using a uniform grade soil containing less than two percent fines and permeability of 3 x 10^{-3} cm/s.

The crack infiltration rate (Ic) prescribed by the FHWA Highway Subdrainage Design manual is 2.4 ft^3/day/ft of crack. It is stated that this value is based on a "minimum amount of research." FHWA-IP-90-012 prescribes an infiltration rate of 0.7 ft^3/day/ft of crack. The equation for the design infiltration rate:

$$q_i = I_c*(N_c/W + W_c/(W*C_s)) + k_p \ (ft^3/day/ft^2), \text{ where}$$

q_i = design infiltration rate per square-foot of base drainage layer

I_c = joint infiltration rate (ft^3/day/ft)

N_c = number of contributing longitudinal joints = number of lanes plus one

W = width of permeable base (ft)

W_c = Length of contributing traverse joints (ft)

C_s = traverse joint spacing (ft)

k_p = PCC pavement permeability ($ft^3/day/ft^2$)

For an I_c = .7 $ft^3/day/ft$, Using N_c = (3 lanes + 1), W = (12+12+14)ft, W_c = W = 38 ft, C_s = 16 ft, and k_p = 0:

$$q_i = .7*(4/38 + 38/(38*16)) + 0 = .117\ ft^3/day/ft^2$$

For an I_c = 2.4 ft3/day/ft, Using the same values stated above:

$$q_i = 2.4*(4/38 + 38/(38*16)) + 0 = .403\ ft^3/day/ft^2$$

The second value for the infiltration rate is 3.4 times larger than that found using .7 $ft^3/day/ft$. The data obtained from preliminary tests conducted on cubic-foot samples supports the higher value for infiltration. The test were conducted on four samples with FDOT permeabilities ranging from 4×10^{-4} to 3×10^{-3} cm/s. The samples were typical Florida soils used for subbase taken from various locations throughout the state. Volumetric outflow rates were measured for a 3.5 cm constant head of water in the propagated joint between slabs. The 3.5 cm of water was used to simulate conditions during a storm where enough water was present to fill the joint. This same approach was used by Ridgeway to take insitu measurements for PCC pavement. The joint infiltration rates measured by Ridgeway ranged from 0 to 1.92 $ft^3/day/ft$ (Stated as .08 $ft^3/hr/ft$).

It was assumed by Ridgeway that the "traverse cracks were sealed, and the longitudinal edge cracks were filled with sand and other debris." In actuality, nothing was installed to seal the edges of the pavement the entire depth of the slab during this experimentation. The absence of known boundary conditions gives a poor assessment of joint infiltration. Although some discrepancy is evident in reading the Ridgeway report, the values for I_c stated in that report are of

the same magnitude as the values obtained from the square-foot model. In the model, the vertical flow ranged from 2.06 to 11.52 ft^3/day/ft. The horizontal flow ranged from .04 to 3.72 ft^3/day/ft. The total combined flow ranged from 1.94 to 15.25 ft^3/day/ft.

The experimentation conducted at the University of Florida was preliminary. The main purpose of the data stated in this report was to begin a standardization, so comparison of different tests on one soil agree in value. The similarity between the insitu measurements of Ridgeway and the data of the square-foot model is reassuring. This test does not represent true field conditions and a strong conclusion should not be yielded. But this testing scenario does give hints of some of the factors involved and was used in order to further evaluate the Florida soils and gain a better understanding of the conditions being tested.

Analysis of soil layering using the 3-in x 6-in x 3-ft infiltration model

Using the 3" x 6" x 36" soil sectioning model, two types of testing environments were developed to study the effects of soil layers with respect to the layer's permeability and thickness and the effects of changing the soil height on the overall drainage of the soil. The permeability of the coarse soil and fine soil were lab tested at 0.078 cm/s and 0.025 cm/s respectively.

1. Testing Scenario 1

The first group of tests used a combination of coarse and fine sand layers to observe the drainage patterns and what effect the layer's thickness and soil properties has on it. Each of the respective tests had the same initial head condition.

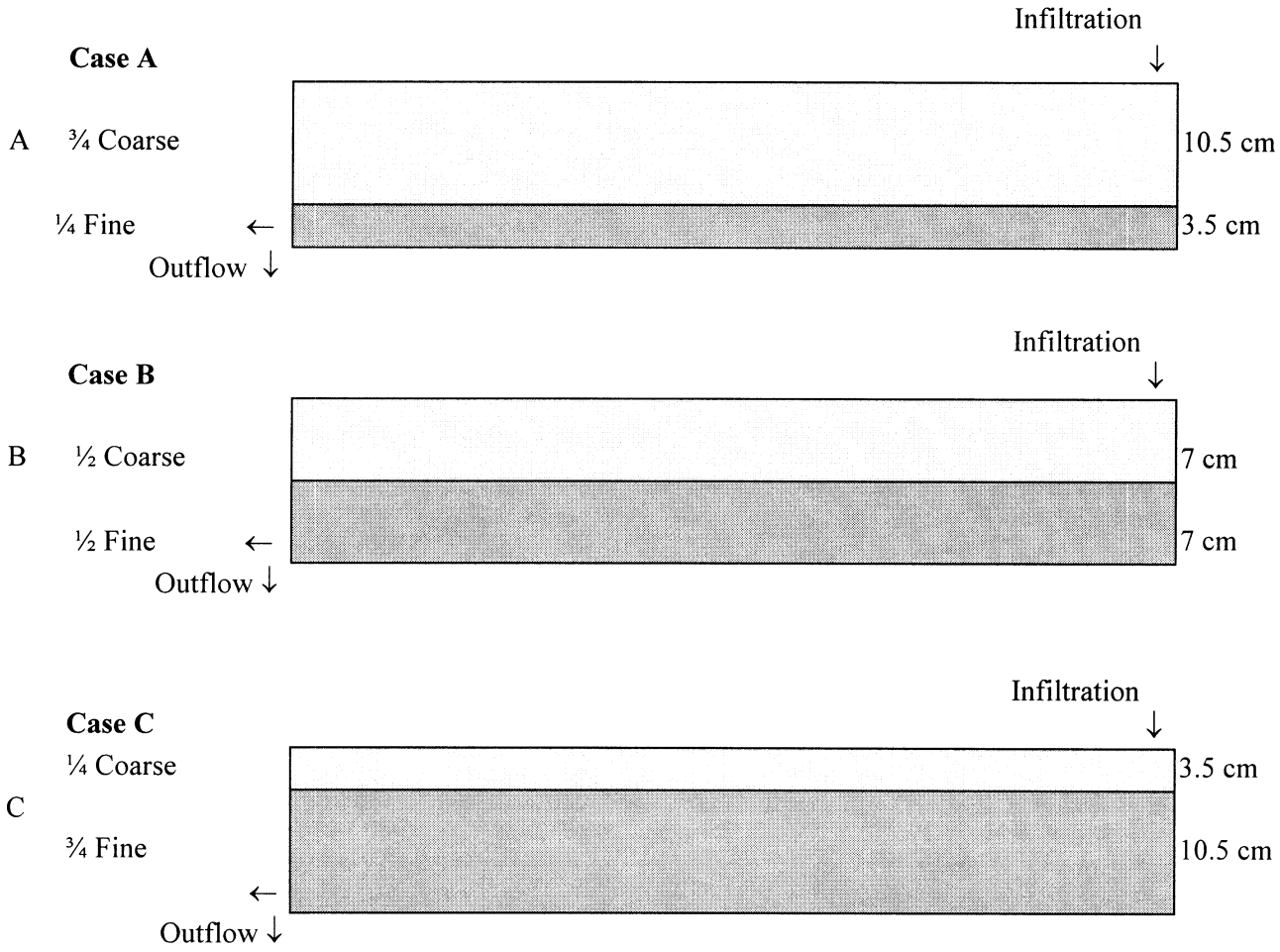

The results of each case are presented on the next few pages.

Results: A - ¼ Fine Sand Layer and ¾ Coarse Sand Layer

Test Results

0% Slope	
Vert. Avg Flow - (cc/s)	5.17
Horiz Avg Flow - (cc/s)	0.51
Total Flowrate - (cc/s)	5.68
% Vert of Total Flow	91.1
% Horiz of Total Flow	8.92

2% Slope	
Vert Avg Flow - (cc/s)	5.48
Horiz Avg Flow - (cc/s)	0.65
Total Flowrate - (cc/s)	6.13
% Vert of Total Flow	89.40
% Horiz of Total Flow	10.60

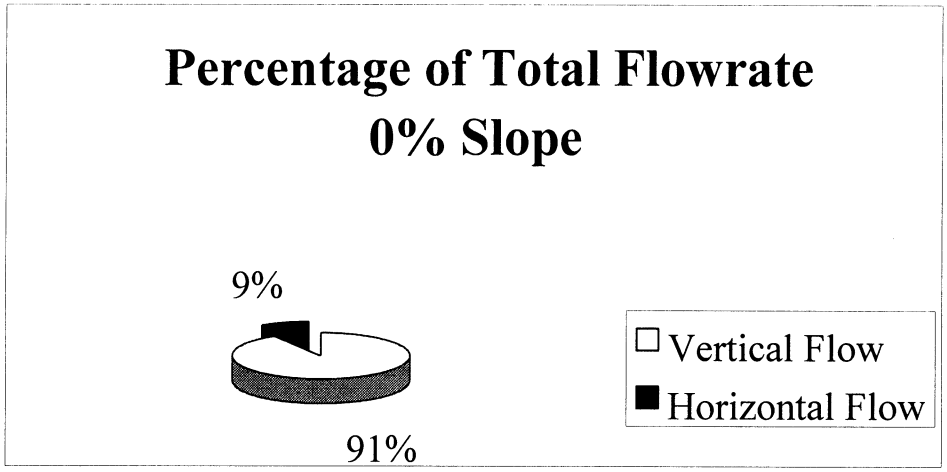

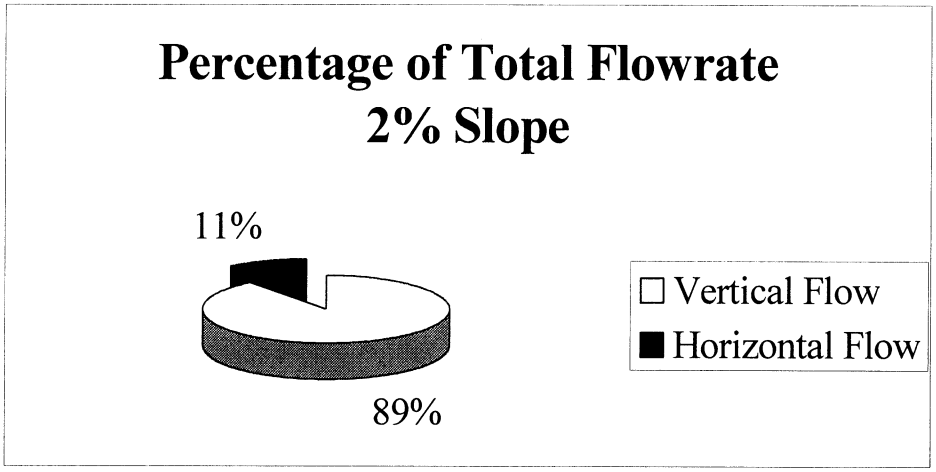

Results: B - ½ Fine Sand Layer and ½ Coarse Sand Layer

Test Results

0% Slope	
Vert Avg Flow - (cc/s)	5.01
Horiz Avg Flow - (cc/s)	0.83
Total Flowrate - (cc/s)	5.84
% Vert of Total Flow	85.7
% Horiz of Total Flow	14.3

2% Slope	
Vert Avg Flow - (cc/s)	4.64
Horiz Avg Flow - (cc/s)	1.30
Total Flowrate - (cc/s)	5.94
% Vert of Total Flow	78.2
% Horiz of Total Flow	21.8

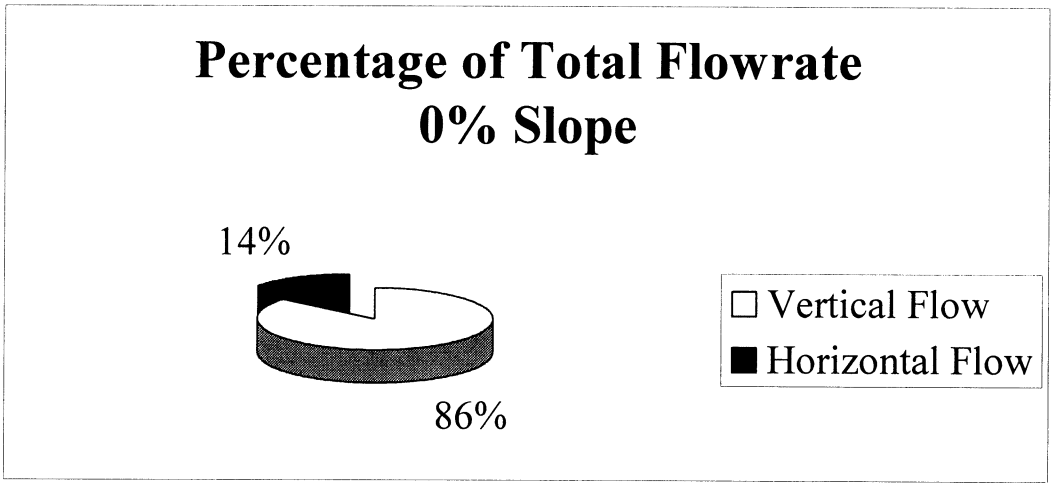

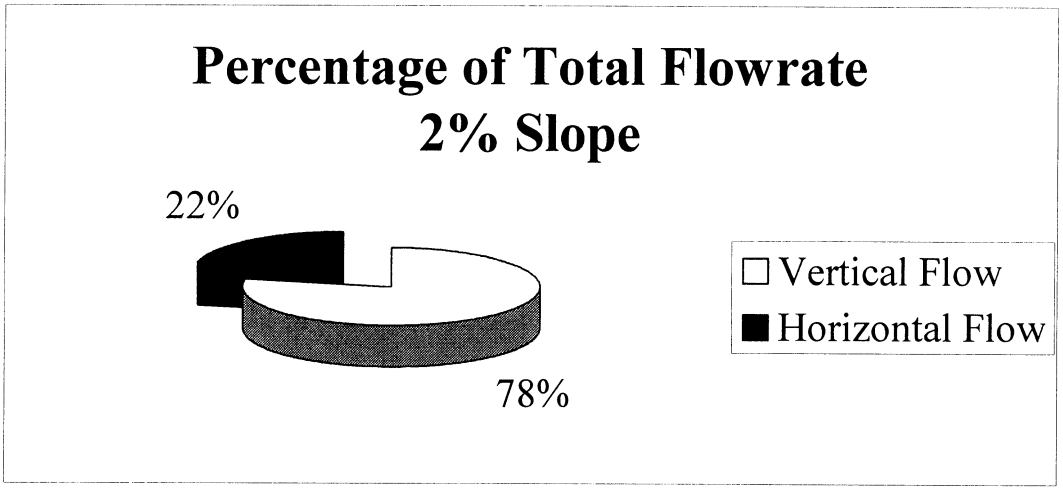

Results: C - ¾ Fine Sand Layer and ¼ Coarse Sand Layer

Test Results

0% Slope	
Vert Avg Flow - (cc/s)	4.11
Horiz Avg Flow - (cc/s)	0.98
Total Flowrate - (cc/s)	5.09
% Vert of Total Flow	80.69
% Horiz of Total Flow	19.31

2% Slope	
Vert Avg Flow - (cc/s)	3.69
Horiz Avg Flow - (cc/s)	1.37
Total Flowrate - (cc/s)	5.06
% Vert of Total Flow	72.98
% Horiz of Total Flow	27.02

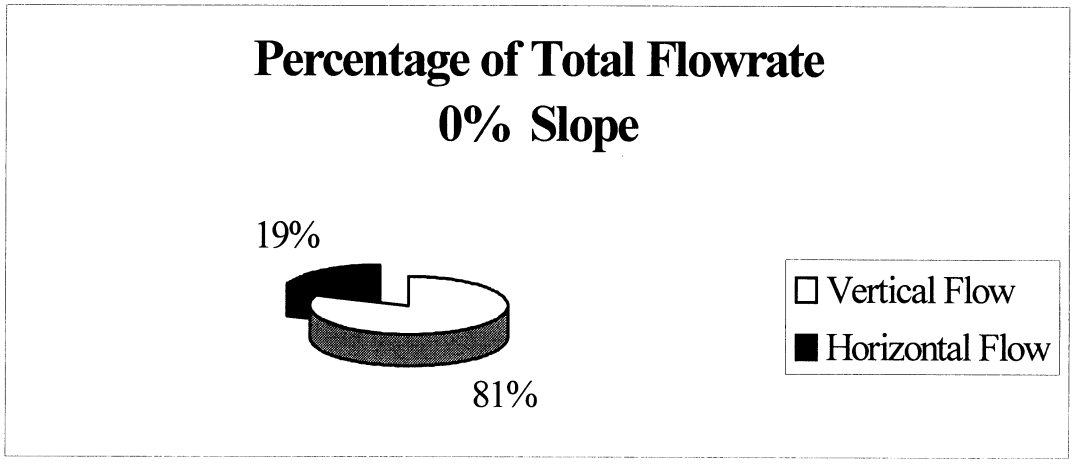

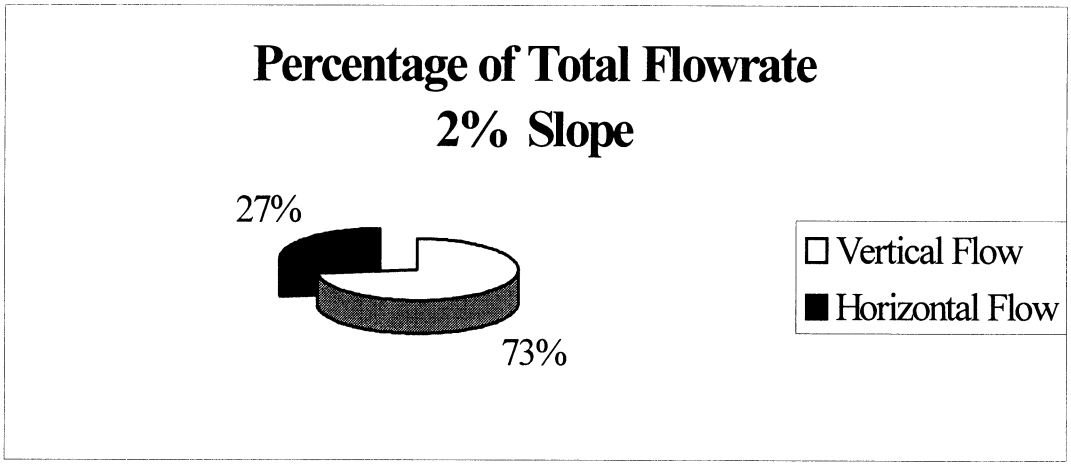

Overall Case Comparison for Testing Scenario 1

Case A had a higher vertical flow and a lower horizontal flow because water drains through the bottom screen faster than through the side screen. This is because the fine sand layer is relatively thin compared to the coarse layer and does not impede the vertical flow a great deal. Meanwhile, Case C has a lower vertical flow and a higher horizontal flow since the water is impeded by the fine sand layer which forces the drainage in the lateral direction.

The flowrates from cases A, B, and C do not vary widely because the k of the coarse and fine material used are 0.078 / 0.025, a 3.12 coarse to fine permeability ratio.

Case A is representative of the situation when the water table is close to the subbase layer, and Case C represents the field case that the water table is low and distant from the subbase.

2. Testing Scenario 2

The second group of tests used a fine sand layer to observe drainage patterns and what effect the layer's height has on it. Observations were made of the soil's ability to effectively drain the water that was infiltrating, as well noting the amount of standing water between the top of the soil layer and the rigid cover. Studying the affects of using layers that are fractions of the model height can help provide an understanding of how much soil needs to be present in a subbase to effectively drain it without standing water developing. The hard-pan scenario was tested by allowing only horizontal side drainage. Obviously, this situation can lead to pumping. Again each of the test cases had the same initial head condition.

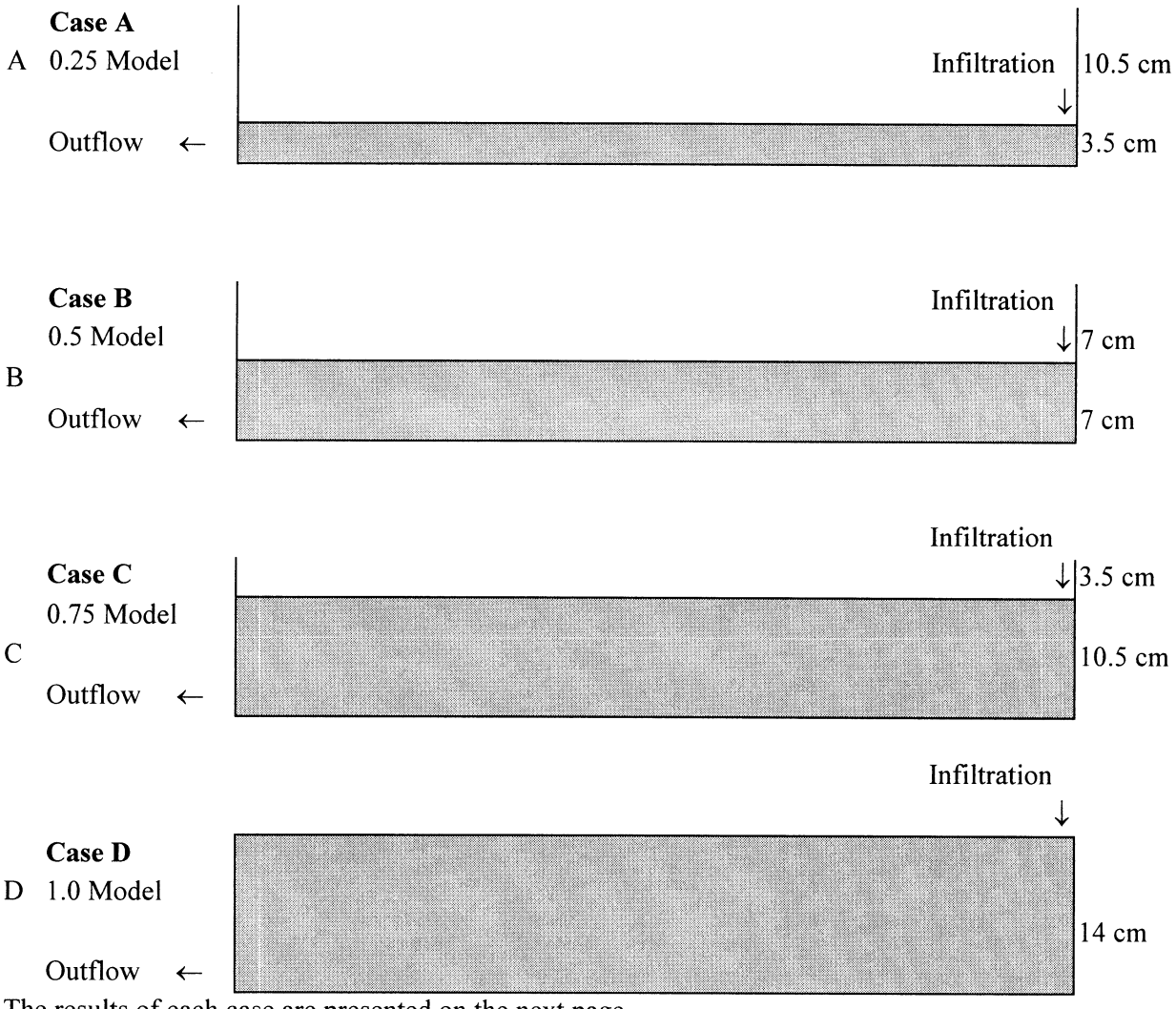

The results of each case are presented on the next page.

Results: Testing Scenario 2

Test Results		
Type of Test Soil Height	Drainage of Soil (cc/s x 10^{-2})	
	0% Slope	2% Slope
A – 0.25	2.32	4.34
B – 0.5	3.39	5.85
C – 0.75	4.56	7.05
D – 1.0	6.53	8.44

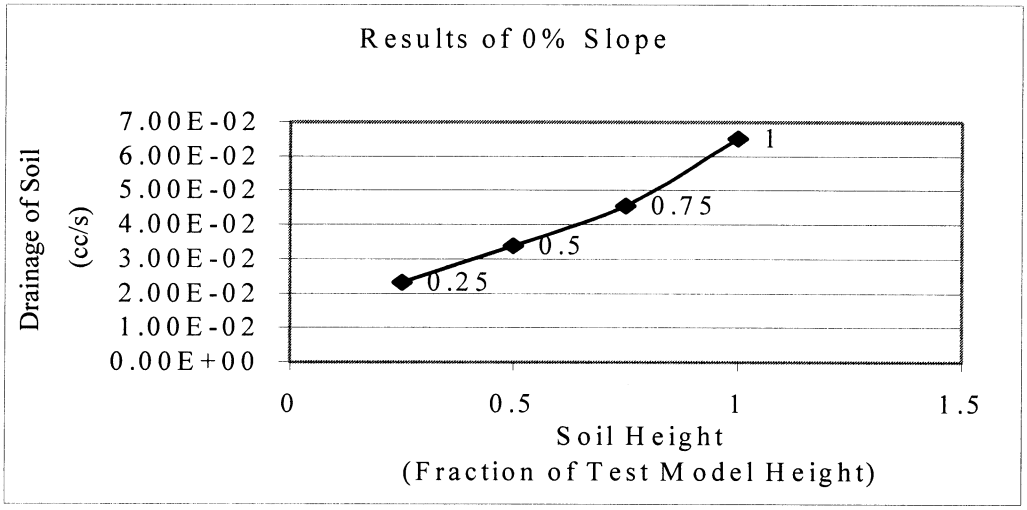

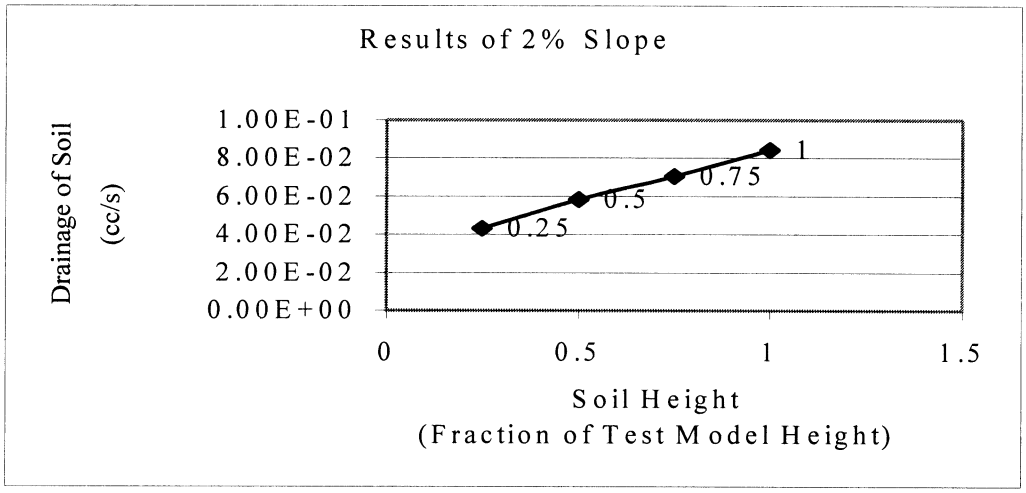

Overall Comparison for Testing Scenario 2

These tests can help to understand what effect a hard-pan layer can have on the drainage of a subbase. As the height of the soil layer is increased the amount of water ponding between the rigid cover and the top of the soil is reduced. This is exhibited by the greater overall drainage of the soil as the soil height is raised.

An effective height of soil must be obtained to ensure proper drainage of the subbase, which will prevent standing water.

3. Testing Scenario 3

This testing scheme uses the same principles and procedures as testing scenario 1 but inverses the layering of the soils. The fine sand is placed on the top layer and the coarse sand is used as the bottom layer. Again these tests were run in order to observe the drainage patterns and what effect the layer's thickness and soil properties has on it. Each of the tests had the same initial head condition.

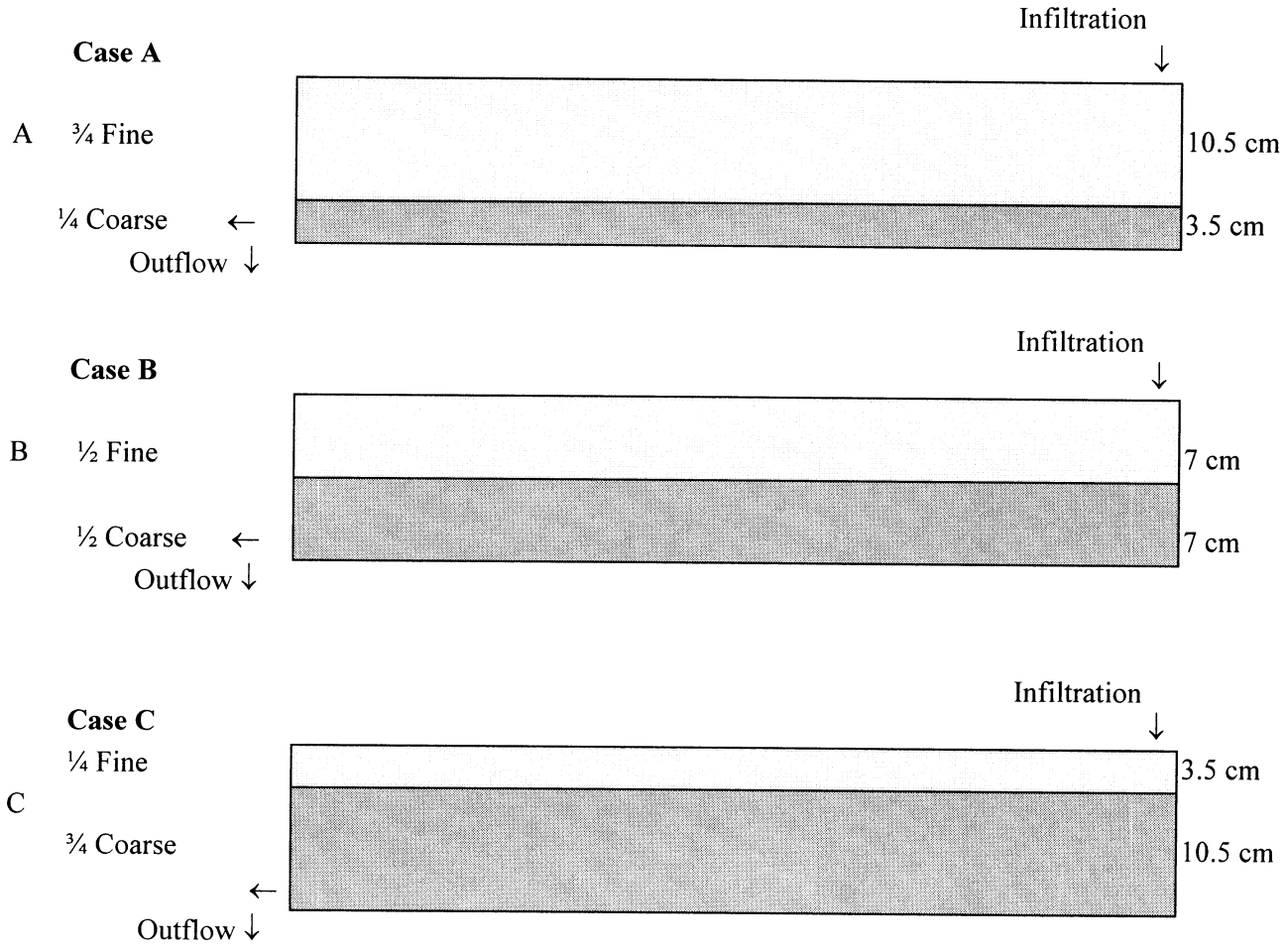

4. Testing Scenario 4

Using the plexiglass model the flowrates of the above testing scheme 3 were measured with only horizontal and then only vertical drainage allowed.

Comparison of Testing Scenarios: Observations and Summary- *Overall graphical*

Testing Scenario 1 Flowrate Comparison

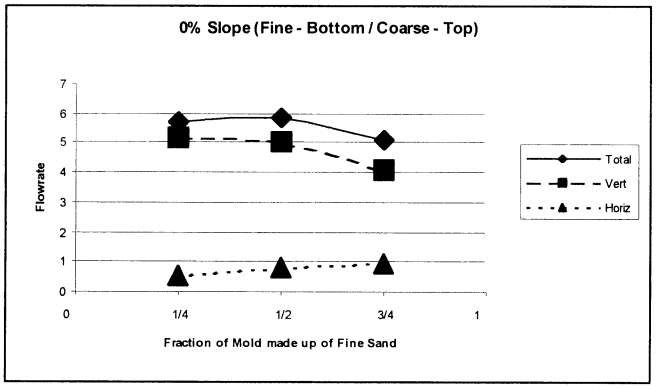

Figure A-1

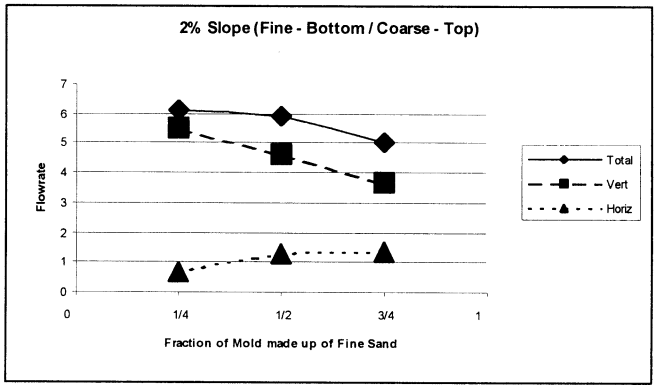

Figure A-2

Testing Scenario 3 Flowrate Comparison

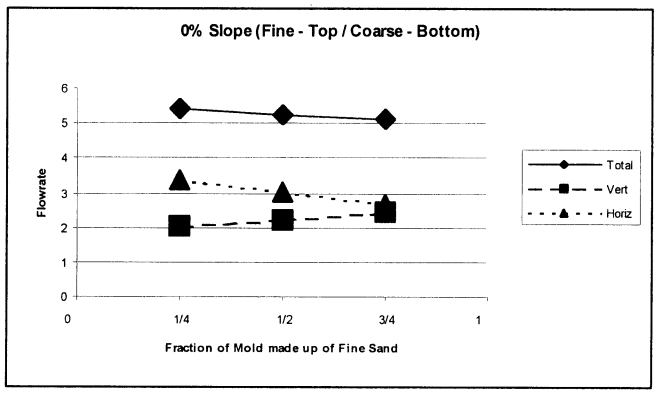

Figure A-3

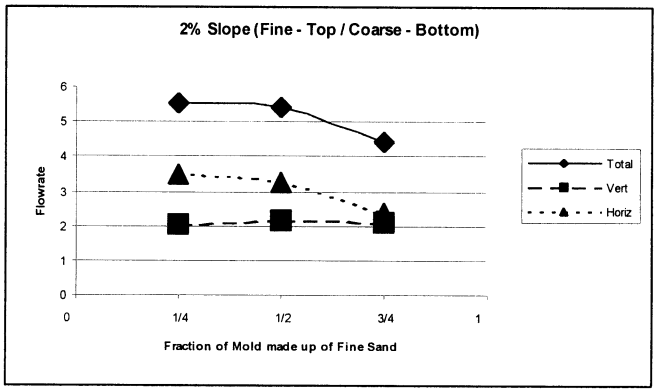

Figure A-4

Testing Scenario 4 Flowrate Comparison

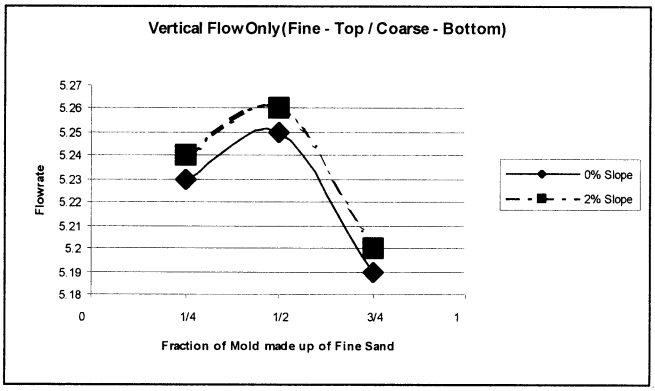

Figure A-5

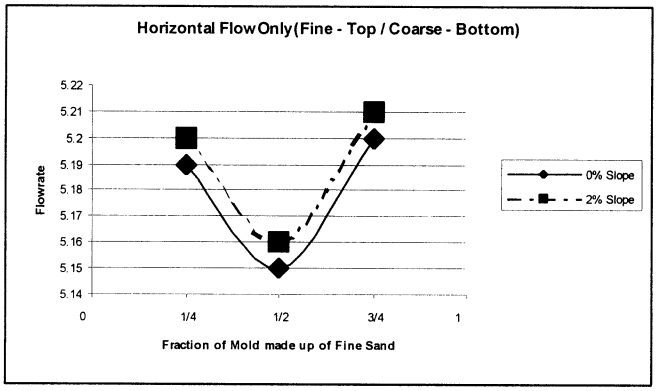

Figure A-6

Conclusions and Recommendations

The model testing data relates the overall drainage of typical subbases and how the drainage of these subbases are effected by grading, ability for vertical flow, and ability for horizontal flow as compared with the layering of soils for each testing scenario.

In testing scenario 1 the fine soil layer was on the bottom and the coarse soil layer was on the top. Figure A-1 shows that the horizontal (side) drainage of the soil increases as the height of the fine soil layer is increased. Figure A-2 shows the same pattern associated with side drainage and fine soil height, as well as showing that a more overall drainage of the soil is accomplished with a 2% side slope.

In testing scenario 3 the fine soil layer was on the top and the coarse soil layer was on the bottom. The data from figures A-3 and A-4 shows that more horizontal (side) drainage is achieved with a fine soil layer on the top. This is due to the lower vertical permeability of the fine soil which impedes vertical flow and causes the drainage to take a more horizontal flow.

Testing scenario 4 was run in order to see how each drainage condition is effected by the layering of the soils. The information from figure A-5 describes how vertical flow is impeded with a greater height of fine soil. Figure A-6 demonstrates how the horizontal (side) drainage of a subbase is highest when the fine soil layer is at its largest height.

It is recommended that further studies would yield more accurate and reliable results if the permeabilities of the two soils differed by several orders of magnitude.

Description of Test Methodology and Results

In order to compare the FEM analysis with the model test, multiple tests had to be performed. Below is the details of how a typical model test was conducted along with photographs of the model on the next few pages showing the changing water level during a test.

Procedure:

1. Prepare a soil sample of desired % fines and permeability.
2. Set drainage condition of the model – horizontal / vertical.
3. Fill the box model with 4 lifts of the soil sample and compact to desired density specification denoting the mass of the entire soil sample added.
4. Place the simulated rigid pavement cover on the model (if test so requires) and begin the water infiltration through the joint. (Note: Water is supplied by a marriot tank with a flowmeter attached which allows for an adjustable infiltration rate delivered with a constant head).
5. Adjust the infiltration rate until a constant head has been established.
6. Using the piezometers labeled 1-8, denote the water levels in the soil at each region of the soil specimen at intermediate time periods.

When the water begins to drain from the vertical or horizontal drain outlets, begin to take mass readings of the drainage water for measured timed intervals. Repeat trials at 25-minute intervals and cease once the soil sample has been in a saturated state for at least a 25-minute time period. (Note: Continue to denote the water level in the piezometers for each trial.)

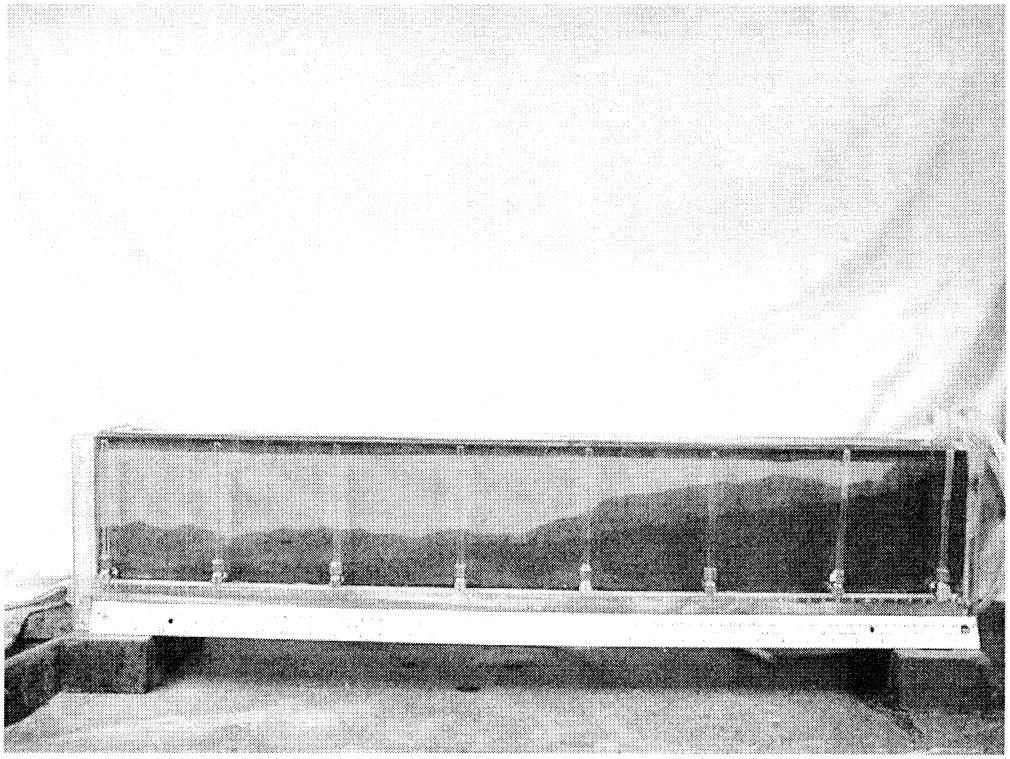

Above: Picture of soil sample #4 in box model: steady flow for 2 hours

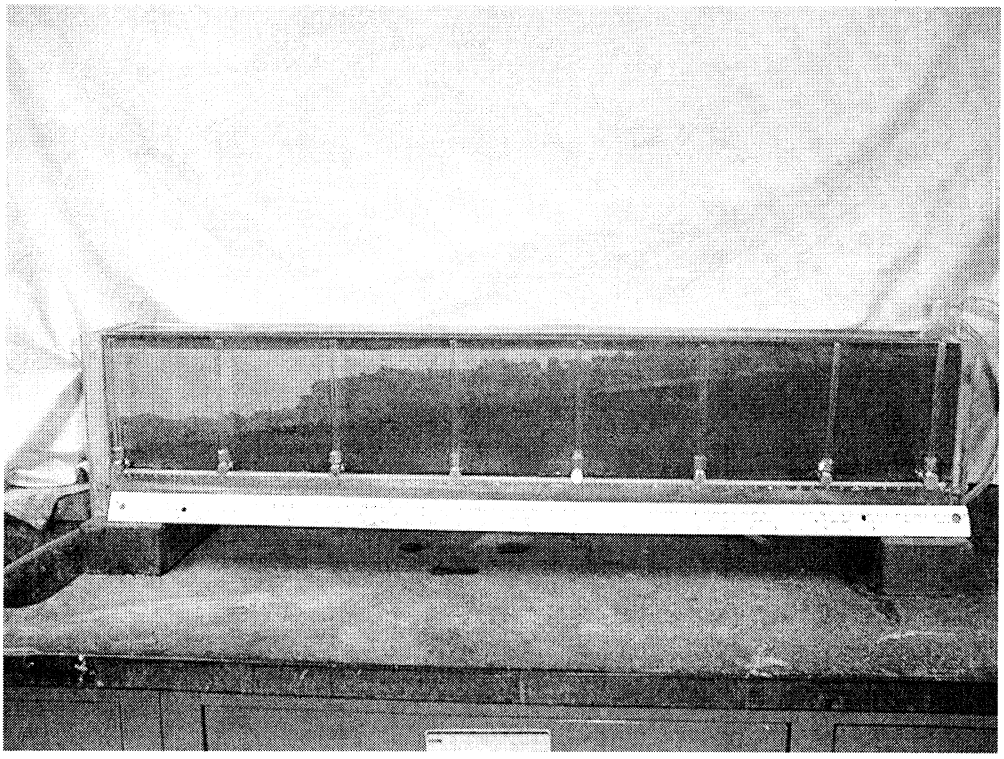

Above: Picture of soil sample #4 after 4 hours with a steady infiltration

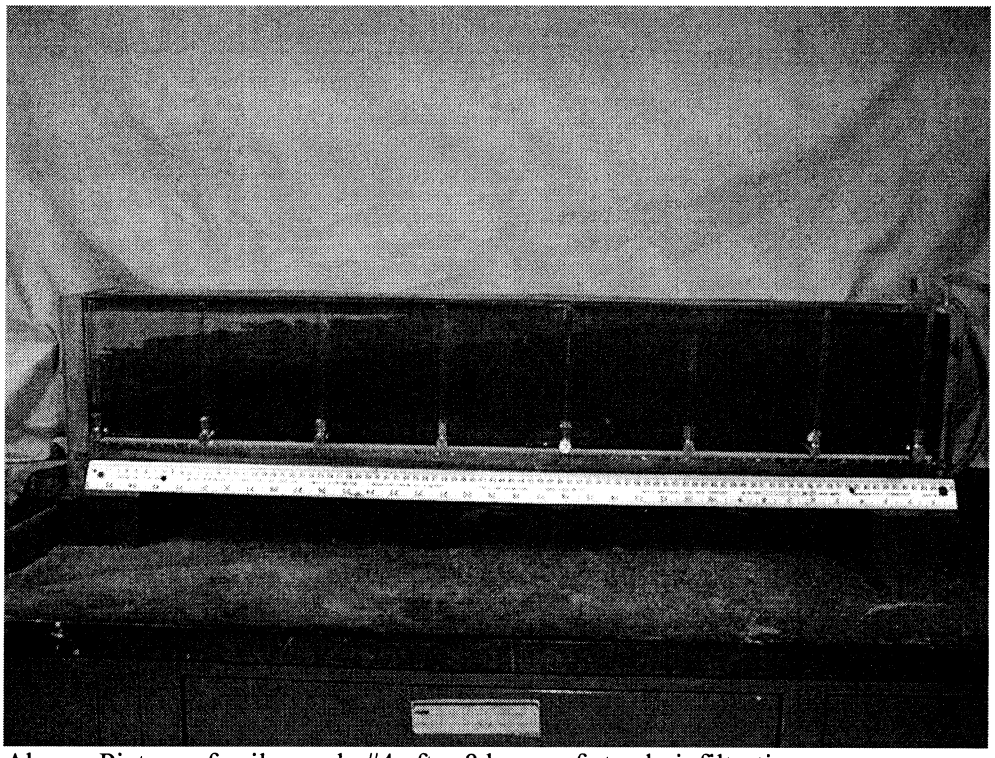

Above: Picture of soil sample #4 after 8 hours of steady infiltration

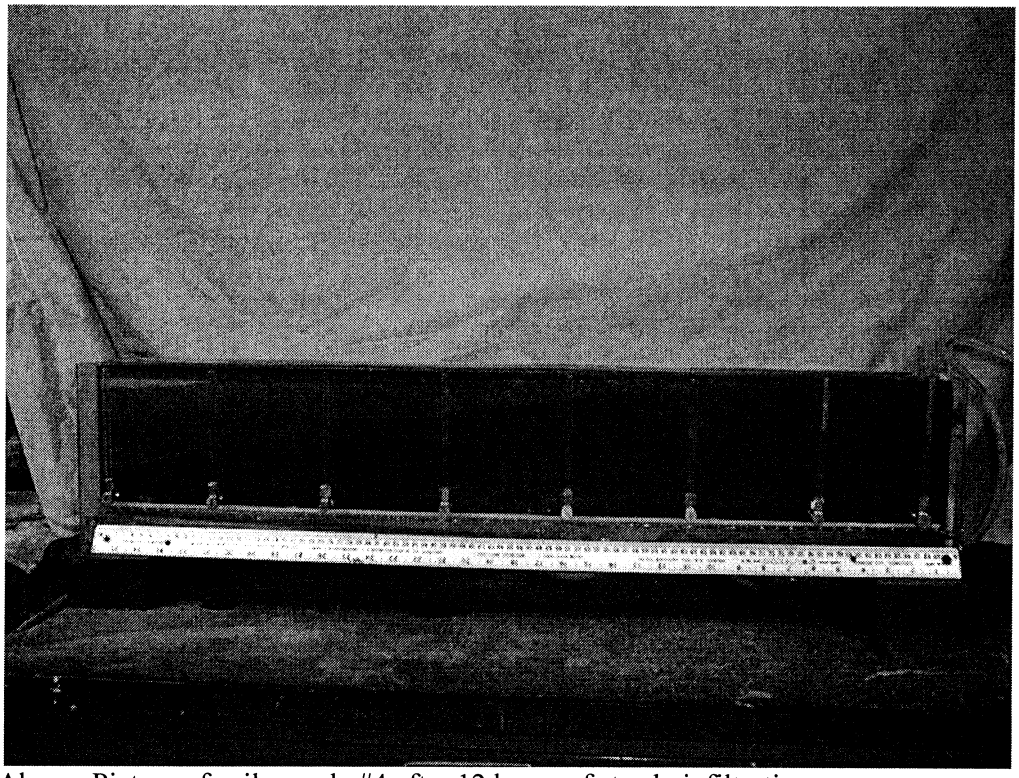

Above: Picture of soil sample #4 after 12 hours of steady infiltration

Using the Results

The information obtained from the box model experiments yielded the infiltration rate for each base slope and soil sample. By using the permeability value of each soil sample from the previous permeability tests, a plot of the test data in the form of q/k vs. base slope can be made.

Relationship of q/k vs. base slope

The plot of the test data for q/k vs. base slope (Figure A-7) has linear best-fit trendlines with R^2 values of more than 0.94. And, the trendlines of soil samples 1, 3, 4 and 6 have a slope and y intercept that is close to the values of the trend lines from the FastSeep analyses (a 2 cm and 20 cm curling gap distance). The exception is soil sample 5. This is most likely due to the difference in compaction between the permeability test sample (ASTM permeameter tests) and the model specimen.

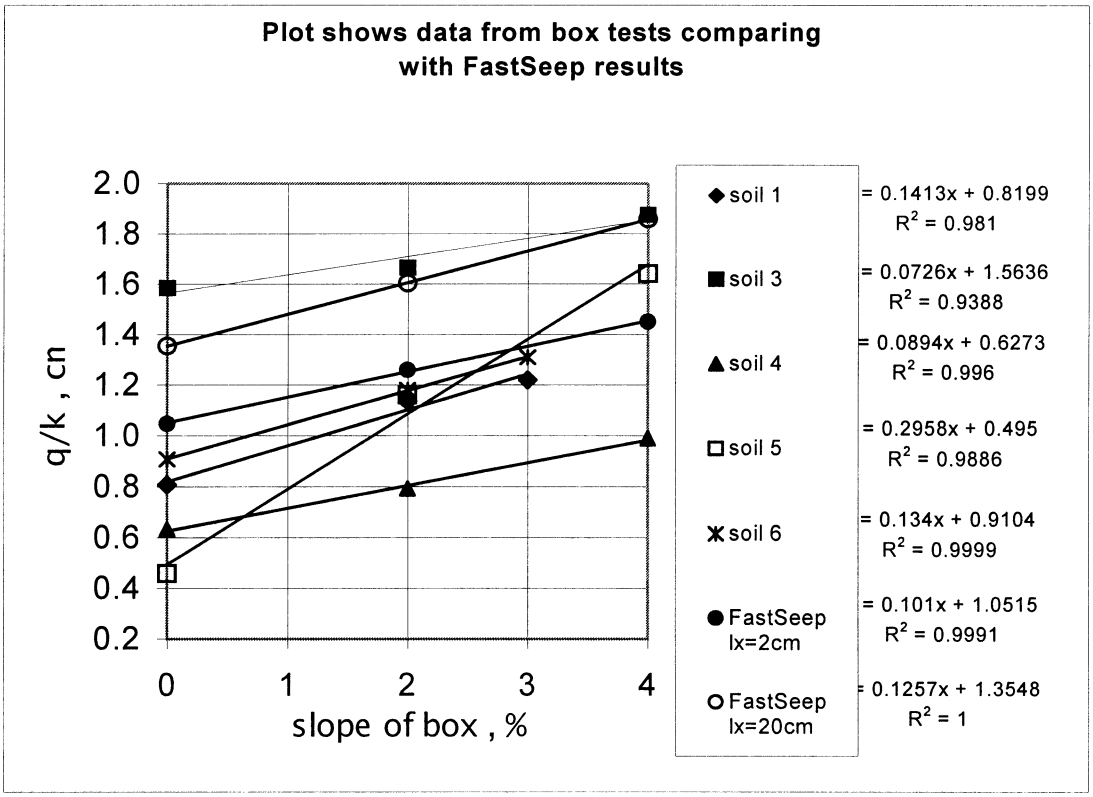

Figure A-7

The adjustment of the k value of soil samples 4 and 6 shifts their trendlines closer to the trendlines of FastSeep analyses. A very minor adjustment of the k value of soil 4 from 2.616 x 10^{-2} cm/s to 1.5 x 10^{-2} cm/s and soil 6 from 1.02 x 10^{-2} cm/s to 9.0 x 10^{-3} cm/s will bring their respective trendlines very close to the FastSeep predicted trendlines. This is shown in Figure A-8. Therefore, one of reasons that the test data does not exactly agree with the FEM analyses is the sensitivity of the output to the permeability of the soil. This is validation to the fact that accurate permeability data is crucial to infiltration predictions.

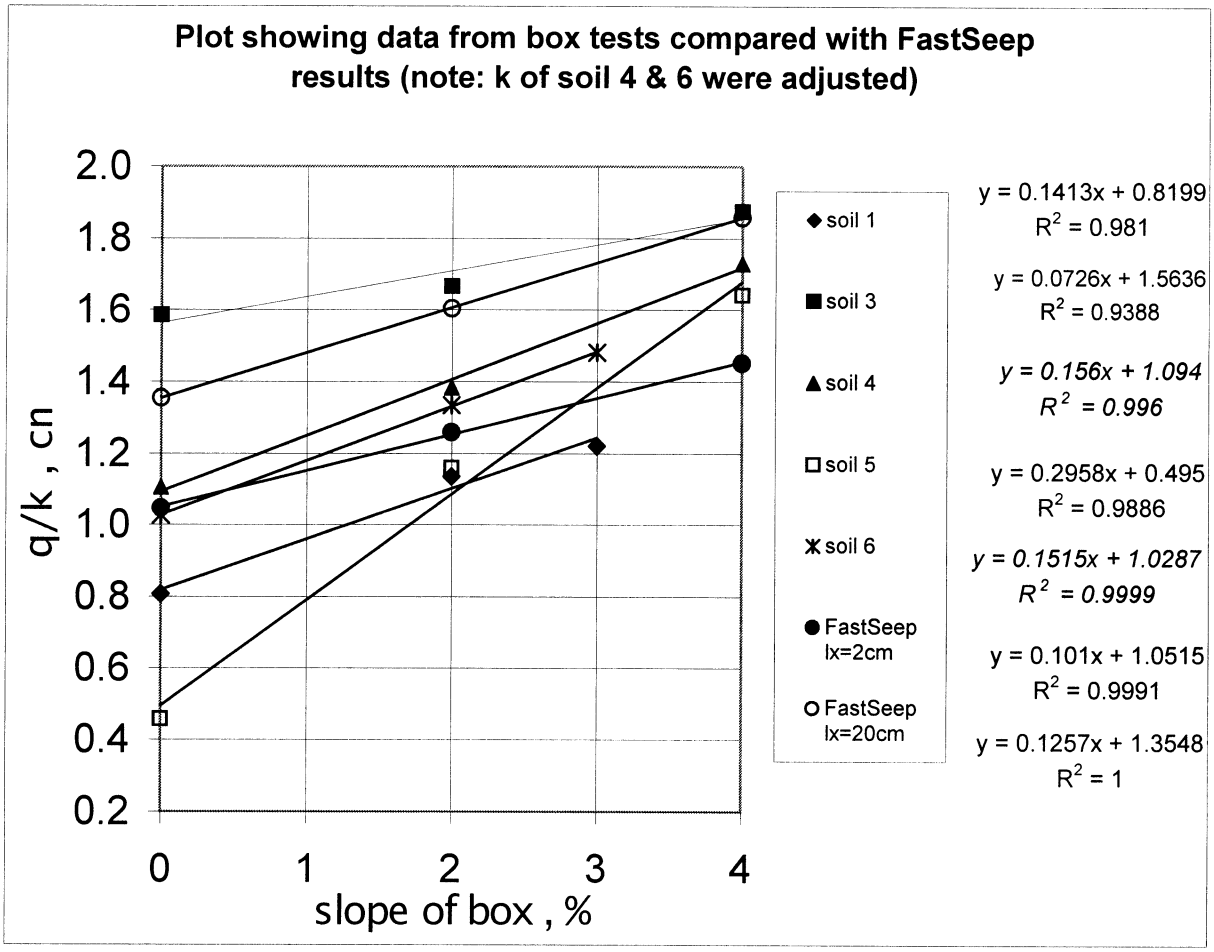

Figure A-8

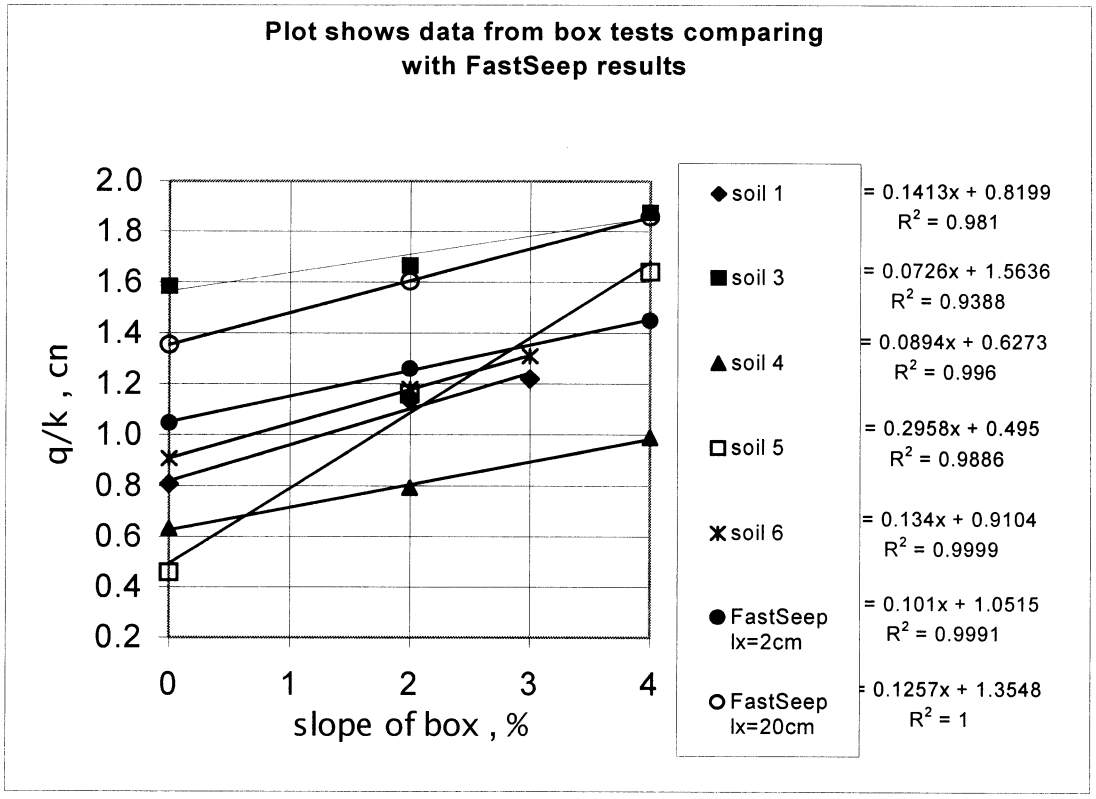

Conclusions

1. The test data agrees within a reasonable error with the FEM analyses.
2. The infiltration rate is linearly dependent on the soil permeability.
3. The infiltration rate is linearly dependent on the base slope.
4. The infiltration rate is linearly dependent on the curl distance due to temperature change under the joint.

The agreement of the test data and the FastSeep analysis provides confidence in the ability to analyze the actual pavement joint infiltration using a finite element program.

Pumping Model

Introduction

Since pumping by definition is the creation of excess pore pressures and the subsequent ejection of fines through the joint, an important aspect is to determine the proximity of the water table to the load required to induce pumping. Hence, a test setup was constructed in order to investigate this phenomenon.

Experimental Model

The setup consists of a standard proctor mold (6 in. deep with an inner diameter of 6 in.) filled with soil. The mold was modified to include both an outlet at the bottom for drainage and an outlet for a manometer tube 2-in. from the bottom of the mold to determine the level of the simulated water table. The pavement surface is substituted with a steel plate that fits atop the soil surface within the mold. To simulate the pressure produced by traffic, the standard proctor hammer, which is capable of applying a consistent blow to the plate, was used. To monitor the development of pore pressures, a miniature pressure transducer was inserted into the soil sample. In theory, the occurrence of pumping should cause an increase in the pore pressure within the soil. The water level was then varied in order to determine the level at which the change in pore water pressure produced by the hammer becomes noticeable.

A Druck PDCR 81 transducer was placed near the bottom of the soil in the center of the mold oriented downward. This model proved effective in providing a detectable change in the pore water pressure (recorded on a digital oscilloscope by pressure changes transmitted by the transducer) at approximately 4.5-in. from the surface of the soil. This test configuration was changed slightly during testing by orientating the transducer horizontally and approximately 3/4 in. from the bottom of the mold instead of vertical. This setup reduced the vibratory readings and gave a clearer waveform. The figure on the next page shows the test setup.

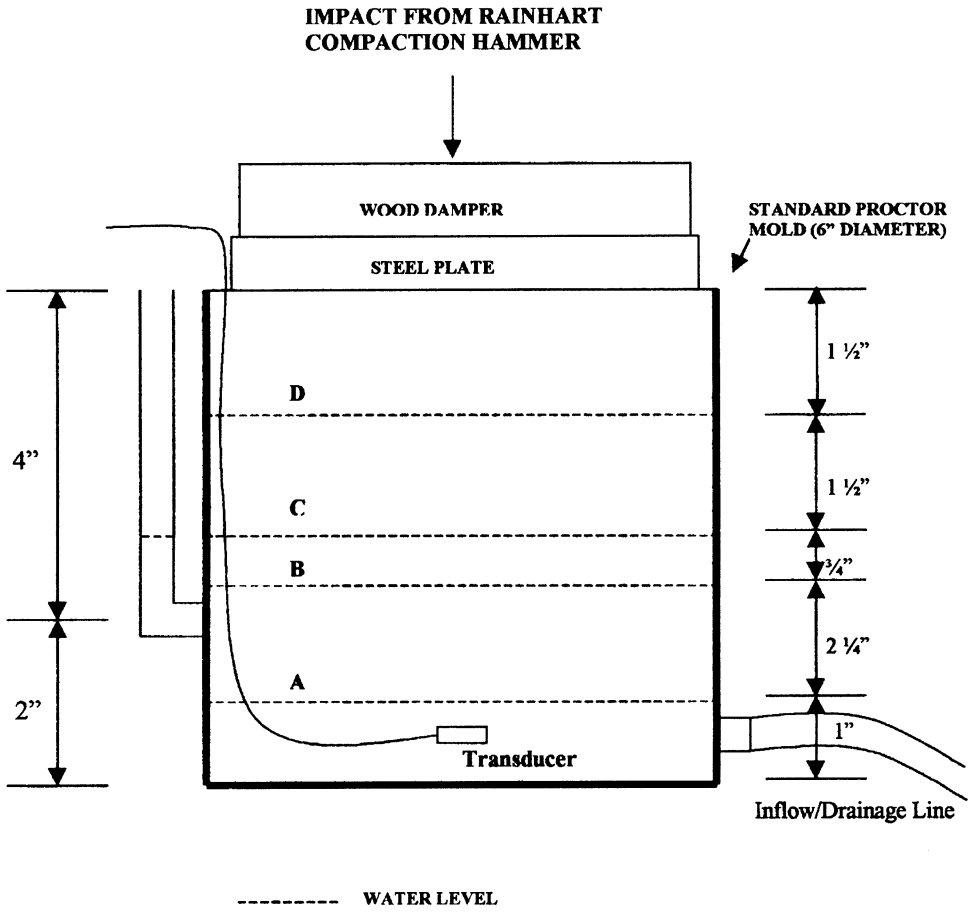

Model Cross Section

Procedure

1. Prepare the watertight testing mold for the soil and pressure transducer.
2. Saturate the transducer by boiling it until there are no longer any air bubbles emerging from the porous stone. Then allow the water to cool and saturate the stone.
3. Place the first lift (approximately 2.5-in.) of soil in the mold and compact to the desired level. The standard Proctor hammer may be used to achieve the desired degree of compaction. Embed the saturated transducer in the soil with the tip oriented horizontally approximately 3/4 in. from the bottom of the mold.
4. Place the subsequent lifts in the mold at the desired degree of compaction.
5. Connect the transducer to the appropriate power source and oscilloscope.

6. Set the oscilloscope to 20mV and 2ms per division (the 20 mV may need to be adjusted for varying excitation voltages). Use the trigger setup to capture the single waveform. Drop the hammer on the dry soil to observe the zero reading.
7. Raise the water table as desired by injecting water through the manometer tube allowing the water sufficient time to infiltrate.
8. Drop the hammer and observe the waveform.
9. Repeat steps 8 and 9 until a large increase in the pore water pressure is observed.

Data

Figures A-9 and A-10 indicate that the pore water pressure increase begins to be seen at approximately 4.5-in. from the surface of the soil. This was based on an essentially zero reading at 5-in. and a well-defined wave at 3.75-in. The first waveform, 5-in. from the surface, does not show the tight dip in pore water pressure that the others display, and is more indicative of inherent noise. Figure A-9 shows the waveforms for water levels of 5-in., 3.75-in., and 3-in. from the soil surface. Figure A-10 shows the waveforms for water levels of 1.5-in. and 0-in. (fully saturated) from the soil surface. Further testing at smaller water level increments may able to more accurately determine the critical water level. Total summary of data is in Table A-1.

Table A-1

Water level [depth from soil surface] (in.)	Peak pore water pressure (psi)
0.00	66.41
1.50	51.04
3.00	45.97
3.75	40.89
5.00	25.52

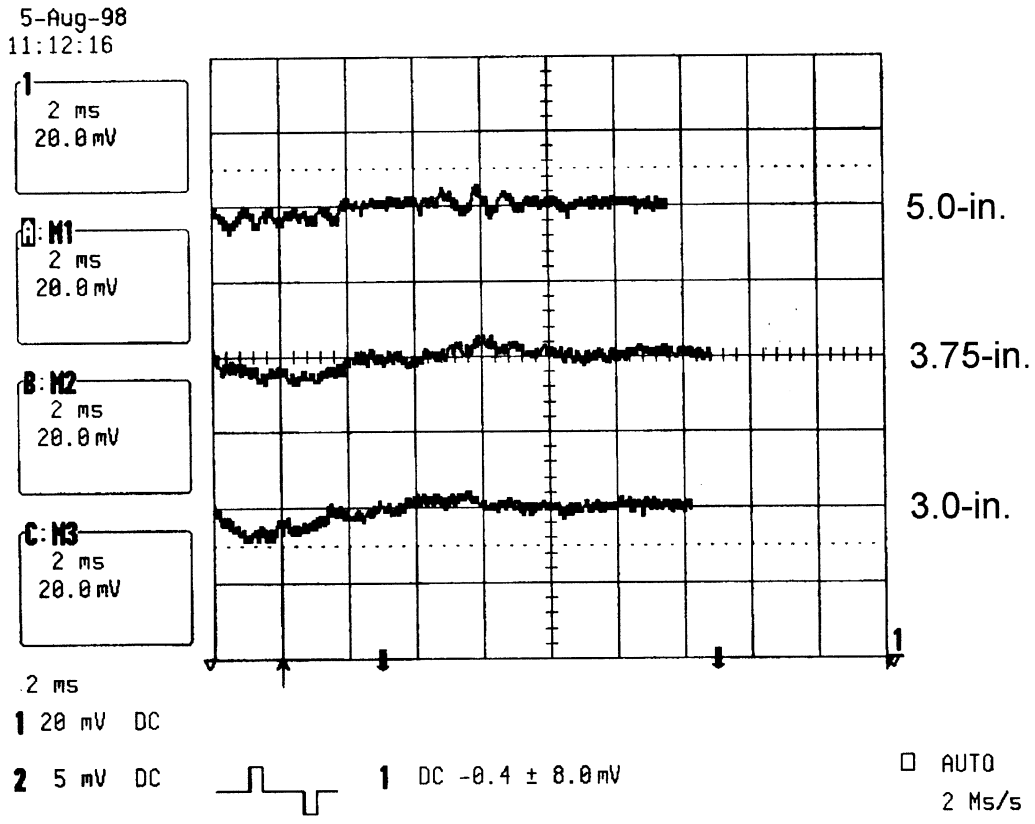

Figure A-9

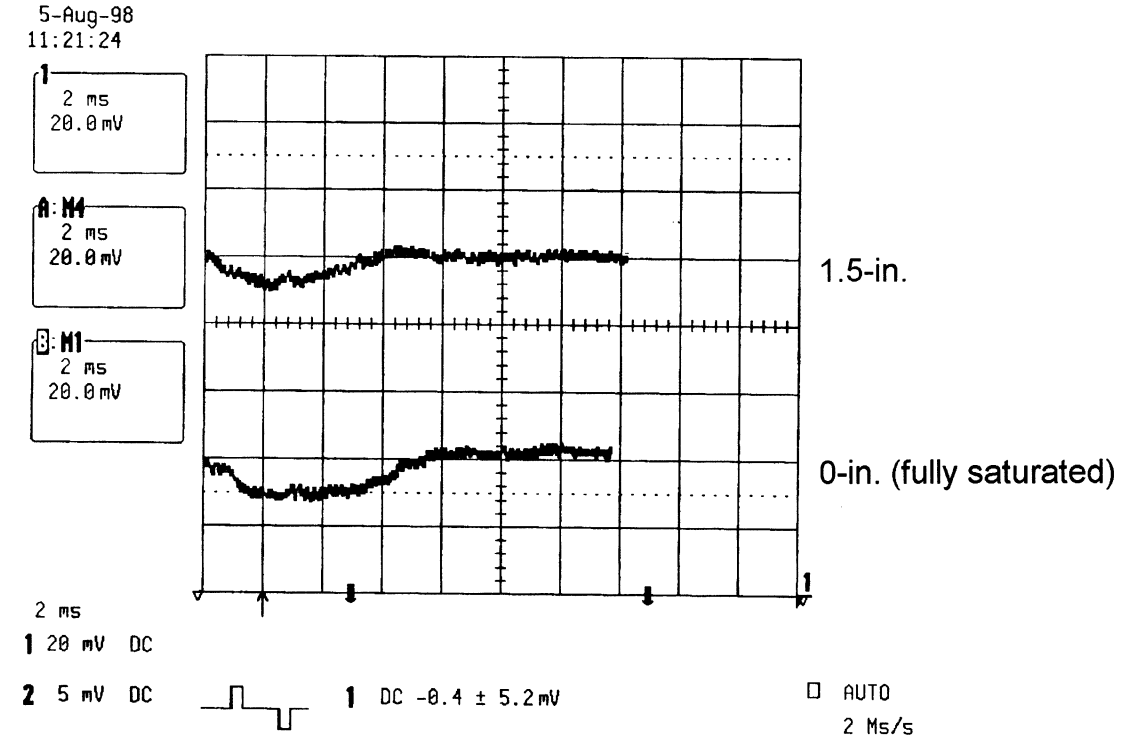

Figure A-10

Field Testing

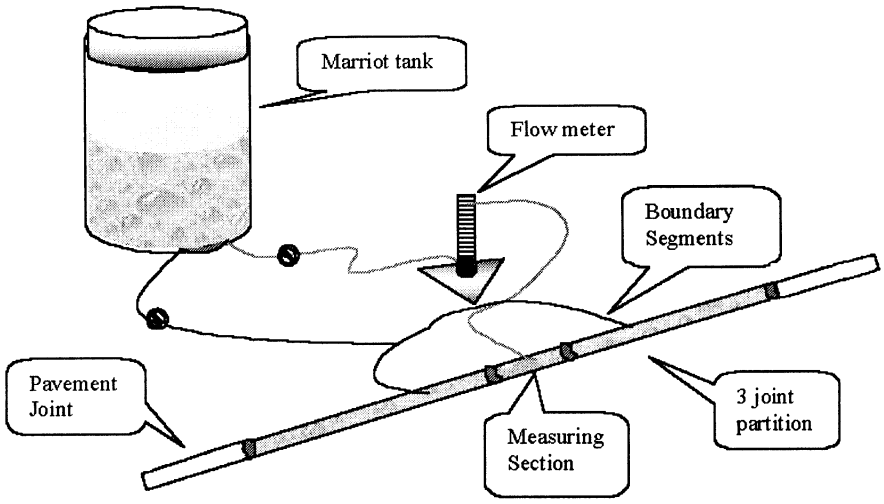

Field Test Procedure

1. Prepare concrete joint by cleaning out fill material and debris. Partition joint into three segments using foam insulation. One 6 in segment will be used as the measuring segment and two 1.5 ft segments will be used as the boundary.
2. Apply silicon around foam insulation in order to ensure water tight seal between segments. Perform seal check. (Add water to 6 in segment and look for leaks.)
3. Position the Marriot tank at a suitable lateral distance and height from the experimental joint.
4. Connect tubing from outlet "A" of the Marriot tank to the "in" of the flow meter. Place the tubing from the "out" of the flow meter at the 6 in measuring segment.
5. Position the two ends of the tubing from outlet "B" of the Marriot tank at the two 1.5 ft boundary segments.
6. Turn on both valves "A" and "B" of the Marriot tank.
7. Adjust the flow of valve "B" at Marriot tank to obtain a constant water level at top of 1.5 ft joint segments.
8. Adjust the flow meter to obtain a constant water level at top of 6 in joint segment
9. Start recording the flow rate versus time until a constant value has been reached.
10. The infiltration rate can be obtained by dividing the constant flow rate by the length of the measuring segment.

Field Testing Data and Results

- Test Site #1 –

Location: concrete campus road, University of Florida

Description: Transverse joint testing on 6in. measuring joint segment

Data and Calculation:

Test #	Flow rate per 6in. joint $cm^3/sec/6in.$
1	0.03
2	0.028
3	0.032
4	0.032
Average	0.0305

Therefore

$$\text{Joint infiltration rate} = (0.0305\frac{cm^3}{sec})(2)(24\times 60\times 60\ \text{sec/day})(\frac{1}{(30.48)^3}\ ft^3/cm^3)$$

$$= 0.186\ ft^3/day/ft$$

- Test Site #2 -

Location: SR24 urban road in Waldo, FL.

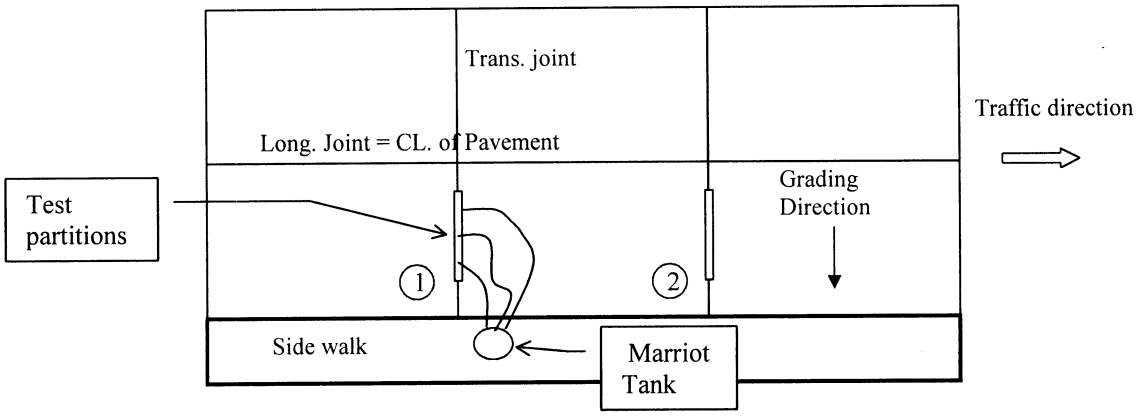

Site Plan View

The joint infiltration testing was performed on one portion of concrete pavement in Waldo, FL. By following the testing procedures, the 18in.-5.2in.-18in. testing partition were prepared over the selected transverse joint (2-18in. as the boundary partitions and the middle 5.2in. as the measuring partition). The water was introduced to the testing joint and after running the test for 3 hours, the infiltration rate into the middle partition was read by using the flow meter. The data was converted to the joint infiltration rate per foot of joint.

* Joint Location # 1

Date of Test: Jun 5, 1998 1-4 pm.

Weather: sunny , hot and dry

Joint Infiltration Rate = 0.516 ft^3/day/ft

- Test Site #2 - (continued)

* Joint Location # 2

Date of Test: Jun 11, 1998 2:30 – 4:30 pm.

Weather: sunny , hot and dry

Time (P.M.)	Elapsed time hour : minute	Flow meter reading	Joint infiltration (ft^3/day/ft)
2:25	0:00	Start	Start
2:35	0:10	74	0.196
2:50	0:25	74	0.196
3:10	0:45	71	0.184
3:25	1:00	75	0.199
3:40	1:15	79	0.215
3:55	1:30	79	0.215
4:10	1:45	79	0.215
4:25	2:00	79	0.215

- Test Site #3 -

Location: North of Tampa on I-4 Eastbound at intersection between I-4 and I-75

Date: Aug.27, 1998

Weather: Clear, hot

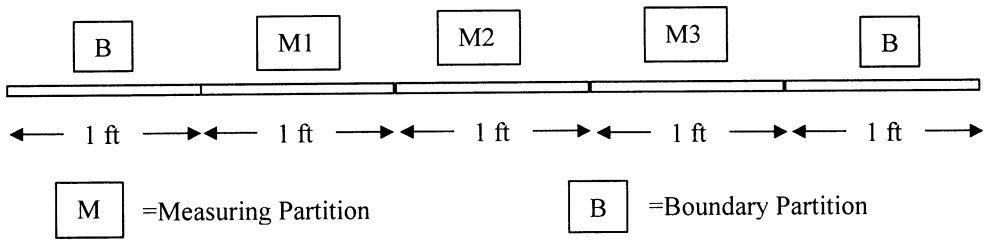

Partition M1		Partition M2		Partition M3	
Time	Infiltration rate (ft^3/day/ft)	Time	Infiltration rate (ft^3/day/ft)	Time	Infiltration rate (ft^3/day/ft)
3:45pm	Start	3:45pm	Start	3:45pm	Start
4:30pm	0.61	4:20pm	0.13	4:00pm	0.135

Date: Sep. 5, 1998

Weather: Clear, hot

Partition M1		Partition M3	
Time	Infiltration rate (ft^3/day/ft)	Time	Infiltration rate (ft^3/day/ft)
6:10am	Start	6:10am	Start
6:27am	2.62	6:27am	0.92
6:37am	2.62	6:37am	0.92
6:47am	2.62	6:47am	0.92
6:57am	2.62	6:57am	0.92
10:50am	Start	10:50am	Start
11:05am	1.60	11:05am	0.46
11:25am	1.49	11:25am	0.45
2:15pm	Start	2:15pm	Start
3:05pm	1.28	2:30pm	0.33
3:18pm	1.28	2:45pm	0.33

- Test Site #4 -

Location: East of Tampa on I-75 Northbound between Exit 48 and 49

Date: Sep.17, 1998

Weather: Mild after raining

No. of testing = 3 locations

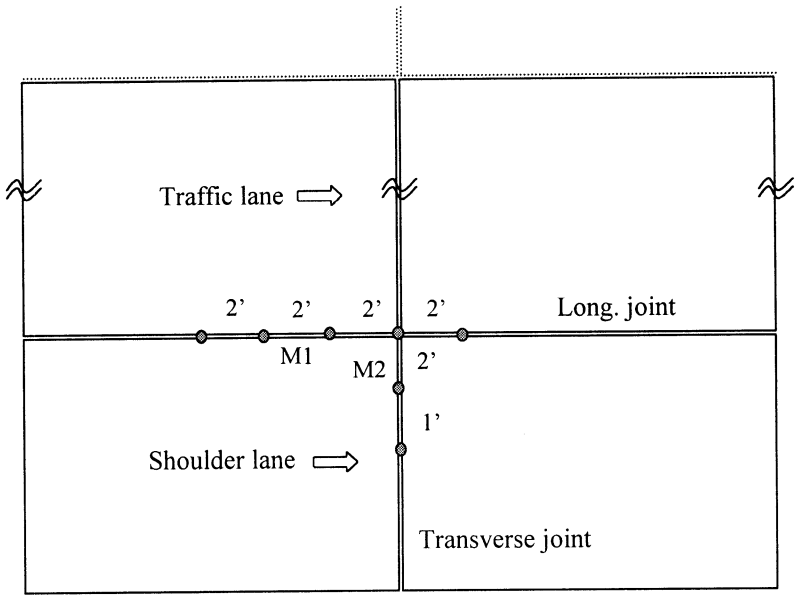

* Joint Location # 1 (M1 and M2)

Partition M1 (Long.)		Partition M2 (Transverse)	
Time	Infiltration rate (ft^3/day/ft)	Time	Infiltration rate (ft^3/day/ft)
2:20 pm	Start	2:20 pm	Start
2:30 pm	0.112	2:30 pm	0.331
2:45 pm	0.109	2:40 pm	0.331
3:00 pm	0.109	2:50 pm	0.366
		3:00 pm	0.366

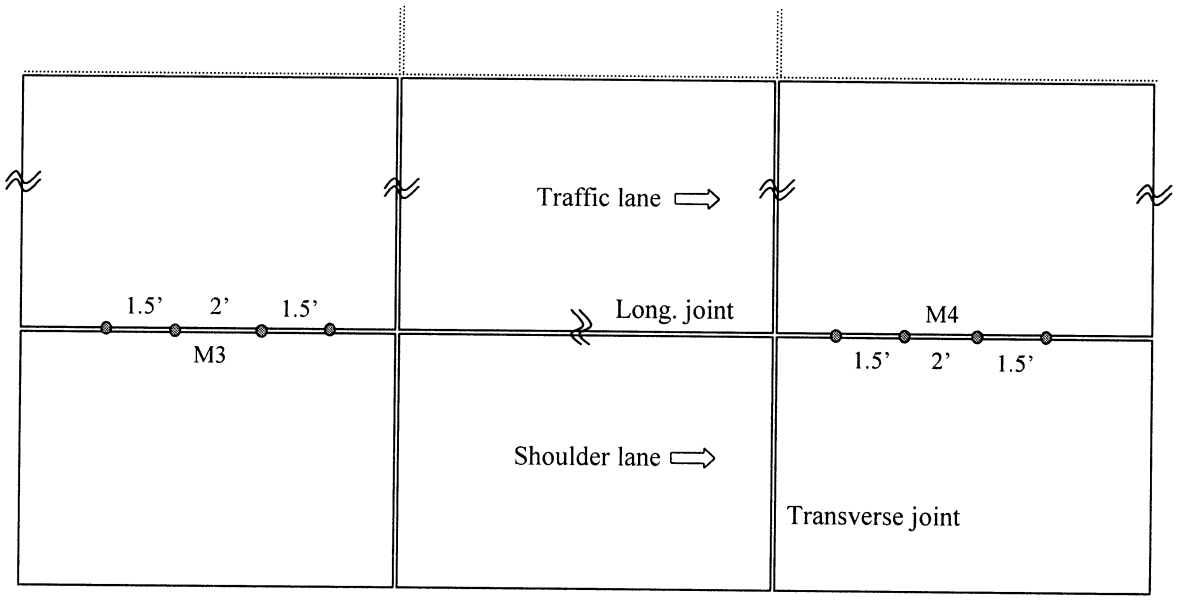

* Joint Location # 2 (M3) and # 3 (M4)

Partition M3 (Long.)		Partition M4 (Long.)	
Time	Infiltration rate (ft^3/day/ft)	Time	Infiltration rate (ft^3/day/ft)
4:00 pm	Start	4:50 pm	Start
4:50 pm	0.058	5:10 pm	1.139
5:05 pm	0.058	5:20 pm	1.139